



This is to certify that the

dissertation entitled

**LAYERED DOUBLE HYDROXIDES:**

**I. SYNTHESIS BY DESIGN**

**II. CATALYSIS BY INTERCALATED  
POLYOXOMETALATES**  
presented by

**Elizabeth Ann Gardner**

has been accepted towards fulfillment  
of the requirements for

Ph.D. degree in Chemistry

  
Thomas J. Pinnavaia  
Major professor

Date December 18, 1998

**LIBRARY  
Michigan State  
University**

**PLACE IN RETURN BOX** to remove this checkout from your record.  
**TO AVOID FINES** return on or before date due.  
**MAY BE RECALLED** with earlier due date if requested.

DATE DUE	DATE DUE	DATE DUE

LAYERED DOUBLE HYDROXIDES:  
I. SYNTHESIS BY DESIGN  
II. CATALYSIS BY INTERCALATED  
POLYOXOMETALATES

by

Elizabeth Ann Gardner

A DISSERTATION

Submitted to  
Michigan State University  
in partial fulfillment of the requirements  
for the degree of

DOCTOR OF PHILOSOPHY

Department of Chemistry

1998

## ABSTRACT

### LAYERED DOUBLE HYDROXIDES: I. SYNTHESIS BY DESIGN II. CATALYSIS BY INTERCALATED POLYOXOMETALATES

by

Elizabeth Ann Gardner

Layered double hydroxides (LDHs) have two predominant properties which can be exploited for materials applications. First, the hydroxylated lamellar framework can possess the desired characteristics, as in their use as antacids. Second, the exchangeable intergallery anions can be chosen for a specific function, with the framework serving merely as an inert support. The oxidation of alkenes by tungstate immobilized on an LDH intercalated with hydrophobic anions is an example which uses both the basicity of the LDH to enhance the selectivity for the epoxide over the diol product and the hydrophobic gallery anions to create a favorable environment for the organic substrate.<sup>1</sup>

Taking advantage of the hydroxylated lamellar structure of the LDH intercalate, a method for making thin LDH films for application as sensors, devices, and flame retardant materials was developed. LDHs were synthesized in organic solvents, resulting in colloidal sized LDH particles which formed well oriented films less than a micron thick, as judged by powder XRD and SEM studies. With this method, films with varying layer charge, intergallery anions, and framework cations are easily synthesized.

Catalysis by intercalated polyoxometalates (POMs) is an example of the second approach. Polyoxometalates are a promising class of anionic catalysts for

intercalation into LDHs and much research has been invested in introducing gallery functionality by intercalation of the POM into LDH layers.

However, there are a few problems which complicate the LDH-POM chemistry. First, the synthesis of an LDH-POM is always accompanied by an impurity phase which results from the reaction of the basic LDHs with acidic polyoxometalates. This problem was to be addressed by using a more acidic  $\text{Zn}_2\text{Al-LDH}$ , which can be synthesized at a pH of 6.2. The second problem arose from discrepancies in the reported d spacing for otherwise identical polyoxometalate intercalates, namely 9.9 and 12.2 Å in the case of LDH- $\text{Mo}_7\text{O}_{24}^{6-}$ , and 12.2 and 14.6 Å for LDH- $\text{H}_2\text{W}_{12}\text{O}_{40}^{6-}$  intercalates. In this case, Raman spectroscopy was used to unambiguously identify the molybdenum polyoxometalate intercalate. Finally, size selective catalysis implies pillaring of the gallery anions. Nitrogen adsorption was used to measure the pore volume of the LDH-POM systems. The catalytic activity of four systems;  $\text{Mg}_2\text{Al-Mo}_7\text{O}_{24}^{6-}$ ,  $\text{Mg}_2\text{Al-H}_2\text{W}_{12}\text{O}_{40}^{6-}$ ,  $\text{Zn}_2\text{Al-Mo}_7\text{O}_{24}^{6-}$ , and  $\text{Zn}_2\text{Al-H}_2\text{W}_{12}\text{O}_{40}^{6-}$  was tested for the peroxide oxygenation of cyclohexene to the corresponding epoxide and diol. However, our results indicate that only the surface bound anions are catalytically active and that the selectivity is a result of the basic nature of the LDH support.<sup>2,3</sup> In addition, the impurity salt may contribute to the catalytic activity. The acidity of the LDH support is not the determining factor in the formation of the impurity salt, but rather the affinity of the POM for the layer cations.

**This Dissertation is dedicated to my son, Mathew Miller**

## TABLE OF CONTENTS

Chapter 1. Thesis Objectives: An Overview .....	1
Chapter 2. Layered Double Hydroxides: A Brief Review .....	8
History .....	8
Applications .....	9
Structure.....	13
Composition .....	15
The Nature of $M^{n+}$ .....	15
The Nature of $A^n$ .....	18
The interlayer water .....	23
Synthesis .....	24
Precipitation .....	25
Salt-Oxide method.....	28
Thermal Treatments .....	31
Physicochemical Characterization.....	31
Chapter 3. Synthesis of $Mg_2Al$ -Layered Double Hydroxides at Acidic pH.....	37
Introduction .....	37
Results and Discussion.....	46
Conclusion.....	52
Experimental Methods.....	52
Chapter 4. The Synthesis of Layered Double Hydroxides with Colloidal-Size Particles .....	54
Introduction .....	54
Results and Discussion.....	56

M-LDHs .....	60
The Precipitate from Methanol .....	75
Conclusions .....	76
Experimental Methods .....	78
Chapter 5. Layered Double Hydroxides Pillared with Polyoxometalate	
Catalysts .....	81
Polyoxometalates .....	83
Applications .....	84
Catalysis by polyoxometalates .....	84
History .....	88
Composition .....	89
Structure .....	90
Polyoxometalate Intercalated Layered Double Hydroxides .....	97
Layered Double Hydroxides Intercalated with	
Isopolyoxometalates .....	99
LDHs Intercalated with Heteropolyoxometalates .....	101
Applications .....	106
Chapter 6. Polyoxometalates and Their Intercalation into Layered	
Double Hydroxides .....	107
Introduction .....	107
Results and Discussion .....	109
Catalyst Synthesis and Characterization .....	109
Catalytic Properties Mg <sub>2</sub> Al- and Zn <sub>2</sub> Al-POMs .....	122
Catalytic Oxidation of Cyclohexene by Zn <sub>2</sub> Al-PJP .....	126
Zn <sub>2</sub> Al-NaP <sub>5</sub> W <sub>30</sub> O <sub>110</sub> <sup>1+</sup> .....	127
Catalytic Oxidation by Zn <sub>2</sub> Al-NaP <sub>5</sub> W <sub>30</sub> O <sub>110</sub> <sup>1+</sup> .....	128
Conclusions .....	133

Experimental Methods.....	138
Refernces .....	139

## LIST OF TABLES

<i>Number</i>	<i>Page</i>
Table 2-1. Different Metals Used in the Synthesis of Layered Double Hydroxides .....	16
Table 2-2 Inorganic Anions That Have Been Intercalated Into Layered Double Hydroxides.....	20
Table 2-3. Organic Anions That Have Been Intercalated Into Layered Double Hydroxides.....	22
Table 2-4. Change in d spacing with Increasing Humidity .....	24
Table 2-5. Identifying Wavenumbers for Common Gallery Anions.....	34
Table 3-1. Three Methods Used to Synthesize MgAl Layered Double Hydroxides .....	40
Table 3-2. Indices ( <i>hkl</i> ) for LDHs Synthesized by the Methods of Miyata and Reichle .....	44
Table 5-1. Applications for Polyoxometalates, Excluding Catalysis and Medicine .....	85
Table 5-2. Summary of Polyoxometalate Intercalated Layered Double Hydroxides .....	102
Table 5-3. Oxidation Reactions with Intercalated Polyoxometalate Catalysts .....	105
Table 6-1. Raman Bands ( $\text{cm}^{-1}$ ) of Isopolymolybdates.....	117
Table 6-2. Peroxide Oxidation of Cyclohexene Over Polyoxometalate Catalysts .....	123

Table 6-3. Peroxide Oxidation of Cyclohexene in the Presence of Different Forms of $\text{NaP}_5\text{W}_{30}\text{O}_{110}^{1+}$ .....	132
--	-----

## LIST OF FIGURES

<i>Number</i>	<i>Page</i>
Figure 2-1. A schematic of a 3:1 $M^{2+}/M^{3+}$ Layered Double Hydroxide .....	12
Figure 2-2. X-ray diffraction pattern of a $Mg_3Al-NO_3^-$ double hydroxide showing Miller indices.....	32
Figure 3-1. Schematic of pH where $M(OH)_n$ and Layered Double Hydroxides form .....	38
Figure 3-2. X-ray diffraction patterns of $MgAl-CO_3^{2-}$ LDHs made by Miyata's coprecipitation at constant pH. The pH is maintained at $10.0 \pm 0.2$ and the reaction is digested for 18 hours at room temperature. a. $Mg/Al = 4$ ; b. $Mg/Al = 3$ ; c. $MgAl/ = 2$ ;. The peak assignments are given in Table 3-2. ....	42
Figure 3-3. $MgAl-CO_3^{2-}$ LDHs made by Reichle's coprecipitation at variable pH. The final pH is in the range of 8-11 and the reaction is digested for 18 hours at room temperature. a. $Mg/Al = 4$ ; b. $Mg/Al = 3$ ; c. $MgAl/ = 2$ ; The Miller indices are given in Table 3-2. ....	43
Figure 3-4. a. Transmission Electron Micrograph of $Mg_3Al-CO_3^{2-}$ made by Reichle's coprecipitation method. b. TEM of $Zn_2Al-NO_3^-$ made by Taylor's induced hydrolysis method. The particle size is considerably larger. c. TEM of a single particle of $Zn_2Al-NO_3^-$ at a higher magnification. ....	47
Figure 3-5. The diffraction patterns of products obtained by the reaction of $Mg(NO_3)_2$ (0.03 mol) and $Al(NO_3)_3$ (0.01 mol) in 200 ml $H_2O$	

in the presence of various amounts of 2.0 M Na(OH). The volumes of NaOH solution added to the reaction mixture are indicated along with the final pH value of the reaction mixture a reaction time of 3 days at 90-95 °C. .... 49

Figure 3-6. FTIR of  $Mg_2Al-NO_3^-$  synthesized at pH = 6.9. The resonance at  $1633\text{ cm}^{-1}$  is assigned to coordinated water,  $1385\text{ cm}^{-1}$  to nitrate, and  $447\text{ cm}^{-1}$  is Al-OH ..... 50

Figure 4-1. X ray diffraction pattern of products prepared in the reaction of a.  $Mg(NO_3)_2$ ,  $Al(NO_3)_3$ , and NaOH in acetonitrile and b. acetone. Synthesis of LDHs in acetone and acetonitrile by standard coprecipitation methods is unsatisfactory due to the insolubility of the Mg and Al salts in these solvents..... 57

Figure 4-2. Powder X-ray diffraction patterns for LDHs and LDH precursor products precipitated from various organic solvents and water. The LDHs synthesized in propanol and butanol were washed with methanol to remove the remaining  $NaNO_3$  salt byproduct..... 58

Figure 4-3. Infrared Spectra of  $Mg_xAl-NO_3^-$ , synthesized in ethanol, methanol, and water. From top to bottom: A  $Mg_3Al-NO_3^-$  synthesized in ethanol; the  $Mg_4Al-NO_3^-$ ,  $Mg_3Al-NO_3^-$ , and  $Mg_2Al-NO_3^-$  product from precipitation in methanol; the  $Mg_2Al-NO_3^-$  precipitation product after suspension in water and an LDH formed by traditional coprecipitation. .... 59

Figure 4-4. The X-ray diffraction pattern of an oriented thin films of  $Mg_3Al-NO_3^-$  a. product prepared by coprecipitation of an in methanol and subsequent hydrolysis in water, 0.030 mole

Mg(NO<sub>3</sub>)<sub>2</sub> and 0.010 mol Al(NO<sub>3</sub>)<sub>3</sub> in 100 ml methanol are dripped into a solution of 0.09 mol NaOH in 100 ml methanol and stirred for 3 days at 55 °C. b.. LDH product prepared by coprecipitation in water at 55 °C under conditions analogous to the synthesis in methanol. The orientation of the LDH layers in pattern a. is evident from the complete lack of in-plane reflections for the M-LDH . c. A less oriented powder pattern of the M-LDH product. The presence of the in-plane reflections verify that the M-LDH is an authentic layered double hydroxide. ....61

Figure 4-5 Scanning electron micrographs of; 6. A 20 mm self supporting Mg<sub>3</sub>Al-NO<sub>3</sub><sup>-</sup> M-LDH film. b. A 0.3 mm Mg<sub>2</sub>Al-Cl<sup>-</sup> film supported on glass.....65

Figure 4:6. Scanning electron micrographs of c. The surface of the Mg<sub>3</sub>Al-NO<sub>3</sub><sup>-</sup> M-LDH film. d. The surface of a 30 mm film of the Mg<sub>3</sub>Al-NO<sub>3</sub><sup>-</sup> control synthesized in water.....67

Figure 4-7. a. X ray diffraction pattern of an M-LDH calcined at 500 °C. b. the same material after being reconstituted in water to reform the LDH. ....69

Figure 4-8. Thermogravimetric analysis of Mg<sub>x</sub>Al-NO<sub>3</sub><sup>-</sup> M-LDH a. M-LDH with a 2:1 Mg:Al ratio. b. M-LDH with a 3:1 Mg:Al ratio. c. Mg<sub>3</sub>Al-NO<sub>3</sub><sup>-</sup> made by coprecipitation in water. d. M-LDH with 4:1 Mg:Al ratio..... 70

Figure 4-9. X-ray diffraction patterns of M-LDHs with theoretical 4:1 (4.0:1.0), 3:1 (3.2:1.0), and 2:1 (3.0:1.0) Mg:Al ratios. The actual ratios are in parentheses. .... 71

Figure 4-10. X ray diffraction patterns for a. M-LDH where the gallery anion of interest was intercalated via an exchange reaction. b. M-LDH where  $\text{Co}^{3+}$  cation of interest is present in a fractional substitution.....73

Figure 4-11. XRD of M-LDH with varying layer cations and anions..... 74

Figure 4-12. FTIR of a.  $\text{Mg}_3\text{Al-NO}_3^-$  dried under ambient conditions. b.  $\text{Mg}_3\text{Al-NO}_3^-$  dried under vacuum at 150 °C. ....77

Figure 5-1. Schematic of the Keggin.<sup>127</sup> The  $\alpha\text{-XM}_{12}\text{O}_{40}$  Keggin ion is shown with common derivatives. The left side shows the three isomers formed by the rotation of 1,2, or 4  $\text{M}_3$  triads. The lacunary ions on the right are formed by the dissociation of neutral  $\text{MO}_3$  octahedra. ( $\text{H}_2\text{W}_{12}\text{O}_{40}^{6-}$ ). The formula for the Keggin ion and its derivatives can be written as  $(\text{XO}_4)_n\text{M}_m\text{O}_{3m}$  where each Keggin ion (excepting  $\text{H}_2\text{W}_{12}\text{O}_{40}^{6-}$ ) has an internal  $\text{XO}_4$  tetrahedra and each addenda atom has one terminal oxygen. The Keggin anions are considered to be very weak bases with great softness.....91

Figure 5-2. Examples of Type 2 structures where each addenda atom has two terminal oxygens.<sup>127</sup> ..... 93

Figure 5-3. Schematic of some representative macropolyanions. a. A Dawson ion made from two  $\text{M}_9\text{O}_{31}$  Keggin lacunary ions. b. A Dawson TSMP complex sandwiching four planar Co octahedra. c. A PJP anion,  $\text{NaP}_5\text{W}_{30}\text{O}_{110}^{14-}$ . The Na cation is displaced from the center of the disk shaped anion. ....95

Figure 6-1. X-ray diffraction patterns of the mixed phase product formed by in situ hydrolysis of  $\text{Na}_2\text{WO}_4$  in the presence of a  $\text{Mg}_2\text{Al-}$

terephthalate: a. thin film sample dried under ambient conditions; the sharp reflections are (00l) lines of  $[\text{Mg}_{12}\text{Al}_6(\text{OH})_{36}](\text{Mo}_7\text{O}_{24})$  with a basal spacing of 12.2 Å, whereas the broad lines are due to a salt-like impurity phase with a spacing of 10.2 Å. b. powder sample, dried under ambient conditions, showing a marked reduction in the intensity of the LDH phase; c. powder sample dried overnight at 120 °C showing the loss of the  $\text{Mg}_2\text{Al}-\text{Mo}_7\text{O}_{24}^{6-}$  phase; d. thin film of sample after use as a catalyst in the oxidation of cyclohexene..... 110

Figure 6-2. Raman spectra of  $(\text{NH}_4)_6\text{Mo}_7\text{O}_{24}$  and the  $\text{Mg}_2\text{Al}-\text{Mo}_7\text{O}_{24}^{6-}$  product formed by in situ hydrolysis of  $\text{MoO}_4^{2-}$  and ion exchange with a  $\text{Mg}_2\text{Al}$ -terephthalate LDH. .... 112

Figure 6-3 X-ray diffraction patterns of the mixed phase product formed by in situ hydrolysis of  $\text{Na}_2\text{WO}_4$  in the presence of  $\text{Mg}_2\text{Al}$ -terephthalate. Parts a-d are analogous to those given in Figure 6-1 for the corresponding molybdate system..... 114

Figure 6-4. X-ray diffraction patterns of  $[\text{Zn}_{12}\text{Al}_6(\text{OH})_{36}](\text{Mo}_7\text{O}_{24})\text{mH}_2\text{O}$  prepared by ion exchange of the corresponding LDH-nitrate with  $\text{Mo}_7\text{O}_{24}^{6-}$ ; a. thin film sample dried under ambient conditions; b. powder sample dried under ambient conditions; c. powder sample dried overnight at 120 °C showing the loss of the LDH phase; d. thin film sample after use as a catalyst in the oxidation of cyclohexene. The broad weak reflection at 10.8 Å in spectrum (b) is due to a salt-like impurity phase..... 116

Figure 6-5 Raman spectra of  $\text{Zn}_2\text{Al}-\text{Mo}_7\text{O}_{24}^{6-}$  after heating to various temperatures: a. the air sample, showing bands analogous to those

in ammonium heptamolybdate; b. After drying at 105 °C, showing the splitting of the terminal Mo=O band at 950 cm<sup>-1</sup>; c. After heating to 220 °C, the terminal Mo=O band at 936 cm<sup>-1</sup> and the Mo-O-Mo polymeric band at 220 cm<sup>-1</sup> decreased in intensity similar to the band for Mo-O-Al in alumina supported molybdate d. The sample dried at 220 °C and then slurried in distilled water, showing the further shift in the terminal Mo-O band to 922 cm<sup>-1</sup>..... 119

Figure 6-6 X-ray diffraction patterns of [Zn<sub>12</sub>Al<sub>6</sub>(OH)<sub>36</sub>](H<sub>2</sub>W<sub>12</sub>O<sub>40</sub>)<sup>6-</sup>mH<sub>2</sub>O prepared by ion exchange of the corresponding LDH-nitrate with H<sub>2</sub>W<sub>12</sub>O<sub>40</sub><sup>6-</sup>: a. thin film sample dried under ambient conditions; b. powder sample dried under ambient conditions; c. powder sample dried overnight at 120 °C; d. thin film sample after use as a catalyst in the oxidation of cyclohexene. The broad line at 11.1 Å is due to a salt-like POM impurity phase..... 121

Figure 6-7 a. XRD pattern of a physical mixture of Zn-H<sub>2</sub>W<sub>12</sub>O<sub>40</sub><sup>6-</sup> salt and Al-H<sub>2</sub>W<sub>12</sub>O<sub>40</sub><sup>6-</sup> salts b. XRD pattern of a physical mixture of Zn-Mo<sub>7</sub>O<sub>24</sub><sup>6-</sup> salt and Al-Mo<sub>7</sub>O<sub>24</sub><sup>6-</sup> salts. .... 125

Figure 6-8. a. Powder XRD pattern of an Aluminum-NaP<sub>5</sub>W<sub>30</sub>O<sub>110</sub><sup>14-</sup> salt analogous to the impurity phase in the synthesis of Zn<sub>2</sub>Al-PJP. The d spacing of the first peak is 15.5 Å. b. XRD of a thin film sample of Zn<sub>2</sub>Al-PJP The d spacing of the LDH is 21.6 Å and the broad reflection due to the impurity phase is 15.1 Å. c. XRD of a thin film sample of Zn<sub>2</sub>Al-PJP with a slightly greater volume of impurity phase. The d spacing of the LDH is 22.0 Å and that of the impurity phase is 15.1 Å. d. XRD of a thin film sample of

Zn<sub>2</sub>Al-PJP with a the greatest volume of impurity phase. The d spacing of the LDH is 21.7 Å and 14.8 Å for the impurity phase. ....129

Figure 6-9. a. MAS-NMR of (NH<sub>4</sub>)<sub>14</sub>NaP<sub>5</sub>W<sub>30</sub>O<sub>110</sub>, with a single peak at -13.9 ppm. The two small peaks are side bands. b. Zn<sub>2</sub>Al-NaP<sub>5</sub>W<sub>30</sub>O<sub>110</sub><sup>1+</sup>, the MAS-NMR of the intercalated anion is the same as a., verifying that only PJP anion is present. c. MAS-NMR of the supported catalyst after use in the oxidation of cyclohexene. The peak at -2.89 ppm is (BuO)<sub>3</sub>PO and the small peaks are side bands. ....130

## Chapter 1. Thesis Objectives: An Overview

My graduate work actually began with the study of oxidative catalysis by polyoxometalates (POMs) intercalated into layered double hydroxides (LDHs). While several of my predecessors in the Pinnavaia group had worked on the synthesis of various LDH-POM systems, I was to be the first student to concentrate on their catalytic applications

Polyoxometalates were first intercalated into LDHs in 1984.<sup>4</sup> Since then, there have been over 45 articles published on the intercalation of POMs into LDHs and catalysis by the LDH-POM systems. The driving force behind all this effort has been the catalytic potential of the LDH supported POMs. Polyoxometalates are the most widely applied class of homogeneous catalysts in industry today. They serve as both hydration<sup>5</sup> and dehydration catalysts, as polymerization catalysts,<sup>6</sup> as co-catalysts with palladium or rhodium, and most importantly for this work, as oxidation catalysts. While many of these POMs serve as homogeneous catalysts, supporting the POM in the layers of an LDH adds the potential value inherent to a heterogeneous catalyst. The LDH-POM can be easily filtered from the reaction mixture and reused, making the catalyst less detrimental to the environment and adding economic value for POMs as industrial catalysts. When the POMs are constrained between the layers of an LDH, selectivity can be added to the reaction scheme. The selectivity can be conformational, where the substrate can only approach the catalyst in one

orientation, or by size, where access to the interlayer region is restricted by the dimensions of the catalyst.

But in many ways, POM-LDHs have not lived up to their potential. There is an impurity byproduct in all POM-LDH intercalation reactions which is the product of a hydrolysis reaction between the acidic POM and basic LDHs. And of all the studies pertaining to catalysis by LDH-POMs, only Tatsumi et al.<sup>7</sup> have shown a direct correlation between the LDH-POM catalysts and substrate selectivity. Small molecules had greater access to the catalyst when  $\text{Mg}_2\text{Al-LDH}$  was intercalated with the catalyst  $\text{H}_2\text{W}_{12}\text{O}_{42}^{10-}$  (d spacing = 12.2 Å) than when  $\text{Mo}_7\text{O}_{24}^{6-}$  was the intercalated catalyst (d spacing = 9.9 Å). The oxidation of cyclohexene (4.7 Å by 6.2 Å) was suppressed to a greater extent than that of the 2-hexene (3.9 Å by 4.7 Å) in the  $\text{Mg}_2\text{Al-Mo}_7\text{O}_{24}^{6-}$  relative to the  $\text{Mg}_2\text{Al-H}_2\text{W}_{12}\text{O}_{40}^{6-}$  system. My project was to take the preliminary results of Tatsumi, add the expertise of our lab in LDHs and the intercalation of POMs, and see how far I could take the chemistry. Specifically to intercalate the oxidation catalysts into a more acidic  $\text{Zn}_2\text{Al-LDH}$  in order to eliminate the impurity phase present in all synthesis of LDH-POMs to date.

The first step was to intercalate  $\text{Mo}_7\text{O}_{24}^{6-}$  and  $\text{H}_2\text{W}_{12}\text{O}_{40}^{6-}$  into  $\text{Mg}_2\text{Al-}$  and  $\text{Zn}_2\text{Al-LDHs}$  and repeat the size selective experiments of Tatsumi et. al. It immediately became obvious that there were some major problems at the most basic level of the experiment. The identity of the catalytic species was equivocal, the catalysts were not stable under the thermal or catalytic conditions of the experiments, and finally, there was an impurity phase, present in all LDH-POMs reported to date,<sup>2</sup> but which is generally ignored.

A search of the literature showed that these problems were the result of ambiguities that have propagated through the literature on LDH-POMs; Diffraction patterns with unassigned peaks and no evidence of ordered

reflections are the only evidence to support the claim that a POM anion has been intercalated into an LDH. Discrepancies in the reported d spacing are discussed in vague terms of 'grafted pillars' and dismissed. In discussions of catalysis by POM intercalated LDHs, any possible catalytic activity by the ever-present impurity phase is ignored. And finally, the X-ray diffraction patterns of oriented film samples are used to determine the relative amount of impurity phase present in an LDH-POM, without acknowledging that impurity phases are obscured in the X-ray diffraction patterns of oriented samples.<sup>8</sup> It was evident that a method for the synthesis of a pure LDH-POM phase was necessary before the catalytic properties of the LDH-POM systems could be investigated. In addition, careful characterization of the LDH-POM system would be necessary, not only to verify the identity of the intercalated POM species, but to substantiate the thermal and catalytic stability of the catalyst.

I was eventually able to untangle the  $\text{Mg}_2\text{Al}$ - and  $\text{Zn}_2\text{Al}$ -POM intercalate systems. Raman Spectroscopy and the known aqueous chemistry of molybdate and tungstate were used to unambiguously identify the intercalated POMs as the  $\text{Mg}_2\text{Al-Mo}_7\text{O}_{24}^{6-}$ ,  $\text{Zn}_2\text{Al-Mo}_7\text{O}_{24}^{6-}$ ,  $\text{Mg}_2\text{Al-W}_7\text{O}_{24}^{6-}$  and  $\text{Zn}_2\text{Al-H}_2\text{W}_{12}\text{O}_{40}^{6-}$ . X-ray diffraction of the LDH-POMs before and after use as catalysts showed that the  $\text{Mg}_2\text{Al-Mo}_7\text{O}_{24}^{6-}$ ,  $\text{Mg}_2\text{Al-W}_7\text{O}_{24}^{6-}$ , and  $\text{Zn}_2\text{Al-Mo}_7\text{O}_{24}^{6-}$  were not stable catalysts. Finally, Al-POM salts synthesized under conditions analogous to the POM intercalation reactions were used to show that the impurity phase has a significant reactivity of its own.

Still, all the previous experiments did not result in any new insight into the synthesis of impurity-free LDH-POMs. It was time to step back and take a fresh look at the problem. POMs are formed by a series of hydrolysis reactions as the pH is lowered. Most POM-LDHs are made at acidic pH where the POM is stable, but LDHs begin to decompose. However, some POMs are stable at

quite basic pH. Why haven't these POMs been intercalated? Also, some LDHs are more acidic; ZnAl-LDH can be synthesized at pH 6.4 and relatively pure Zn<sub>2</sub>Al-POMs are easily synthesized. But much work focuses on intercalating POMs into MgAl-LDHs. Why? Nowhere did I see an analytical discussion of the relative merits of a MgAl- versus a ZnAl-LDH or any other M<sup>2+</sup>M<sup>3+</sup>-LDH as a support for POM catalysts; nor was there any discussion of why a particular POM was chosen to be intercalated into an LDH for catalysis or any other purpose.

The impurity phase is believed to be the product of an acid/base reaction between the acidic POMs and the basic LDHs. The synthesis of the POMs, the LDHs, and the final LDH-POM is done in aqueous solution. The acid/base reaction is very much a result of the aqueous solvent system. An LDH in 0.1 M acetic acid will decompose overnight, while after 3 days in glacial acetic acid, there is very little decomposition of the LDH. How would replacing the water with an organic solvent affect the acid/base reaction between the POM and LDH?

All these questions led me to believe that before I could figure out the best way to intercalate POMs into LDHs, I needed to thoroughly understand the LDH support. It is generally stated that the pH required for LDH precipitation reactions is equal to or higher than the pH where the more soluble cation precipitates. However, MgAl-LDHs are routinely synthesized at pH greater than 12, where Mg<sup>2+</sup> precipitates, but Al<sup>3+</sup> is soluble. In addition, ZnAl-LDHs are synthesized at pH = 6.2, where Zn<sup>2+</sup> is soluble. It seemed that the pH required for precipitation reactions would be any pH where the least soluble cation precipitates. If this were true, then it should be possible to synthesize MgAl-LDHs at pH less than 8.

In a similar vein, it is generally accepted that contamination by carbonate is inevitable because of the preference of LDHs for  $\text{CO}_3^{2-}$  anions. There are two factors that make  $\text{CO}_3^{2-}$  highly favored for intercalation into LDHs. The first factor is the divalent charge; since LDHs have a high layer charge, multivalent anions are preferentially intercalated. Second, the structure of  $\text{CO}_3^{2-}$  is such that the three oxygens fit into adjacent sites of the LDH layers. But is carbonate really that favorable, or is it merely ubiquitous? Since  $\text{CO}_2$  from the air easily dissolves in basic, aqueous LDH reaction systems and forms  $\text{CO}_3^{2-}$ , synthesis of LDHs is generally done under an inert atmosphere ( $\text{N}_2$ ), or at a pH less than 7 where  $\text{HCO}_3^-$  is the predominant species. What would be the effect be if the entire LDH precipitation reaction was done at an elevated temperature where  $\text{CO}_2$  is less soluble? What would the effect be if the solvent system was organic, where again  $\text{CO}_2$  is less soluble?

These questions generated from the literature did suggest two sets of experiments on the fundamental chemistry of LDH synthesis. My first study dealt with the synthesis of MgAl-LDHs at pH < 8. Even a slightly acidic pH might make the intercalation of POMs into MgAl-LDHs result in a more crystalline LDH-POM product. My second study was the synthesis of LDH in organic solvents. Not only would contamination by  $\text{CO}_3^{2-}$  be minimized, the organic solvent system might be useful in POM intercalation reactions.

The results of these experiments led me in some unexpected directions. The synthesis of LDHs in MeOH results in a colloidal LDH which makes very thin, oriented LDH films. There are several possible applications for the colloidal LDHs in the areas of catalysis, sensors and devices, and fire retardant materials.

This is all very far from the initial purpose of finding better ways to intercalate POMs cleanly into LDHs. But while I didn't find a direct application

of the two new methods to the synthesis LDH-POM catalysts, I did begin to see a new interpretation of the LDH-POM systems. While the majority of the catalytic activity demonstrated by the LDH-POM systems is probably attributable to the impurity salt surface sorbed to the LDH, the selectivity is enhanced by the basicity of the LDH support. Through such effects as increasing access to the catalysts, selective adsorption of substrate on the surface of the LDH, and enhancing product selectivity, the LDH acts as a co-catalyst in conjunction with the POM. These arguments are clarified in the final catalytic oxidation experiments using  $\text{Zn}_2\text{Al}-(\text{NaP}_5\text{W}_{30}\text{O}_{110})^{1+}$  as the catalyst.

## **I. SYNTHESIS BY DESIGN**

## Chapter 2. Layered Double Hydroxides: A Brief Review

Most simply stated, LDHs consist of positively charged mixed metal hydroxide sheets with charge balancing interlayer anions. Sometimes designated anionic clays in reference to the anionic intercalates, they are the only general class of layered anion exchange materials. Three contemporary review articles on LDH chemistry are available: one by Vacarri in 1991,<sup>9</sup> another by De Roy in 1992<sup>10</sup> and a 1998 review by Jones,<sup>11</sup> which focuses mainly on LDHs containing organic intercalates.

### History

LDHs are relatively rare natural materials generally associated with serpentines in metamorphic formations or in saline deposits. They have been linked to prebiotic chemistry and it is postulated that they may have played a role in the origin of life.<sup>11</sup> The first layered double hydroxide to be identified was hydrotalcite,  $([\text{Mg}_6\text{Al}_2(\text{OH})_{16}]\text{CO}_3 \cdot 4\text{H}_2\text{O})$ . Discovered in Sweden around 1842, it is easily crushed into a white powder like talc. Also like talc, it occurs in nature as a foliated material with contorted plates or in fibrous masses. Pyroaurite, a MgFe-LDH that is similar in appearance to gold when heated, was discovered at about the same time. It was later recognized to be isostructural to hydrotalcite

The formula for LDHs was determined in 1915 by E. Manasse<sup>12</sup> and in 1930, Aminoff and Broomè<sup>13</sup> recognized the existence of two polytypes of hydrotalcite, one with rhombohedral symmetry and a second one with hexagonal symmetry which was called manasseite after Manasse. The papers by Manasse

and Aminoff and Broome went relatively unnoticed, so it was not until 1941 that Frondel<sup>14</sup> recognized the interrelations between hydrotalcite, pyroaurite and several other minerals. The first laboratory synthesis was done in 1942 when Feichtknecht<sup>15</sup> reacted metal salt solutions with base.

There was a considerable time gap between the discovery and synthesis of LDHs and the determination of their structure due to their nonstoichiometric nature and the difficulty in obtaining crystals large enough for X-ray analysis. The proposed structure went through several successions before Allman<sup>16</sup> and Taylor<sup>17</sup> determined the correct configuration to be a layered structure with cations located in the same layer with anions and water in the interlayer.

Meanwhile, catalysis by LDHs took a separate but parallel path beginning in 1924 with coprecipitated NiAl-LDH as a hydrogenation catalyst.<sup>18</sup> This continued until 1970 when the two paths merged in a patent for the preparation of a hydrotalcite-like material as catalyst precursors.<sup>19</sup>

## **Applications**

LDHs are an excellent example of materials by design. A variety of framework cations, layer charges, and intergallery anions can be incorporated into the LDH structure, and it is this very versatility that allows LDHs to be utilized in exceedingly diverse areas. Industrial applications of LDHs can be loosely divided into four areas; pharmaceuticals, anion exchangers and adsorbents, the improvement of materials properties, and catalysis.

An early application of LDHs in pharmaceuticals was in the treatment of peptic ulcers. The buffering pH of MgAl-CO<sub>3</sub><sup>2-</sup> is around 4, it has a high antipeptic activity, dissolves completely, and intestinal absorption is low. The high anion exchange capacity is utilized by replacing the carbonate with salicylic

acid for use as an anti-inflammatory medication.<sup>20</sup> Isocarbostyryl derivatives used in the treatment of heart disease are stabilized by intercalation into LDHs.<sup>21</sup> Many forms of LDHs are not only non-toxic but can also supply essential nutrients. Iron-containing LDHs are used in treating iron deficiencies.<sup>22</sup> Other uses include ointments and poultices<sup>9</sup> for the protection of damaged skin.

There are a wide variety of applications of LDHs as anion exchangers and adsorbents in the area of environmental remediation. The ion exchange capacity, 2-3meq/g, is similar to that of anion exchange resins, but because of their higher thermal stability, LDHs are used in the treatment of the cooling water in nuclear reactors.<sup>23</sup>  $Mg_3Al-CO_3^{2-}$  can be used to remove low levels of acidic impurities in synthetic lubricant oils and plasticizers that can not be eliminated by traditional adsorbents.<sup>24</sup> MgAl-LDHs have been tested for adsorption of  $Tc^{7+}$  from radioactive wastes.<sup>25</sup> Stereoselective isomer separation can be achieved through anion exchange reactions.<sup>26</sup> Perhaps the most important applications are the adsorption of ecologically undesirable anions from dilute waste streams and of halogens in polyolefin production.<sup>27,28</sup>

Flame retardation, purification, and stabilization of polymers are the main applications of LDHs in the improvement of material properties. Resistance to combustion in polymers is attained through alteration of the degradation or combustion processes by the addition of certain chemicals. LDHs act mainly by dilution and by the generation of non-flammable gases. The thermal decomposition of LDHs creates large amounts of non-flammable  $CO_2$  and  $H_2O$ , reducing the concentration of  $O_2$  at the flame front. The metal oxide products of LDH combustion also act as a diluent, reducing the concentration of combustible material.

The greatest number of LDH patents in recent years have been for the purification and stabilization of polymers. An LDH will adsorb HCl produced

as vinyl chlorides degradation by heat or UV light, thus protecting them from further degradation.<sup>28</sup>

Another materials improvement applications is compression mouldability. LDHs are more compressible than the standard microcrystalline cellulose, capping does not occur and the flaky crystals are oriented, producing product with good luster. One to two tons of pressure/cm<sup>2</sup> will form a 1 mm thick transparent plate which can be used in agricultural films.<sup>29</sup>

When added in small amounts LDHs can improve the flexibility and mouldability of a material. This is useful in producing molded heat resistant insulation parts such as switchboards, capacitors and insulation wires.<sup>30</sup>

Additional materials applications include:

1. Spacer sheets in electrolytic capacitors<sup>31</sup>
2. Corrosion inhibitors in paints and coatings<sup>32</sup>
3. Protection against bacterial corrosion<sup>33</sup>

Perhaps the largest area of industrial applications for LDHs is in catalysis. There are two approaches to using LDHs as catalysts. The first concentrates on the framework cations. Mixed metals oxides produced by calcining LDHs at 500 °C, form a large group of industrial catalysts.<sup>9</sup> Very recently, MgAl-LDHs have been used as co-catalysts in the oxidation of alkenes to epoxides. The basicity of the LDH aids in oxygen transfer and increases product selectivity.<sup>34</sup> The second approach concentrates on the intercalated anion. Many catalytic species are anionic, and intercalation into LDHs can prevent catalyst degradation, control access to the catalysts or transform a homogeneous catalyst to a heterogeneous catalyst. Catalyst degradation can occur through different routes. Loss of ligands can occur in many

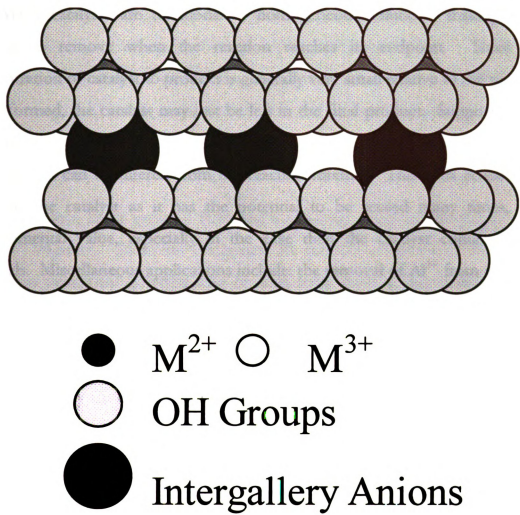


Figure 2-1. A schematic of a 3:1  $M^{2+}/M^{3+}$  Layered Double Hydroxide

organometallic catalysts as the organic ligands are oxidized. Cannibalism can occur when the catalyst reacts with itself to form an inactive species

Many catalysts are functional in homogeneous solutions, making them difficult to remove when the reaction reaches its endpoint. Since the concentration of catalyst to product is generally very small relative to the product being formed, the catalyst may just be left in the final product. Supporting the catalyst by intercalating it into an LDH transforms it into a heterogeneous catalysts that can be filtered from the reaction mixture. This adds economical value to the catalyst as it has the potential to be reused many times, and environmental value, especially in the case then the catalyst contains toxic materials. Miscellaneous applications include: the removal of  $\text{Al}^{3+}$  from recovery systems of a closed kraft pulp mill,<sup>35</sup> novel conducting materials,<sup>36</sup> and clay-modified electrodes.<sup>37</sup>

Recent research efforts into applications for LDHs include phenol hydroxylation by Cu containing LDHs,<sup>38</sup> LDHs as molecular containers for the preparation of microporous carbons,<sup>39</sup> clay modified electrodes,<sup>40</sup> and as photochromic sensors,<sup>41</sup> Myristate intercalated LiAl-LDH membranes can partition styrene from a methanol/water solution.<sup>42</sup> Heating MgAl-dodecylsulfate resulted in the formation of  $\text{C}_{60}$  between the layers indicating that LDHs are useful in the preparation of new materials.<sup>43</sup> The interaction of  $\text{TiO}_x$  with LDH-porphyrins results in a catalyst for the photodegradation of pollutants.<sup>44</sup>

## Structure

The most detailed investigations into the structure of LDHs were done by Allmann<sup>45</sup> and Taylor.<sup>46</sup> The main characteristics are the brucite-like sheets, the

positions of interlayer anions and water, and the type of stacking. The layers are composed of infinite sheets of edge sharing  $M^{2+}$  and  $M^{3+}$  octahedra with 6-fold coordination to  $OH^-$  (Figure 1). The interlayer domains are in a quasiliquid<sup>47</sup> state with the anions solvated by one or two layers of water.

The divalent and trivalent cations randomly occupy the octahedral holes in the close packed configuration of  $OH^-$  ions. The interlayer anions and water are free to move by breaking and reforming hydrogen bonds with the layer  $OH^-$ .

LDHs consist of two polytypes,<sup>48</sup> a 3-layer polytype with rhombohedral crystal structure, space group =  $R\bar{3}m$  and a two-layer hexagonal polytype, space group =  $P6_3mmc$ . These are designated 3R and 2H, respectively. In natural LDHs the hexagonal polytype may be high temp form of the rhombohedral. The d spacing,  $c = 23.4 \text{ \AA}$ , is 3 times the first order peak for a 3R LDH, where  $c' = 7.80 \text{ \AA}$ . The hexagonal lattice parameters for  $Mg_3Al-CO_3^{2-}$  in the  $a,b$  plane are  $3.06 \text{ \AA}$ , the average distance between neighboring metal cations in the hydroxide bilayer. The cation distances are unaffected by the polytype.

As stated in the previous section, the  $M^{2+}/M^{3+}$  ratio varies continuously, and integer values of the stoichiometric coefficients are favorable for the appearance of superstructure, ex. for  $M^{2+}/M^{3+} = 2:1$ ,  $a = a_0\sqrt{3}$ ; for  $M^{2+}/M^{3+} = 3:1$ ,  $a = 2a_0$ . A superstructure has only been detected in the case of  $Mg_2Al$ -LDHs, verifying the random distribution of the cations.

Heterostructures with regularly alternating interlayer anions, have been seen when both  $CO_3^{2-}$  and  $SO_4^{2-}$  are intercalated into an LDH. The d spacing is the sum of the two layer heights with a total d spacing of  $16.5 \text{ \AA}$  ( $7.6 \text{ \AA} + 8.9 \text{ \AA}$ ).<sup>49</sup>

## Composition

Anionic clays are two-dimensional solid bases composed of positively charged sheets of di- and trivalent metal hydroxides with shared octahedral edges and contain intergallery anions and water.<sup>9</sup> The parent material is brucite  $\text{Mg}(\text{OH})_2$  composed of neutral layers held together by H-bonding and Van der Waals interactions. Substitution by a trivalent anion such as  $\text{Al}^{3+}$  results in a net positive charge compensated by solvated anions in the interlayers with a general formula of  $\text{M}^{2+}_{(1-x)}\text{M}^{3+}_x(\text{OH})_2\text{A}^{n-}_{x/n}m\text{H}_2\text{O}$ . (Figure 1) The ratio of  $\text{M}^{2+}/\text{M}^{3+}$  ranges from approximately 4 to 2, which translates into an x value of 0.20 to 0.33.

The divalent cations can be  $\text{Mg}^{2+}$ ,  $\text{Zn}^{2+}$ ,  $\text{Ni}^{2+}$ , or any divalent cation with a radius less than that of  $\text{Ba}^{2+}$ . The charge is introduced into the layers by fractional substitution of  $\text{M}^{2+}$  with a trivalent cation such as  $\text{Al}^{3+}$ ,  $\text{Cr}^{3+}$ , or  $\text{Fe}^{3+}$ . The layer charge, while quite high when compared to cationic clays, is easily manipulated by controlling the  $\text{M}^{2+}/\text{M}^{3+}$  ratio. Although the charge balancing anion,  $\text{A}^{n-}$ , can be almost any negatively charged species, multiply charged anions such as carbonate are preferentially intercalated.<sup>50</sup> The intergallery anions are solvated by water molecules. The number of water molecules (m) varies with x, n, and the size of the anion.<sup>51</sup>

### The Nature of $\text{M}^{n+}$

A list of the cation combinations used in to synthesis LDHs is shown in Table 1. Cations with an ionic radius in the range of 0.50-0.74 Å allows them to fit in the  $\text{O}_h$  holes of close packed  $\text{OH}^-$  groups. Ions such as  $\text{Be}^{2+}$  (0.59 Å) are too small, and  $\text{Ba}^{2+}$  (1.35 Å) is too large to occupy an  $\text{O}_h$  position without lattice distortion. For bigger cations such as  $\text{Ca}^{2+}$  (0.98 Å) and

Table 2-1. Different Metals Used in the Synthesis of Layered Double Hydroxides

MgAl <sup>a</sup>	CuZnAl	CuZnCr
CuAl	ZnCr	CoAl
MgAl	ZnAL	LiAl
NiAl	CuCoAl	CuCoCr
MnAl	MgCr	MgAlV <sup>52</sup>
NiAl	FeAl	
NiMgAl	CuCoZnAl	

a. From references 9 and 10, unless otherwise annotated

$\text{Cd}^{2+}$  (0.97 Å), the octahedral environment becomes unstable. While  $\text{Ca}^{2+}$  and  $\text{Cd}^{2+}$  are borderline, LDHs have been synthesized from these metals.<sup>53,54</sup> All trivalent anions from 0.5 to 0.8 Å form LDHs, though  $\text{V}^{3+}$  and  $\text{Ti}^{3+}$  are not air stable. In addition, LDHs with more than 2 cations are possible.

Copper containing LDHs can only be made when another  $\text{M}^{2+}$  is present in the greater concentration. When the  $\text{Cu}^{2+}$  cations are separated by another divalent anion, the  $\text{Cu}^{2+}$  forms the undistorted octahedra typical of LDHs. When the  $\text{Cu}^{2+}/\text{M}^{2+}$  ratio is greater than one, adjoining  $\text{Cu}^{2+}$  octahedra can form a copper compound with a Jahn Teller distortion energetically favored over the hydrotalcite structure.

The fractional substitution,  $x$ , ( $x = \text{M}^{3+}/(\text{M}^{2+} + \text{M}^{3+})$ ) can range from 0.5 to 0.167, but pure phases appear only in the range of 0.33 to 0.2 and the 0.2 value has been disputed. Another way of expressing the amount of substitution by  $\text{M}^{3+}$  is the  $\text{M}^{2+}/\text{M}^{3+}$  ratio. Therefore, when  $x = 0.33$ ,  $\text{M}^{2+}/\text{M}^{3+} = 2$ ; when  $x = 0.2$ ,  $\text{M}^{2+}/\text{M}^{3+} = 5$ . The theoretical maximum limit  $\text{M}^{3+}$  substitution is  $\text{M}^{2+}/\text{M}^{3+} = 2$ . If the substitution by  $\text{M}^{3+}$  were greater, there would be positive charges in adjacent octahedra. When  $\text{M}^{2+}/\text{M}^{3+} = 5$ , the high density of divalent cations leads to the formation of brucite-like  $\text{M}(\text{OH})_2$ .

There is a statistical distribution of trivalent cation substitution in LDHs. This random occupation of all octahedral sites allows the  $\text{M}^{2+}/\text{M}^{3+}$  ratio to vary continuously throughout the allowable range of  $x$ . The ratio of  $\text{M}^{2+}/\text{M}^{3+}$  added to the reaction is the ratio found in the final LDH product, although this is somewhat dependent on the synthetic method. This ratio can be easily verified by the size of the unit parameter  $a$ , which is not affected by intergallery anion. LDHs adhere to Vegard's law which states that increasing substitution by a

smaller anion will cause a proportional decrease in the size of the unit cell. The in-plane parameters,  $a=b$ , have been indexed with hexagonal axes. In an ideal structure,  $a=2^{1/2}r_{(M-O)}$  where  $r$  = the distance between the  $M^{2+}$  and O centers. For brucite, where  $x = 0$ , this is equal to 3.15. In an LDH,  $r_{(M-O)}$  is replaced with the mean ionic radius,  $z$ , where  $z = [(1-x)r_{M^{2+}} + x(r_{M^{3+}})]$ . Therefore,  $a=2^{1/2}z$ . Since  $a \propto x$ , they can be plotted to form a line with a slope of  $-2^{1/2}[r_{M^{2+}} - (r_{M^{3+}})]$ . This is valid within the range of  $x = 0.2$  and  $0.33$ . Miyata<sup>55</sup> observed an increase in  $a$  when  $x < 0.2$ , but in addition to the LDH, brucite and hydromagnesite were observable by XRD. Above  $x = 0.33$ ,  $a$  becomes constant. Pausch<sup>56</sup> claims that LDHs with  $x = 0.44$  is possible for MgAl LDHs and that the constancy of  $a$  is due to the  $Al^{3+}$ - $Al^{3+}$  repulsion balancing the decrease in  $z$ .

In addition to the most common  $M^{2+}/M^{3+}$  LDH, other combinations of metal cations are possible. The  $M^{1+}/M^{3+}$  combination of LiAl-LDH has been extensively studied and there have been reports of  $M^{2+}/M^{4+}$  combinations of Co and Ti.

### **The Nature of $A^n$**

The anion exchange properties are one of the more spectacular characteristics of LHDs. There is almost no limit to the nature of  $A^n$  and exchange reactions are extremely simple. The sample to be exchanged is maintained in an aqueous solution of anion to be inserted. The only problems are contamination by carbonate and forming pure crystalline material. It is generally assumed that the interlayer anions are present in the precise amount to attain charge neutrality, but there are exceptions. Hansen and Koch<sup>57</sup> have found a charge imbalance ranging between +0.77 and -1.09 eq per formula unit in MgFe-LHDs. The charge imbalance depended linearly on  $x$  and was attributed to the amphoteric properties of the hydroxyl groups.

Powder X-ray diffraction and infrared spectroscopy are the two main methods used study anion exchange reactions in most LDH- $A^{n-}$  systems. Infrared spectroscopy is often used to verify the presence of the intercalated anion and powder X-ray diffraction is used to track the change in layer spacing caused by the exchange reaction. The diffraction pattern can lend insight into the number, size, and orientation of the anions as well as the strength of the bonds between  $A^{n-}$  and the  $\text{OH}^-$  groups of the LDH layer.

The anion affects the thickness of interlayer regions in two ways. The greatest effect on the layer separation (the d spacing minus 4.8 Å, the thickness of a brucite layer) is the physical size of the anion. For example, the d spacing for an LDH intercalated with  $\text{F}^-$  is 7.51 Å and for  $n\text{-C}_{18}\text{H}_{37}\text{SO}_4^-$  it is 32.6 Å.<sup>58</sup> Similarly, the d spacing increases linearly with the chain length of an organic acid and with the ionic radius of halogens.

The orientation of the intergallery anion also has an effect on the layer spacing. When  $a\text{-P}_2\text{W}_{18}\text{O}_{62}^{6-}$  is intercalated into an LDH with the  $D_{3h}$  axis perpendicular to the layers the d spacing is 2.1 Å greater than when the  $D_{3h}$  axis is parallel to the layers.<sup>59</sup> The same argument has been put forth for the differences in d spacing between  $\text{SO}_4^{2-}$  and  $\text{ClO}_4^-$ .

These isostructural anions have a difference in d spacing of 0.3 Å when intercalated into LDHs (see Table 2-2). Tetrahedral  $\text{XO}_4^{n-}$  anions can have at least two orientations with respect to the LDH layers. An orientation with one apical oxygen pointing to one hydroxyl plane and the other three pointing to the adjacent hydroxyl plane. This orientation corresponds to the larger d spacing and would allow more of the monovalent  $\text{ClO}_4^-$  anions to be intercalated. Another orientation would have two oxygens coordinating to the opposite hydroxyl planes and two in the interlayer region. This corresponds to the minimum layer separation and could be adopted by  $\text{SO}_4^{2-}$ . However, Bish<sup>60</sup>

**Table 2-2 Inorganic Anions That Have Been Intercalated Into Layered Double Hydroxides**

Anion	LDH Framework	d spacing/Å	Ref
OH <sup>-</sup>	MgAl	7.55	
CO <sub>3</sub> <sup>2-</sup>	MgAl	7.65	
F <sup>-</sup>	MgAl	7.66	
Cl <sup>-</sup>	MgAl	7.86	
Br <sup>-</sup>	MgAl	7.95	
I <sup>-</sup>	MgAl	8.16	
NO <sub>3</sub> <sup>-</sup>	MgAl	8.79	
SO <sub>4</sub> <sup>2-</sup>	MgAl	8.9	
ClO <sub>4</sub> <sup>-</sup>	MgAl	9.2	
IO <sub>3</sub> <sup>-</sup>			
S <sub>2</sub> O <sub>3</sub> <sup>2-</sup>			
WO <sub>4</sub> <sup>2-</sup>			
CrO <sub>4</sub> <sup>2-</sup>			
Fe(CN) <sub>6</sub> <sup>3-,4</sup>			61
SiO(OH) <sub>3</sub> <sup>-</sup>			
Ru(BPs) <sup>3+,b</sup>	MgAl		62
TcO <sub>4</sub> <sup>2-</sup>	MgAl		25
ReO <sub>4</sub> <sup>2-</sup>	“	“	“
SP <sup>c</sup>	MgAl	17.7	63
PTS <sup>d</sup>	“	“	“
IC <sup>e</sup>	MgAl	17-22	81
NC <sup>f</sup>	“	“	

a. From Cavani et. al<sup>9</sup> and references within, unless otherwise noted.

b. BPS = 4,7-diphenyl-1,10-phenanthrolinedisulphonate

c. SP = sulphonated indolinespirobenzopyran

d. PTS = p-toluenesulfonate

e. IC = disodium 2-(1,3-dihydro-3-oxo-5-sulpho-2H-indol-2-ylidene)-2,3-dihydro-3-oxo-1H-indole-5-sulphonate

f. trisodium 7-hydroxy-8-[(4-sulpho-1-naphthalenyl)azo]-1,3-naphthalene disulphonate

states this orientation would destroy the rhombohedral symmetry and Miyata<sup>64</sup> attributes the difference in d spacing to the greater electrostatic attraction between the OH<sup>-</sup> and the divalent SO<sub>4</sub><sup>2-</sup> as opposed to monovalent ClO<sub>4</sub><sup>-</sup>. This is the second way the anion can affect the d spacing of an LDH, through the strength of the electrostatic interactions between the anion and the layers.

In addition to the great number of inorganic anions which can be intercalated into LDHs, there are an impressive number of organic anions that have been intercalated into LDHs (Table 2-2). In many way, the behavior of LDH-organics mirrors that of cationic clays. Layered double hydroxides intercalated with alkyl sulfates and alkyl sulphonates undergo substantial swelling in n-alkylalcohols or n-alkylamines.<sup>58</sup> Dodecylsulfate intercalated into NiAl-, MgAl-, or ZnCr-LDHs can take on three packing arrangements. The shortest interlayer spacing, 26 Å correlates to a perpendicular monolayer. The intermediate d spacing, 36 Å was attributed to a bilayer with a tilt of approximately 40 ° or an interleaving vertical bilayer. The largest d spacing, 47 Å was consistent with a vertical bilayer of dodecylsulfate.<sup>65</sup> The most thoroughly studied organic intercalates have been terephthalate (TA) and benzoate. These studies demonstrate the balance of forces that determine the interlayer arrangement of anions. In a 2:1 MgAl-TA, the gallery height was 9.2-9.6 Å (the physical length of TA = 9.9 Å). The d spacing of MgAl-benzoate was 15.2-15.5 Å (benzoate = 8.8) which is proposed to be a bilayer with a tilt angle of 35 °. The d spacing was the same for TA and benzoate in a 3:1 MgAl-LDH before drying. But when the 3:1 MgAl-LDHs were dried at 60 °C, both TA and benzoate oriented with the long axis parallel to the layers. The gallery height of 3.5 Å is the thickness of a benzene ring. The change in orientation was reversible for repeated cycles of rehydration and drying. The ability of

**Table 2-3. Organic Anions That Have Been Intercalated Into Layered Double Hydroxides**

Anion	LDH Framework	d spacing/Å	Synthesis	Ref.
$C_nH_{2n}(CO_2)_2$ n=0-8	ZnAl	9.4-18 <sup>a</sup>	Exchange	66
alkyl sulfate	ZnCr		Exchange	67
aromatic			Exchange	68
diphosphonates				
b-cyclodextrin	MgAl		Exchange	69
	MgAl		Rehydration	70
	MgAl		Rehydration <sup>b</sup>	71
naphthalenecarboxylate			Rehydration	72
Co(II)phthalocyanine			Rehydration	73
tetrasulfonate				
sebacate	MgAl		Thermal exchange	74
caprate,			Thermal exchange	75
phenylphosphate				
terephthalate	MgAl	14.6	Coprecipitation	76
benzoate		15.2		36
$C_nH_{2n+1}SO_4^-$	ZnCr	21.1-32.6 <sup>a</sup>		77
naphthalenedisulfonate	ZnAl			78
9,10-anthrquinone-2,6-disulfonate	MgAl	12, 19 <sup>c</sup>	Coprecipitation	79
BHMBS <sup>d</sup>	ZnAl		Exchange	80
TSPP <sup>e</sup>	MgAl	22.4	Exchange	81
phosphonates	MgAl, CdAl		Exchange	68, 82
organo polymers	MgAl, CaAl		Exchange	
$Ru(BPS)_3^+$	MgAl	22	anion exchange	62

- The d spacing increases linearly with the aliphatic chain length.
- Glycerol was added as a swelling agent
- D spacing was found to be dependent on the orientation of the 9,10-anthrquinone-2,6-disulfonate gallery anion
- 5-benzoyl-4-hydroxy-2-methoxybenzenesulfonate 5,10,15,20-tetra(4-sulfonatophenyl) porphyrine

water to stabilize the vertical packing for 3:1 MgAl-LDH emphasizes the importance of the hydrophobic/hydrophilic interactions

### The interlayer water

There are two types of water associated with LDHs, interlamellar (intrinsic) water and surface sorbed (extrinsic) water. Recent  $^1\text{H}$  NMR studies have shown that in  $\text{MgAl-CO}_3^{2-}$  LDHs, the interlayer water is freely spinning with its  $\text{C}_2$  axis perpendicular to the LDH layers.<sup>83</sup> The number of water molecules ( $m$ ) varies with layer charge, anion charge and size and temperature and humidity. A formula by Miyata used to calculate the maximum amount of water illustrates the above relationships;

$$m=1-Nx/n$$

in terms of  $\text{M}^{2+}_{(1-x)}\text{M}^{3+}_x(\text{OH})_2\text{A}^{n-}_{x/n}m\text{H}_2\text{O}$ , where  $N$  is the number of sites occupied by the anion,  $x = \text{M}^{3+}/(\text{M}^{2+}+\text{M}^{3+})$ , and  $n$  is the charge on the anion.

When  $N$  increases, the number of sites in the close packed configuration of oxygen atoms that decreases, leaving fewer sites for occupation by water. The same relationship is true for  $x$ , as  $x$  increases, more charge balancing anions are required. There is a reverse relationship with  $n$ , as the charge on the anion increases, fewer are needed leaving more sites for water. For hydrotalcite,  $\text{Mg}_3\text{Al-CO}_3^{2-}$ ,  $m=1-3(.25)/2$ . In this case  $m = 0.625$  or  $\text{Mg}_6\text{Al}_2(\text{OH})_{16}\text{CO}_3\cdot 5\text{H}_2\text{O}$ , which is higher than the measured value of  $m=4$ .

The amount of water is measured by thermogravimetric analysis as measured by weight loss with increasing temperature. The weight loss is reversible at low temperatures, but at 60-80 °C, it becomes irreversible. A similar effect is seen in  $\text{LDH-SO}_4^{2-}$  and  $-\text{ClO}_4^-$ . Both of these LDHs have an reversible

increase in d spacing when placed in an environment with >50% humidity. The d spacing does not change with humidity when anions such as  $\text{CO}_3^{2-}$  or  $\text{NO}_3^-$  are the gallery anion.

**Table 2-4. Change in d spacing with Increasing Humidity**

	Low humidity d spacing/Å	50% humidity d spacing/Å
LDH- $\text{SO}_4^{2-}$	8.9	10.8
LDH- $\text{ClO}_4^-$	9.2	11.7

In addition, an LDH in aqueous suspension will not absorb more than one or two layers of water. This illustrates an important difference between LDHs and traditional cationic clays, LDHs are non-swelling in aqueous solution due to the high layer charge,  $25 \text{ \AA}^2$  /unit charge. An exception to this is seen when the gallery anion is a long chain organic. These LDHs will expand in alcohols and glycols<sup>84</sup> in proportion to the size of the solvent molecule.

In addition to interlayer solvation of the guest anions, there is also water adhering to the surface of LDH crystals. Since this water had been found to effect the proton and ionic conductivity's, acid/base activity, and ion exchange properties, it should be included when considering an LDH intercalated system.

## Synthesis

In addition to being easy to synthesis in the lab, LDHs are truly 'materials by design.' The layer charge, layer cations, and gallery anions are remarkably variable. Still, this does not eliminate the need for a precise chemical foundation in the choice of synthesis conditions. The nature of the final product is very dependent upon the reaction conditions. The choice of the original  $\text{M}^{2+}/\text{M}^{3+}$

composition, precipitation conditions, hydrothermal treatment, type of reagents, aging, washing, drying, calcination, and activation all affect the homogeneity, crystallinity and particle size of the final product. There are a few requirements which are general to any LDH synthesis; the right ratio of cations and anions must be present, the pH domain of anion and LDH must overlap, and the desired anions must be present in higher concentration and have greater affinity for the LDH than any other anions present in the reaction. For many of these reactions, the ratio of  $M^{2+}/M^{3+}$  in the reactants is directly reflected in the product, especially in the range of  $M^{2+}/M^{3+} = 2-4$ . Carbonate from dissolved air must be rigorously excluded, usually by running the reaction under an inert atmosphere, and still cannot be completely excluded. Finally, the anions must have a greater affinity for the LDH than any of the cations. From there, each synthetic method has its own advantages and requirements. However, in all these methods, a small amount of  $CO_3^{2-}$  is present in the gallery, no matter what precautions are taken.

There are three general methods for the synthesis of LDHs which can be loosely defined by the starting reagents: coprecipitation from metal salts, synthesis from metal oxides, and synthesis using a preformed LDH.

### **Precipitation**

Precipitation from metal salts is recognized as the most reliable, reproducible technique and is used in almost all LDH synthesis. The advantages of synthesis by precipitation include the preparation of an LDH with a definite composition, the anion is fixed by the metal salts or in solution, and the crystallinity and particle size are easily controlled. This method is often used to make LDHs precursors for subsequent anion exchange reactions as the crystallinity of the LDH of the original LDH is maintained in subsequent

treatments. In precipitation reactions the structural and physicochemical properties depend on:

1. method of precipitation
2. nature of the reagents
3. temperature
4. presence of impurities
5. aging times
6. washing conditions
7. drying conditions

Precipitation methods are usually done under conditions of supersaturation. Within this general class there are two types of precipitation reactions, coprecipitation and sequential precipitation.

Coprecipitation reactions necessitate aqueous mixtures of  $M^{3+}$  and  $M^{2+}$  at a pH equal to or higher than the one at which the more soluble cation precipitates and can be done at high or low supersaturation. In precipitation reactions done at high supersaturation, a mixed metal solution containing the divalent and trivalent cations is added very quickly to a solution of NaOH or  $NaHCO_3$ . The reaction is generally aged at a temperature of 60-90 °C. The product obtained by coprecipitation at high supersaturation is generally less crystalline than an LDH precipitated at low supersaturation due to the high number of crystallization nuclei.

Coprecipitation at low supersaturation is accomplished by the slow addition of the  $M^{2+}/M^{3+}$  solution with the simultaneous addition of base (KOH, NaOH, or  $NaHCO_3$  if a carbonate LDH is desired) in two dilute streams into a single flask containing a solution of the interlayer anion. This reaction is often done at a constant pH. These products are generally aged at 60-80 °C and result in a more crystalline product than coprecipitation as high supersaturation.

The second type of precipitation reactions are sequential precipitation or the increasing pH method. Here supersaturation can be achieved either by evaporation or more generally by raising the pH. Taylor's induced hydrolysis is an example of sequential precipitation. For example, a solution of  $\text{Al}(\text{NO}_3)_3$  is precipitated at pH 7, then  $\text{Zn}(\text{NO}_3)_2$  is added, maintaining the pH at 6.4 with  $\text{NaOH}_{(\text{aq})}$ . These reactions are an advantage for LDHs containing metals such as Ni which precipitates at a lower pH or preparations with  $\text{Cu}^{2+}$  and  $\text{Zn}^{2+}$  which form several mono and binary compounds.<sup>85</sup> A disadvantage of the sequential precipitation reaction is that often the  $\text{M}^{2+}/\text{M}^{3+}$  ratio added to the reaction is not reflected in the product.

The previously described reactions are all done in aqueous solution. There are a few examples of LDH synthesis done in non-aqueous solvents. In a 1992 patent, Burba et al.<sup>86</sup> reported on the synthesis of layered mixed metal hydroxides from metal alkoxides in organic solvents such as diethylene glycol or methanol. In these examples, a stoichiometric amount of water was added as the source of hydroxide.

Malherbe et al.<sup>87</sup> synthesized layered double hydroxides in a mixture of organic solvent and water in an  $\text{N}_2$  environment. The solvent systems were 50:50 mixtures of water with methanol, ethanol, propanol, acetone or glycols. Their method resulted in microtextural modification of the surface and porous properties of the LDHs.

While precipitation conditions are the most widely used method for attaining a crystalline LDH, they are not always necessary as:

1. aging can rectify improper precipitation
2. sequential precipitation does not occur
3. pure LDH may not be required and synthesis may be followed by thermal treatments and/or ion exchange.

## Salt-Oxide method

Another method for LDH synthesis is called the salt-oxide method.<sup>10</sup> It has also been labeled hydrothermal synthesis, but it becomes hard to differentiate between hydrothermal synthesis and hydrothermal treatments. Here the salt oxide method is defined as a synthetic method where at least one of the cations is present as a solid in the reaction. These reactions can range from high temperature, high pressure reactions to reactions done under ambient conditions. Reactions at temperatures above 273 °C are done in an autoclave or in a sealed tube under pressure. The first synthesis of an LDH from a mechanical mixture of MgO and Al<sub>2</sub>O<sub>3</sub> was reported by Roy et al.<sup>88</sup> in 1988. The mixtures were autoclaved under CO<sub>2</sub>, at a temperatures to 325 °C, and pressures to 130 Mpa. The product was a mixture of LDH, magnesite and hydromagnesite. Synthesis at higher temperatures resulted in the decomposition of the LDH.

Thermal methods for LDH synthesis generally consist of calcining metal oxides at temperatures under 600 °C and pressures from 13 to 130 Mpa under water vapor and CO<sub>2</sub>. The LDH forms very slowly, and the reaction is typically incomplete.

The final methods for the synthesis of an LDH-A<sup>n</sup> are those that begin with a preformed LDH. Most of these synthetic methods can be typed as anion exchange or structure reconstruction. Anion exchange reactions can be accomplished through several routes including: exchange of an easily replaced anion such as OH<sup>-</sup> or NO<sub>3</sub><sup>-</sup>,<sup>9</sup> synthesis of an LDH with a large anion and exchanging with a metalate anion,<sup>76</sup> and swelling the LDH layers with glycols prior to the anion exchange reaction.<sup>89</sup>

Anion exchange reactions of LDHs are very easy considering the high layer charge. Mica, one of the most highly charged silicate clays, is a poor cation

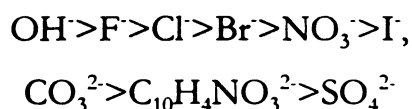
exchanger. LDHs do not delaminate in solution like clays, so the exchange reactions are topotactic. The first mention of the anion exchange properties of LDHs was in 1973, where the selectivity coefficients for  $\text{NO}_3^-$ ,  $\text{ClO}_4^-$ ,  $\text{Cl}^-$ ,  $\text{CH}_3\text{COO}^-$ ,  $\text{CO}_3^{2-}$ ,  $\text{CrO}_4^{2-}$ , and  $\text{SO}_4^{2-}$  were given.<sup>50</sup> In 1977, Bish and Brindley<sup>90</sup> found that the basic LDH structure of takovite treated with HCl was not destroyed. The only change was in the d spacing which had expanded to accommodate the intercalation of  $\text{Cl}^-$  anions. Since these initial experiments, LDH exchange reactions have become a very important method for synthesizing the desired LDH- $\text{A}^n$  system and much research has been done on optimizing the exchange reactions.

Many of the requirements of exchange reactions are similar to those of any of the other synthetic methods:

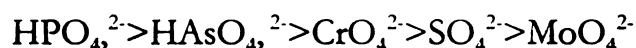
1. matching the anionic charge density with the charge density of the layers
2. matching the acid/base characters of anions and host structure
3. matching the redox characters of anions and host structure
4. insuring hydrophilic or hydrophobic sites for organic anions
5. the absence of too high energetic barrier in the case of anion exchange reactions.<sup>10</sup>

Clearfield<sup>91</sup> stated that thermodynamically, anion exchange reactions of LDHs depend on the electrostatic interactions between positively charged sheets and exchanging ions and to a lesser extent on the free energy of hydration. In addition, the equilibrium constant increases as ionic radius decreases, favoring exchange ions with a high charge density.

Selectivity series for anion intercalation have been determined for several anionic species. Miyata<sup>92</sup> in 1983 found the selectivities for the following monovalent and divalent anions:



Miyata's results were verified by Yamaoka<sup>93</sup> who added these divalent anions:



Exchange reactions can be facilitated by running the reaction at a pH where the anion to be exchanged is protonated. In Drezdson's method for intercalating isopolyoxometalates via exchange with terephthalic acid, the exchange reaction is done at pH = 4.4 where the terephthalate is protonated. Exchange of carboxylate anions into a LDH-CO<sub>3</sub><sup>2-</sup> should be done at pH 4-6, in order to protonate the carbonate and expel it in favor of the exchange anion.

Organics anions can be directly exchanged from inorganics. For example, LDH nitrates have been successfully exchanged with n-C<sub>m</sub>H<sub>2m+1</sub>SO<sub>4</sub><sup>2-</sup>, n=8,12,14,16,18<sup>94</sup> or 5,10,15,20-tetra sulphonato phenyl porphyrin.

A relatively new method for preparing LDH-organics has been developed by Carlino and Hudson.<sup>74</sup> A mixture of sebacic acid and preformed MgAl-CO<sub>3</sub><sup>2-</sup> is heated to 20-30 °C above the melting point of the acid. This method has also been used to intercalate caprate<sup>95</sup> and phenylphosphonate, although the reaction is not complete

The final LDH synthesis method takes advantage of the memory effect of LDHs calcined at 450-500 °C. At these temperatures the LDH loses its hydroxyl groups to form mixed metal oxides solid solution. While the crystalline structure is lost, as evidenced by the X-ray diffraction pattern, scanning electron micrographs showed that calcination does not change the morphology, nor was there exfoliation of the layer structure.<sup>96</sup> When the solid solution is placed in water, it rehydrates and combines with anions to reform an LDH. This reaction

is so favorable that a synthetic meixnerite ( $\text{MgAl-OH}^-$ ) will form in the absence of any other anion.

Thermal/anion exchange methods recently developed by Chibwe and Jones<sup>97</sup> begins with the synthesis of a highly crystalline LDH formed by a controlled pH at low supersaturation. The product is then calcined under  $\text{N}_2$  at  $500^\circ\text{C}$  to form the mixed metal oxides. The metal oxides are added to degassed water where the LDH restructures with  $\text{OH}^-$  as the interstitial anions. These are easily replaced with the desired organic or inorganic anion in a subsequent anion exchange reaction.

### **Thermal Treatments**

Aging or digestion is generally done at a relatively low temp  $<100^\circ\text{C}$  for a period of 18 hours to seven days. The time for aging is dependent on the gallery anion, for example an  $\text{LDH-NO}_3^-$  needs a longer aging time than  $\text{CO}_3^{2-}$ .

### **Physicochemical Characterization**

Characterization of LDHs is done by X-ray diffraction (XRD), Fourier transform infrared spectroscopy (FTIR), thermogravimetric analysis (TGA), Inductively Coupled Plasma (ICP), scanning electron microscopy (SEM), and RAMAN spectroscopy.

#### **XRD**

Single crystal analysis of LDHs has been possible with only a few materials making powder X-ray analysis the main analytical technique for layered double hydroxides with the presence of both sharp basal peaks and diffuse in plane peaks. The general features of LDHs are intense sharp basal (00l) peaks at low

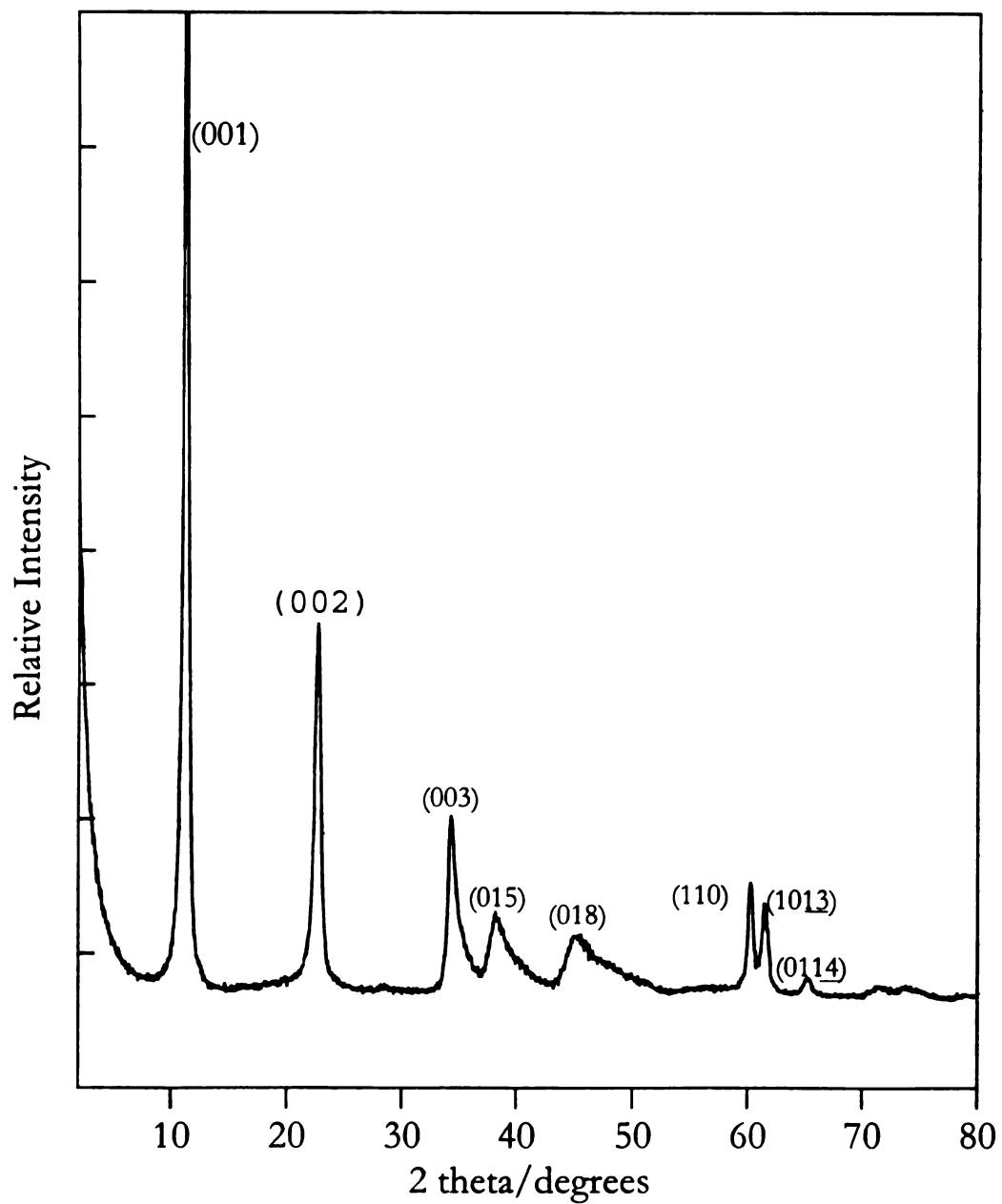


Figure 2-2. X-ray diffraction pattern of a  $\text{Mg}_3\text{Al-NO}_3^-$  double hydroxide showing Miller indices.

$2\sigma$ , corresponding to successive orders of reflection of the layer spacing. At higher  $2\sigma$ , the less intense, asymmetric inplane are evident (Figure 2-2). Turbostratic disordering can make the inplane reflections quite broad.

Poor crystallinity, disorder, and the inherent non stoichiometric nature in the layer stacking of LDHs can lead to broad, asymmetric diffraction lines with differing relative intensities. The basal (00 $l$ ) reflections correspond to successive orders of the basal spacing  $c'$ , and can be used in Bragg's Law to calculate the layer distance ( $d$ )

$$d = n\lambda/2 \sin\sigma$$

The basal reflections are designated as the  $c$  axis in LDHs. The (001) reflection in Figure 2-2 is actually the (003) reflection, or  $c'$ . True  $c$  is a multiple of  $c'$ ,  $2c'$  for 2H and  $3c'$  for 3R. The height of LDH layers is known, (in the case of Mg/AL = 4.8 Å) and can be subtracted from the  $d$  spacing to find the gallery height, verifying intercalation of the desired anion. Increasing  $M^{3+}$  substitution will cause a decrease in layer separation, due to both smaller ionic radius of the  $M^{3+}$  valence, and increased electronic attraction caused by the increase in layer charge.

The in plane reflections are indexed on a hexagonal axis, and are independent of layer stacking and dependent only the cationic species and  $x$ . The crystal parameter  $a$  can be calculated from the (110),  $a=2d_{(110)}$  dependent only upon cation,  $x$  and the degree of hydration.

LDH samples for XRD tend to be oriented due to the platy morphology of LDH particles. Orientation will increase the intensity of reflections of the  $c$  axis relative to the in plane reflections. It will also tend to mask the presence of

**Table 2-5. Identifying Wavenumbers for Common Gallery Anions**

Anion	Characteristic wavenumber/cm <sup>-1</sup>	Ref.
CO <sub>3</sub> <sup>2-</sup>	1355	9
NO <sub>3</sub> <sup>-</sup>	1385	98
SO <sub>4</sub> <sup>2-</sup>	1100	
carboxylate	1560, 1400	
carboxylic acid	1700	
Fe(CN) <sub>6</sub> <sup>3-</sup>	2147	99

impurities and so unoriented powder samples should be used when looking at the relative purity of an LDH product.

### *FTIR*

Gallery anions retain much of their IR features after being intercalated into LDHs, so FTIR is useful, not only for the characteristic absorption features of the LDH, but also for verifying retention of the guest structure.

In MgAl-CO<sub>3</sub><sup>2-</sup> LDHs there is a strong adsorption band at 3512-3448 cm<sup>-1</sup> indicating H-bound layer hydroxyl groups. When x=0 (brucite) the OH band is 3700 cm<sup>-1</sup> and increasing Al<sup>3+</sup> substitution causes broadening and a shift to lower frequency. The half width decreases with 2:1 LDH indicating cation ordering. A shoulder at 3000 cm<sup>-1</sup> is caused by H-bonding with the gallery anion. Interstitial water has a bending mode at about 1635 cm<sup>-1</sup>. The identifying band for CO<sub>3</sub><sup>2-</sup> is an ν<sub>3</sub> band at 1350-1380 cm<sup>-1</sup> (1355 cm<sup>-1</sup> in these spectra). A shoulder at 1400 or a doublet at 1399 and 1362 cm<sup>-1</sup> from the splitting of the CO<sub>3</sub><sup>2-</sup> ν<sub>3</sub> suggests a lowering from the ideal D<sub>3h</sub> symmetry for the interlayer anion. In addition, a ν<sub>2</sub> band at 850-880 cm<sup>-1</sup> can be assigned as a vibration of CO<sub>3</sub><sup>2-</sup>. A band at 1624 could be evidence of HCO<sub>3</sub><sup>2-</sup>. Nitrate is distinguishable by a band at 1485 cm<sup>-1</sup> and SO<sub>4</sub><sup>2-</sup> by a band at 1110 cm<sup>-1</sup>

### *TGA*

There are two main features in the thermal behavior of LDHs, both endothermic. The first feature is the loss of surface and interlayer water and the second transition is the loss of hydroxyl groups from the layers and the gallery anions. Many factors affect the two transition states; M<sup>2+</sup>/M<sup>3+</sup> composition and ratio, type of anions, thermal treatments, and aging.

Each transition can have two stages. The first stage in  $\text{Al}^{3+}$  containing LDHs ranges from 97-297° C, with increasing  $\text{Al}^{3+}$  substitution leading to increasing transition temperature. The two stages can be attributed to extrinsic surface water, and intrinsic water in the gallery. Samples with small crystalline dimensions may have large amounts of physisorbed water and the dehydration and dehydroxylation transitions may overlap. The loss of interlayer water is not accompanied by loss of structure, and at low temperatures is reversible<sup>100</sup>

In the second transition state, the two stages correlate to the loss of  $\text{OH}^-$  from  $\text{Al}^{3+}$  and then  $\text{OH}^-$  loss from  $\text{Mg}^{2+}$  and  $\text{CO}_3^{2-}$  in hydrotalcite  $\text{Mg}_6\text{Al}_2(\text{OH})_{12}(\text{CO}_3)_4\text{H}_2\text{O}$ , for example. The temperature at which the loss of  $\text{OH}^-$  and anions occurs is dependent on  $\text{M}^{2+}/\text{M}^{3+}$  ratio, type of anion, low temperature thermal treatment, and in the case of oxidizable elements such as  $\text{Cr}^{3+}$ , the gas used in heat treatment. For example, NiAl-LDHs dehydroxylate at a lower temperature than MgAl-LDHs and Cr containing LDHs at a higher temperature. If calcined below 500 °C, the LDH will regenerate in water even though the XRD pattern shows a change in the structure to that of mixed metal oxides. If calcined above 550 °C the irreversible formation of spinel occurs.

### *ESR*

Electron Spin Resonance has been used to study the decomposition of  $\text{Cu}^{2+}$  containing LDHs.<sup>101</sup>

### *SEM/TEM*

Along with transmission electron microscopy (TEM), scanning electron microscopy (SEM) indicates textural and crystal morphology. TEM can also be used to calculate interlayer distance and compared to the value obtained through XRD.

# SYNTHESIS OF $Mg_2Al$ -LAYERED DOUBLE HYDROXIDES AT ACIDIC PH.

## INTRODUCTION

It is generally accepted that the synthesis of an LDH should be done at a pH where the most soluble  $M(OH)_n$  precipitates.<sup>9</sup> However, there are many exceptions to this rule. A very relevant example is Taylor's<sup>i</sup> induced hydrolysis method of LDH synthesis by sequential precipitation. In this method, a fully hydrolyzed cation causes the rapid hydrolysis of the second cation at 0.2-0.5 pH units below that at which the second cation would normally precipitate. A modified form of Taylor's induced hydrolysis method was used by Kwon<sup>ii</sup> to form pure  $Zn_2Al-NO_3$ . Synthesizing the LDH at pH 6.2 eliminated the byproduct  $Zn_5(OH)_8(NO_3)_2$ , which forms at basic pH.

Obviously there is some uncertainty as to what pH should be used to synthesize a specific LDH. In a 1992 review of LDH, De Roy<sup>10</sup> et al. states, "If one tries to relate individual precipitation pH of metals and the precipitation pH of mixed hydroxides no clear relation appears," (Figure 3-1).<sup>10</sup> For example,  $Al^{3+}$  will form a well ordered  $ZnAl$ -LDH at pH 6.2, while the synthesis of  $ZnCr$ -LDH must be done at a lower pH (4.4-5.5) even though the pH for  $Cr(OH)_3$  formation encompasses that for  $Al(OH)_3$ . (The figure from reference 10 indicates that a well ordered  $ZnAl$ -LDH forms at pH 7-9, but that does not preclude the presence of the Zn impurity which is avoided by synthesis at pH 6.2.).

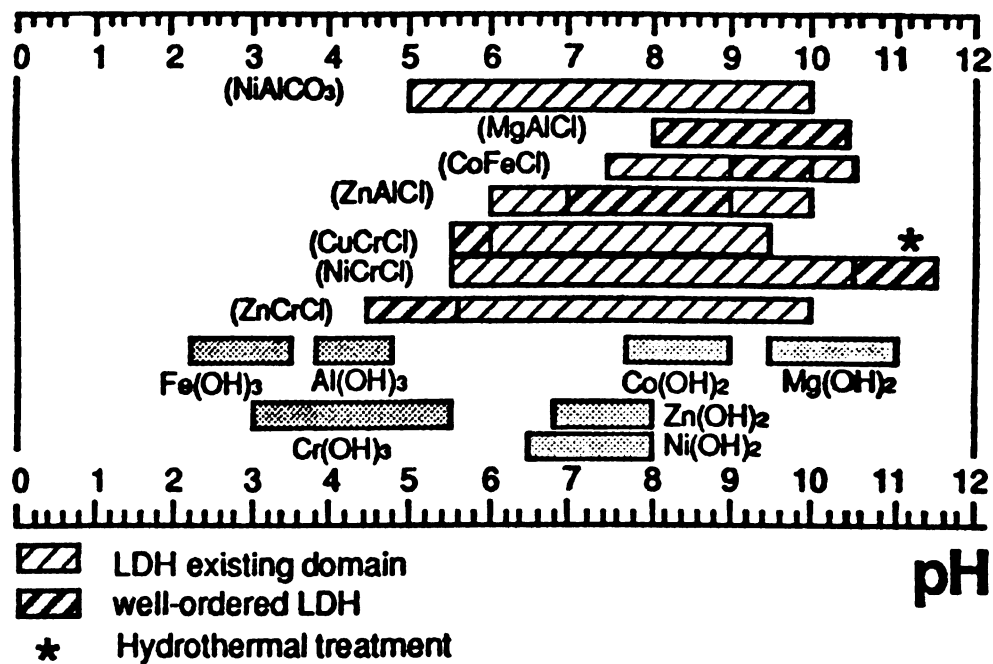


Figure 3-1. Schematic of pH where  $M(OH)_n$  and Layered Double Hydroxides form

One problem encountered with the synthesis a Cr-LDH is the number of oligomeric  $\text{Cr}(\text{OH})_3$  species that form in the pH range 6-10. So the first criteria should be to avoid any pH where undesirable byproducts form. In the case of ZnAl-LDH, this means avoiding a pH greater than 6.4. But how does the pH control the formation of an LDH? The most thoroughly studied LDHs are MgAl-A<sup>n</sup> and these have been synthesized at pH values ranging from 8 to above 12. Even Taylor<sup>17</sup> did not synthesize MgAl-LDHs at a pH lower than 8.

Three fundamental methods for MgAl-LDH synthesis in the pH range of 8 to 12 and above are methods by Miyata,<sup>104</sup> Reichle,<sup>105</sup> and Drezdson.<sup>76</sup> These methods, along with Taylor's induced hydrolysis method for  $\text{Zn}_2\text{Al}$ -LDHs are described in Table 3-1. Miyata's method of coprecipitation at constant pH is the one generally recommended as the easiest method for producing crystalline  $\text{Mg}_x\text{Al}$ -LDH with accurate control of the  $\text{M}^{2+}/\text{M}^{3+}$  ratio. At pH 10, both Mg and Al hydroxides will precipitate as well as the desired LDH product. To insure that the ratio of cations in the final product reflects the ratio of the reactants, very careful pH control is required in order to avoid the formation of  $\text{M}(\text{OH})_2$  and/or  $\text{M}(\text{OH})_3$  byproducts.<sup>11</sup> The advantage of this method is that the digestion step may be very short or completely eliminated.

Reichle's method is coprecipitation at high supersaturation with variable pH. A solution of  $\text{Mg}^{2+}$  and  $\text{Al}^{3+}$  is added rapidly and with good stirring to a solution of sodium hydroxide and sodium carbonate. The amount of the hydroxide should be equal to two times the Mg and three times the Al content in moles. The amount of carbonate should be three times of greater than the stoichiometric amount required to balance the layer charge. While the final pH should be in the range of 8-11, when the mixed metal solution is first added to the caustic solution, the pH is greater than 12. At this point only  $\text{Mg}(\text{OH})_2$  and

**Table 3-1. Three Methods Used to Synthesize MgAl Layered Double Hydroxides**

<b>Method</b>	<b>pH</b>	<b>Precipitates</b>	<b>Method used to prevent <math>\text{CO}_3^{2-}</math> contamination</b>
<b>Miyata</b> <sup>104</sup> coprecipitation at low supersaturation, constant pH	10	$\text{Mg}(\text{OH})_2$ , $\text{Al}(\text{OH})_3$ , $\text{Mg}_x\text{Al-Cl}$ , $\text{NO}_3^-$ , etc.	The reaction is run under $\text{N}_2$
<b>Reichle</b> <sup>105</sup> coprecipitation at high supersaturation, variable pH	8-11	$\text{Mg}(\text{OH})_2$ , $\text{Mg}_x\text{AL-CO}_3^{2-}$ or $\text{Mg}_x\text{Al-OH}^-$	The reaction is run under $\text{N}_2$ in the case of meixnerite
<b>Drezdron</b> <sup>76</sup> coprecipitation at low supersaturation	>12	$\text{Mg}(\text{OH})_2$ , $\text{Mg}_3\text{Al-terephthalate}$	Reaction is run under inert $\text{N}_2$
<b>Taylor</b> <sup>102</sup> sequential precipitation at constant pH	6.2	$\text{Al}(\text{OH})_3$ , $\text{Zn}_2\text{Al-NO}_3^-$	Sparging the reaction with $\text{N}_2$ is will prevent contamination by $\text{CO}_3^{2-}$

$Mg_xAl-CO_3^{2-}$  will form a precipitate, although the pH decreases over the course of the reaction. When 2:1, 3:1, and 4:1 MgAl-LDHs shown in (Figure 3-3) were made, the final pH did not go below 11. A longer digestion period (normally 18 hours at an elevated temperature) is required for this reaction. The powder XRD patterns of 2:1, 3:1, and 4:1 MgAl-LDHs made by Miyata's and Reichle's methods are shown in Figure 3-2 and Figure 3-3, respectively. Except for the 2:1  $Mg_2Al-CO_3^{2-}$ , LDHs synthesized by Miyata's coprecipitation at constant pH did not result in a well ordered product, although other groups have found this to be a very satisfactory method. The key to the synthesis of well ordered LDHs by Miyata's method is careful control of the pH.

The two remaining methods are done at a pH outside of the range 8-11, where both  $Mg(OH)_2$  and  $Al(OH)_3$  precipitate. In Drezdson's coprecipitation at low supersaturation, a mixed metal solution is added to a basic solution of terephthalate (TA). The final pH is above 12 where  $Al^{3+}$  is present as the soluble  $Al(OH)_4^-$ . Again, the only precipitates are  $Mg(OH)_2$  and  $Mg_3Al-TA$ . The reaction is allowed to digest for 18 hr. at 74-75 °C. The  $Mg^{2+}/Al^{3+}$  ratio of the reactants is maintained in the product.

The final method is Taylor's sequential precipitation of  $Zn_2Al-NO_3^-$  performed at a pH = 6.2, where  $Zn(OH)^{2+}$  is soluble. This method demonstrates a method where the pH is below that where the divalent cation precipitates, even though Taylor did not synthesize MgAl-LDHs at a low pH. Using the modified method by Kwon,<sup>103</sup>  $Al(OH)_3$  is precipitated at pH 7, and allowed to digest for one hour. A solution of  $Zn(NO_3)_2$  is added simultaneously with 2 M NaOH, in order to maintain a pH of 6.2. Careful control of the pH is not as essential in this method as the final pH is below the pH where  $Zn(OH)_2$  precipitates. There is a long digestion period, one week at 95 °C, just below the

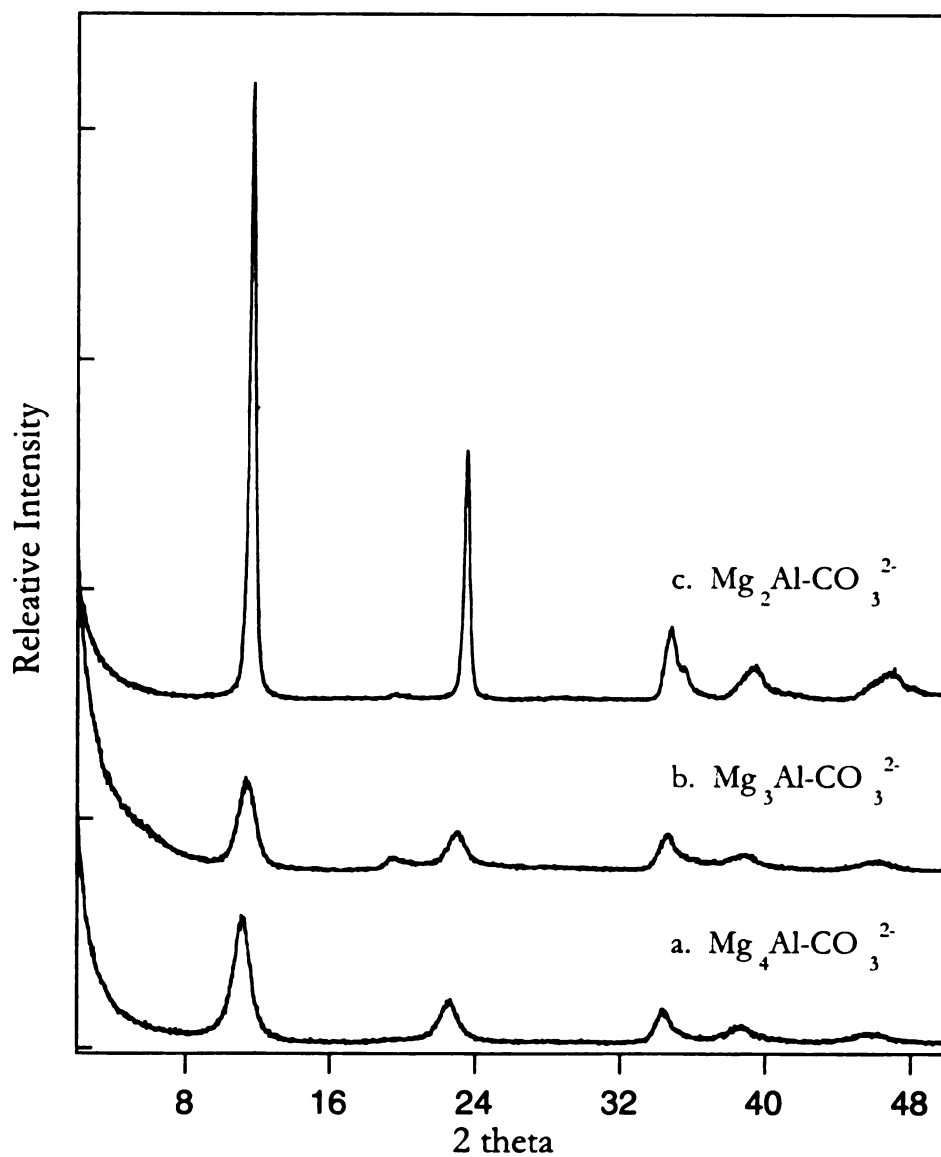


Figure 3-2. X-ray diffraction patterns of MgAl-CO<sub>3</sub><sup>2-</sup> LDHs made by Miyata's coprecipitation at constant pH. The pH is maintained at 10.0 ± 0.2 and the reaction is digested for 18 hours at room temperature. a. Mg/Al = 4; b. Mg/Al = 3; c. MgAl/ = 2;. The peak assignments are given in Table 3-2.

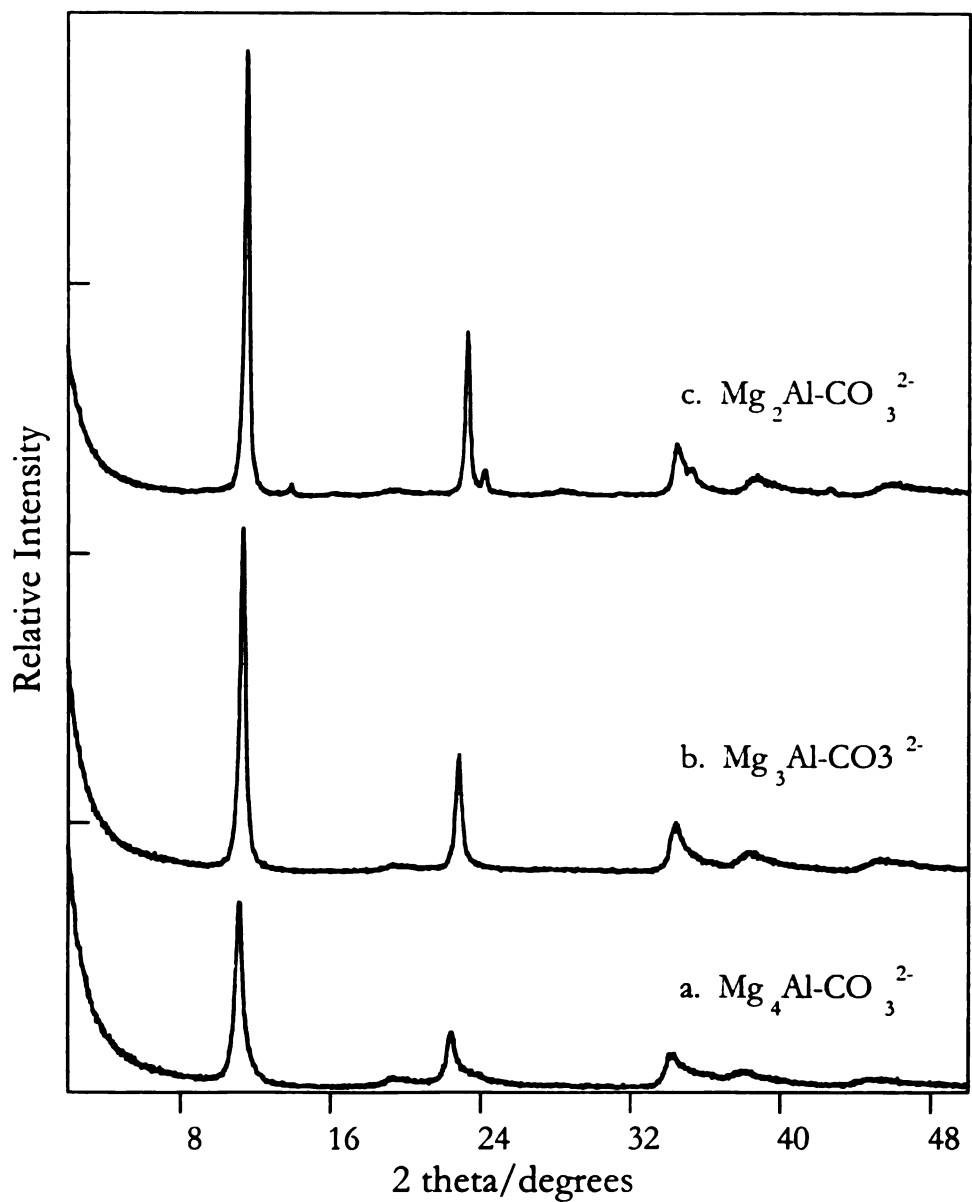


Figure 3-3.  $\text{MgAl-CO}_3^{2-}$  LDHs made by Reichle's coprecipitation at variable pH. The final pH is in the range of 8-11 and the reaction is digested for 18 hours at room temperature. a.  $\text{Mg}/\text{Al} = 4$ ; b.  $\text{Mg}/\text{Al} = 3$ ; c.  $\text{Mg}/\text{Al} = 2$ ; The Miller indices are given in Table 3-2.

**Table 3-2. Indices (*hkl*) for LDHs Synthesized by the Methods of Miyata and Reichle**

Sample	d spacing							
	(001)		(002)		(003)		(015)	(018)
<b>Miyata</b>								
2:1	7.57	4.57	3.78		2.58	2.53	2.28	1.94
3:1	7.79	4.52	3.86		2.59		2.32	1.97
4:1	7.96		3.93		2.61		2.32	1.99
<b>Reichle</b>								
2:1	7.62	6.35	3.81	3.67	2.60	2.54	2.32	1.98
3:1	7.78		3.88		2.59		2.33	1.99
4:1	7.94	4.57	3.96		2.62		2.34	2.02

boiling point of the LDH. The disadvantage of this method is that only a 2:1 ZnAl-NO<sub>3</sub><sup>-</sup> LDHs can be synthesized. No matter what the initial cation ratio is in the reactants, the product ratio is 2:1. The advantage is a very well ordered, large particle LDH. Figure 3-4 shows the transmission electron micrographs of a Mg<sub>3</sub>Al-CO<sub>3</sub><sup>2-</sup> synthesized by Reichle's method. The Zn<sub>2</sub>Al-NO<sub>3</sub><sup>-</sup> in Figure 3-4 is of a much larger particle LDH. Figure 3-4 is a single particle of the Zn<sub>2</sub>Al-LDH at a higher magnification. The large particle size is manifested in an effect called 'streaming,' where the sheer forces of the particles flowing across each other cause a visible opalescent effect in dilute suspensions (approx. 0.01g/ml) of the LDH.

To summarize, it is clear that LDHs can be synthesized at the pH where at least one M(OH)<sub>n</sub> will precipitate. In the middle pH range where both cations precipitate and at higher pH where only the divalent cation precipitates the M<sup>2+</sup>/M<sup>3+</sup> ratio can be made to reflect the ratio of the reactants. This is achieved by careful control of the pH or by a long digestion period, respectively. When the synthesis is done at low pH, where only the trivalent cation precipitates, only a 2:1 M<sup>2+</sup>/M<sup>3+</sup> ratio will result.

Since a well ordered 2:1 Mg<sub>2</sub>Al-LDH can be made at any of the pH ranges in these experiments, it is likely that the 2:1 M<sup>2+</sup>/M<sup>3+</sup> ratio is the most stable ratio. In the middle range, where both cations precipitate, the cation distribution is statistical. In the situations where only one cation precipitates, the driving force would seem to be the removal of charged species from the solution. At pH above 12, both Mg(OH)<sub>2</sub> and LDH are possible, but only the more stable LDH product is expected to be present at equilibrium. As long as the ratio of M<sup>2+</sup>/M<sup>3+</sup> reactants is greater than two, the Mg(OH)<sub>2</sub> will accommodate all the aluminum.

Under low pH conditions, where only the  $M^{3+}$  cation precipitates, the incorporation of the divalent cation will be limited to the stable 2:1 cation ratio. Finally, the minimization of possible byproducts enhances the formation of a pure well ordered LDH.

If these conclusions are valid, it should be possible to synthesize a MgAl-LDH at a pH below 8. The minimum pH for MgAl-LDH synthesis will probably be above that of the ZnAl-LDH and the Mg/Al ratio in the product will be 2, no matter what the ratio of the reactants.

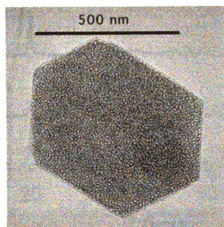
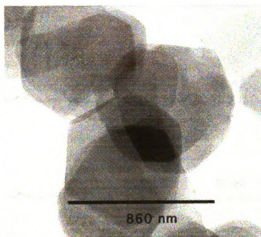
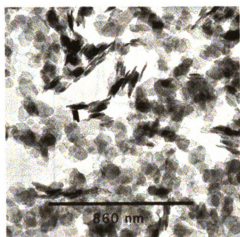
Synthesis of MgAl-LDH at a pH less than 8 would have another advantage; minimal contamination by carbonate. Carbonate is preferentially intercalated into LDHs due to its divalent charge and conformation that matches the LDH. Whatever precautions are taken to eliminate carbonate from the reaction medium, there is always some carbonate present in the product. But at pH 7 and below, the predominate species in solution is monovalent  $HCO_3^-$ . Monovalent bicarbonate should be no more favorable than nitrate for intercalation into LDHs.

The hypothesis is that a  $Mg_2Al$ -LDH can be synthesized at a pH significantly less than 8.4, that the Mg:Al ratio will equal 2 regardless of the initial cation ratio, and that contamination by carbonate will be minimized.

## **Results and Discussion**

The reaction conditions were as follows;  $Mg(NO_3)_2$  (0.03 mol) and  $Al(NO_3)_3$  (0.01 mol) were dissolved in 200 ml water and the temperature was raised to 90-95 °C. The elevated temperature aided in the elimination of dissolved  $CO_2$ . The pH of the reaction mixture was controlled by the addition of predetermined amounts of 2 M NaOH (10-45 ml) to the mixed metal ion

Figure 3-4. a. Transmission Electron Micrograph of  $\text{Mg}_3\text{Al-CO}_3^{2-}$  made by Reichle's coprecipitation method. b. TEM of  $\text{Zn}_2\text{Al-NO}_3^-$  made by Taylor's induced hydrolysis method. The particle size is considerably larger. c. TEM of a single particle of  $\text{Zn}_2\text{Al-NO}_3^-$  at a higher magnification.



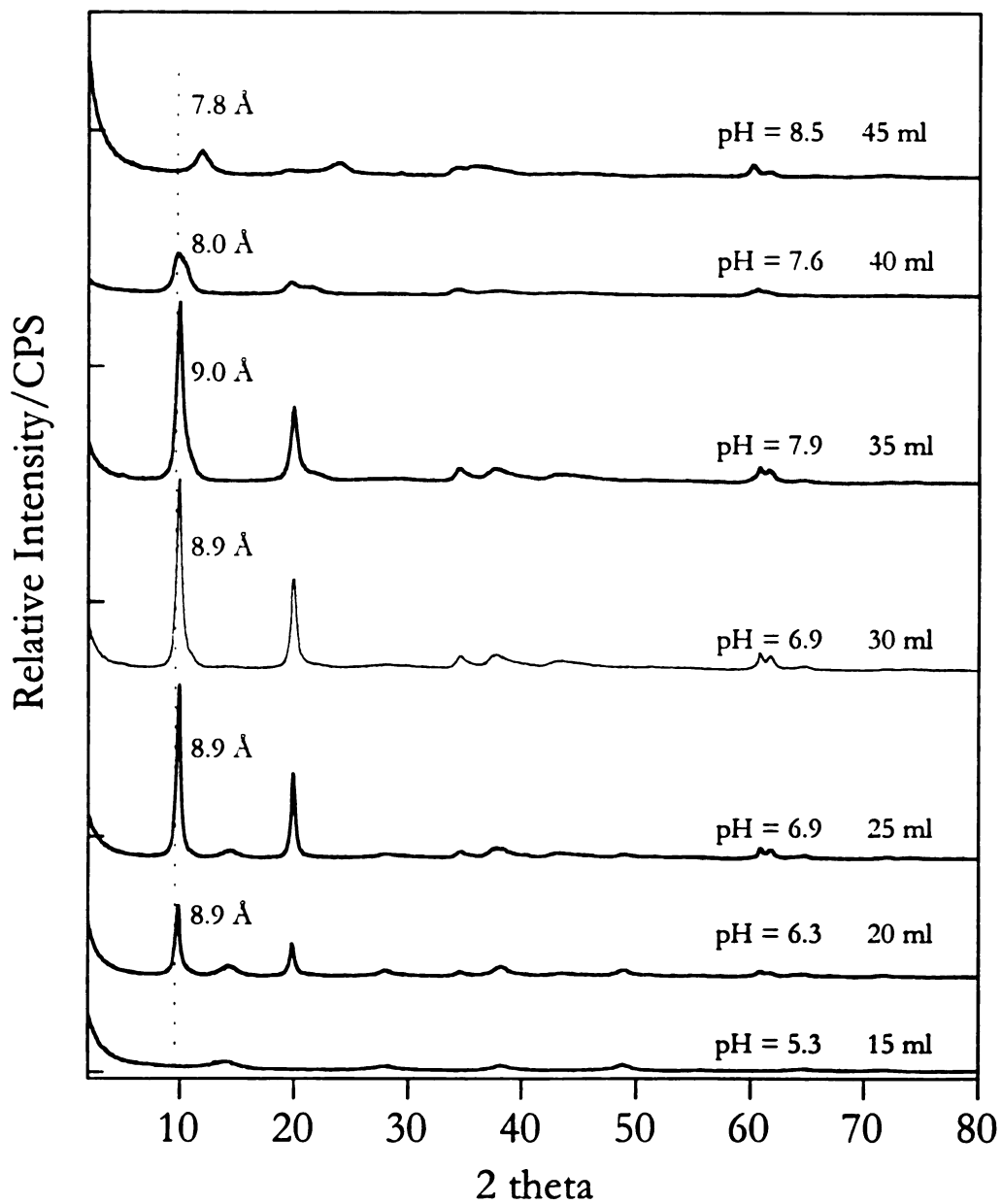


Figure 3-5. The diffraction patterns of products obtained by the reaction of  $\text{Mg}(\text{NO}_3)_2$  (0.03 mol) and  $\text{Al}(\text{NO}_3)_3$  (0.01 mol) in 200 ml  $\text{H}_2\text{O}$  in the presence of various amounts of 2.0 M  $\text{Na}(\text{OH})$ . The volumes of  $\text{NaOH}$  solution added to the reaction mixture are indicated along with the final pH value of the reaction mixture a reaction time of 3 days at 90-95 °C.

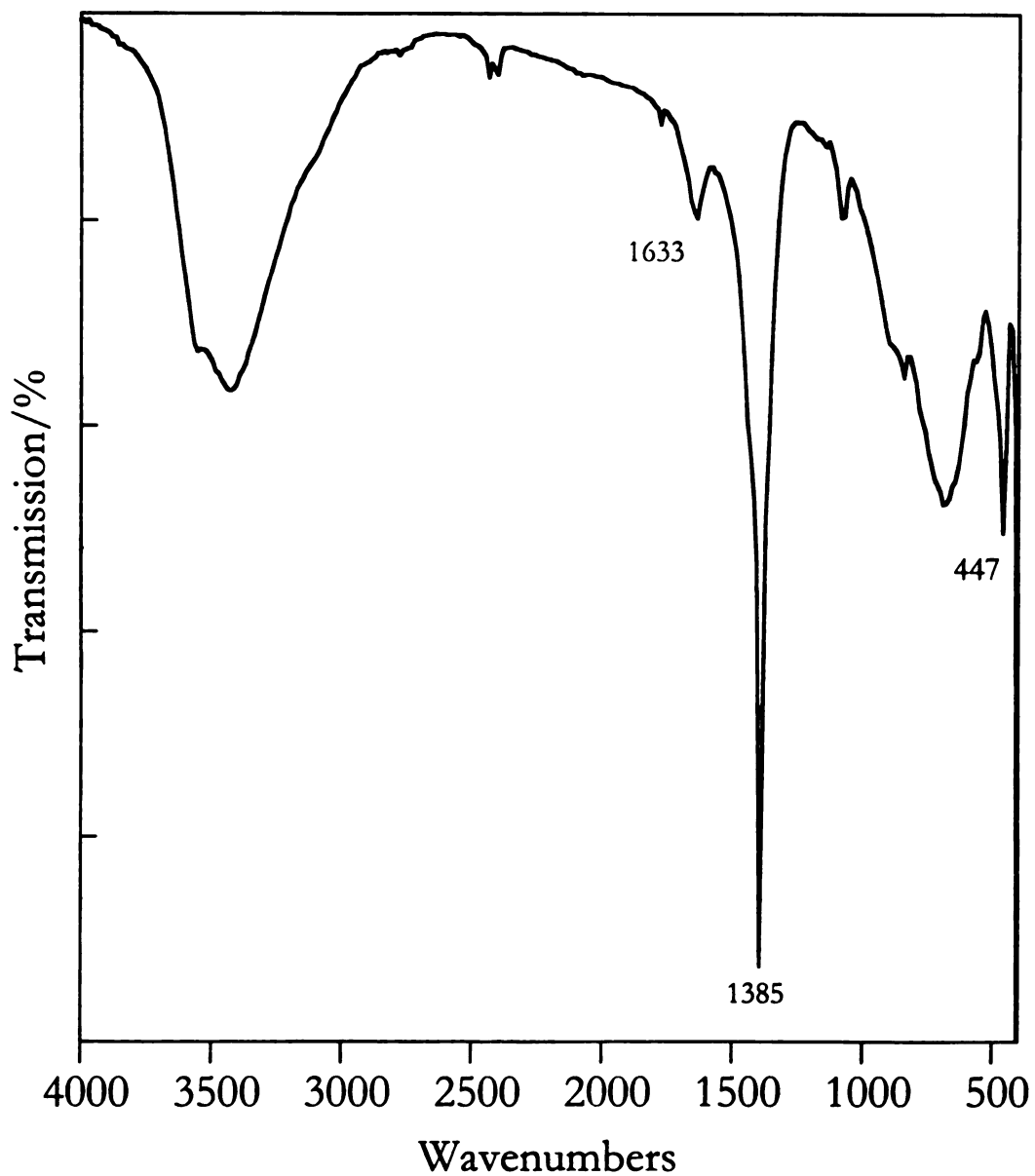


Figure 3-6. FTIR of  $\text{Mg}_2\text{Al-NO}_3^-$  synthesized at  $\text{pH} = 6.9$ . The resonance at  $1633 \text{ cm}^{-1}$  is assigned to coordinated water,  $1385 \text{ cm}^{-1}$  to nitrate, and  $447 \text{ cm}^{-1}$  is Al-OH

solution. The reaction digested at 90-95 °C for three days. The products were centrifuged and the pH of the decantate was recorded as the pH of the synthesis.

The XRD of the products obtained as the volume of 2 M NaOH added to the mixed metal solution is increased by 5 ml increments are shown in Figure 3-5. When 15 ml of base (0.03 mol) is added, the final pH is 5.3 and the only precipitate is pseudo boehmite. The pH increases to 6.3 when 20 ml base (0.04 mol) are added to the mixed metal solution. At this pH, a well ordered LDH is already beginning to form, although it is accompanied by pseudo boehmite. The d spacing is 8.9 Å, consistent with  $\text{Mg}_2\text{Al-NO}_3^-$ . The final pH is 6.9 when 25 to 30 ml base is added. The product from the addition of 25 ml (0.05 mol) has intense LDH peaks and some pseudo boehmite. The addition of 30 ml of NaOH (0.06 mol) has the stoichiometric amount of  $\text{OH}^-$  needed to form a 2:1 MgAl-LDH. (There would be excess  $\text{Mg}^{2+}$  in solution as the Mg:Al ratio of the reactants is 3.) Very little pseudo boehmite or  $\text{Mg}_2\text{Al-CO}_3^{2-}$  (d spacing = 7.6 Å) is evident in the XRD. When more than 30 ml of 2 N NaOH (greater than 0.03 mol) is added, the pH begins to rise above 7.0. Even though the pH is now nearly 8 when 35 ml (0.07 mol) base is added, the main product is a  $\text{MgAl-NO}_3^-$  LDH. The Mg:Al ratio of the products obtained in the addition of 30 and 35 ml 2 N NaOH was two, as analyzed by ICP.

Surprisingly, the pH is lower when 40 ml base is added than when 35 ml is added. The XRD peaks are broad and low in intensity and contamination by carbonate is evident in the tailing of the (00l) peaks. By the time the pH reaches 9.7 (45 ml, 0.09 mol NaOH) the primary product is  $\text{Mg}_2\text{Al-CO}_3^{2-}$ , ascertained from the 7.8 Å d spacing. The LDH is poorly ordered because even though carbonate is favored at this pH, the concentration is limited by the solubility of  $\text{CO}_2$ . Even in a traditional synthesis done a high pH, carbonate is added in a three times excess relative to the  $\text{Al}^{3+}$  concentration.

## Conclusion

These results show that Mg<sub>2</sub>Al-LDHs can be synthesized at a pH appreciably lower than the literature value of 8.0. The elevated reaction temperature and low pH, precludes the intercalation of CO<sub>3</sub><sup>2-</sup>. When the reaction is run in the pH range of 7.5-8.0, the product is poorly crystalline, probably due to increased competition between nitrate and contamination by carbonate from the atmosphere. This may explain why the synthesis at pH lower than 8 has not been attempted. In conclusion, when determining the optimum pH for LDH synthesis, the following criteria should be considered;

1. Minimization of byproducts
2. At least one metal hydroxide should be a precipitate, bearing in mind that only a 2:1 M<sup>2+</sup>/M<sup>3+</sup> LDHs form when M<sup>3+</sup> is the precipitate.

Synthesis of Mg<sub>2</sub>Al-LDHs at low pH a practical application where mild conditions are required or when a minimal volume of caustic waste is desirable.

## Experimental Methods

### *Synthesis of Mg<sub>2</sub>Al-CO<sub>3</sub><sup>2-</sup> by Miyata's method<sup>20</sup>*

A 1.0 molar mixed metal solution of Mg(NO<sub>3</sub>)<sub>2</sub> and Al(NO<sub>3</sub>)<sub>3</sub> was added to a round bottom flask with the pH maintained at 10.0 ± 0.2 by the simultaneous addition of a solution of 1.0 M Na<sub>2</sub>CO<sub>3</sub> and 2 M NaOH. The mixture was stirred during the reaction. The reaction was stirred for 18 hour at room temperature. The solid product was rinsed times by centrifuging and resuspending the pellet in water until the decantate was neutral, about four times.

*Synthesis of  $Mg_2Al-CO_3^{2-}$  by Reichle's method<sup>27</sup>*

An aqueous solution of  $Mg(NO_3)_2$  and  $Al(NO_3)_3$  ( $Mg + Al = 0.04$  mol) were added rapidly and with good stirring to a solution of NaOH and  $Na_2CO_3^{2-}$ . The amount of  $OH^-$  should equal the sum of two times the concentration of the magnesium and three times the concentration of the aluminum. The carbonate should be three or more times the stoichiometric requirement. The reaction was stirred for 18 hour at room temperature. The product was rinsed times by centrifuging and resuspending the pellet in water until the decantate was neutral, about four times.

*Synthesis of  $Mg_2Al-NO_3^-$  at low pH.*

Aluminum Nitrate  $Al(NO_3)_3 \cdot 9H_2O$  (0.01 mol) and  $Mg(NO_3)_2 \cdot 6H_2O$  (0.03 mol) were dissolved in 200 ml water and the temperature raised to 95 °C. Thirty ml of 2 M NaOH was added all at once. The reaction was stirred for three days at 95 °C. The product was rinsed two times by centrifuging and resuspending the pellet in water.

## Chapter 4. The Synthesis of Layered Double Hydroxides with Colloidal-Size Particles

### Introduction

Layered double hydroxides (LDHs), also called anionic clays or hydrotalcite-like compounds, are versatile materials with a wide range of applications including catalysis, environmental remediation, and pharmacology.<sup>9,10</sup> However, while traditional cationic clays such as montmorillonite, fluorohectorite, and vermiculite have been used in film applications since 1983,<sup>106</sup> a parallel development has not been seen for anionic clays. Even though the conductivity, capacitance, and the potentiometric, calorimetric, and colorimetric properties of LDHs have the potential to be applied in sensor technologies,<sup>107</sup> progress in this area as well as in fire resistant coatings and barriers has been hampered by the difficulty in making thin continuous films of LDHs.

Layered double hydroxides are easily synthesized in the lab. Methods of preparation include coprecipitation, the salt-oxide method, and induced hydrolysis. In all cases, the product is a precipitate or gel which is rinsed and generally dried before use. The dried LDH particles form aggregates which cannot be easily resuspended into a non-settling dispersion. Films made from these materials consist of powdery aggregated LDH particles which do not adhere well to the substrate, typically glass. However, there is an example where films as thin as 100 nm were made from an LDH synthesized by coprecipitation.

The air dried product was sonicated for 1 hour to disperse the aggregated platelets and then centrifuged at 2,000 rpm for 1 hour to remove the largest particles. Only the small fraction of suspended fine particles which remained in suspension was used for making films, in effect selecting only the colloidal size particles.<sup>37</sup> The remainder of the LDH was discarded.

The problem was to make the colloidal size particles directly, avoiding both the extra step of sonicating the LDH and the loss of product. The solution is to synthesize the LDH in an organic solvent where particle interactions are less favorable. All other conditions are analogous to standard coprecipitation methods.

There are a few examples of synthesis of LDHs in organic solvents. In a 1992 patent, Burba et al.<sup>86</sup> reported on the synthesis of layered mixed metal hydroxides from metal alkoxides in organic solvents such as diethylene glycol or methanol. In these examples, a stoichiometric amount of water was added as the source of hydroxide. No free base hydroxide (e.g. NaOH) was added to the reaction mixture and the reactions were performed under nitrogen. These LDHs can be used in applications where the presence of water is detrimental, such as electrorheological fluids for high temperature applications and as additives to polymers, oil-based paints, and coatings. A similar method using metal alkoxides in ethanol through sol-gel synthesis was used to synthesize hydrotalcite with a high specific area (150 m<sup>2</sup>/g) compared to natural hydrotalcite.<sup>108</sup>

Malherbe et al.<sup>87</sup> synthesized layered double hydroxides from the nitrate and chloride metal salts in a mixture of organic solvent and water in an N<sub>2</sub> environment. The solvent systems were 50:50 mixtures of water with methanol, ethanol, propanol, acetone or glycols with NaOH as the hydroxide source. Their method resulted in microtextural modification of the surface and porous

properties of the LDHs. The LDH synthesized in water and water/ethylene glycol had nitrogen adsorption/desorption isotherms characteristic of plate-like particles with slit-shaped pores. The LDHs formed in ethylene glycol/water system had pores with regular geometry while the glycerol/water system produced a  $\text{MgAl-CO}_3^{2-}$  with a variable geometry pore structure. This affected the surface area in that the LDH synthesized in water/ethylene had a surface area twice that of the LDH synthesized in water and there was a loss of surface area in the sample synthesized in a glycerol/water mixture.

## Results and Discussion

Magnesium aluminum layered double hydroxides have been made using primary alcohols, acetone, or acetonitrile as the only solvent without other alteration to the standard conditions of synthesis by coprecipitation (Figure 4-1). The reactions in acetone and acetonitrile produced LDHs with a high volume of undesirable  $\text{Mn}^+(\text{OH})_n$  byproducts. Consequently, acetonitrile and acetone are not considered to be adequate solvents under standard coprecipitation conditions.

The X-ray diffraction patterns of the products precipitated from methanol, ethanol, propanol, butanol, and a control reaction in water are shown in Figure 4-2. The intensity of the diffraction patterns increases with the chain length of the alcohol used as the solvent and the LDH formed in water gave the most crystalline product as judged by x-ray diffraction. The products precipitated from ethanol, propanol and butanol are equivalent to the LDH synthesized in water and are authentic LDHs. The gallery anions in a traditional LDH are solvated by water ( $d$  spacing = 7.9 Å,  $[\text{Mg}_3\text{Al}]\text{NO}_3\cdot m\text{H}_2\text{O}$ ], see Figure 4-2 water) so it was possible that LDHs synthesized in alcohols would have the respective

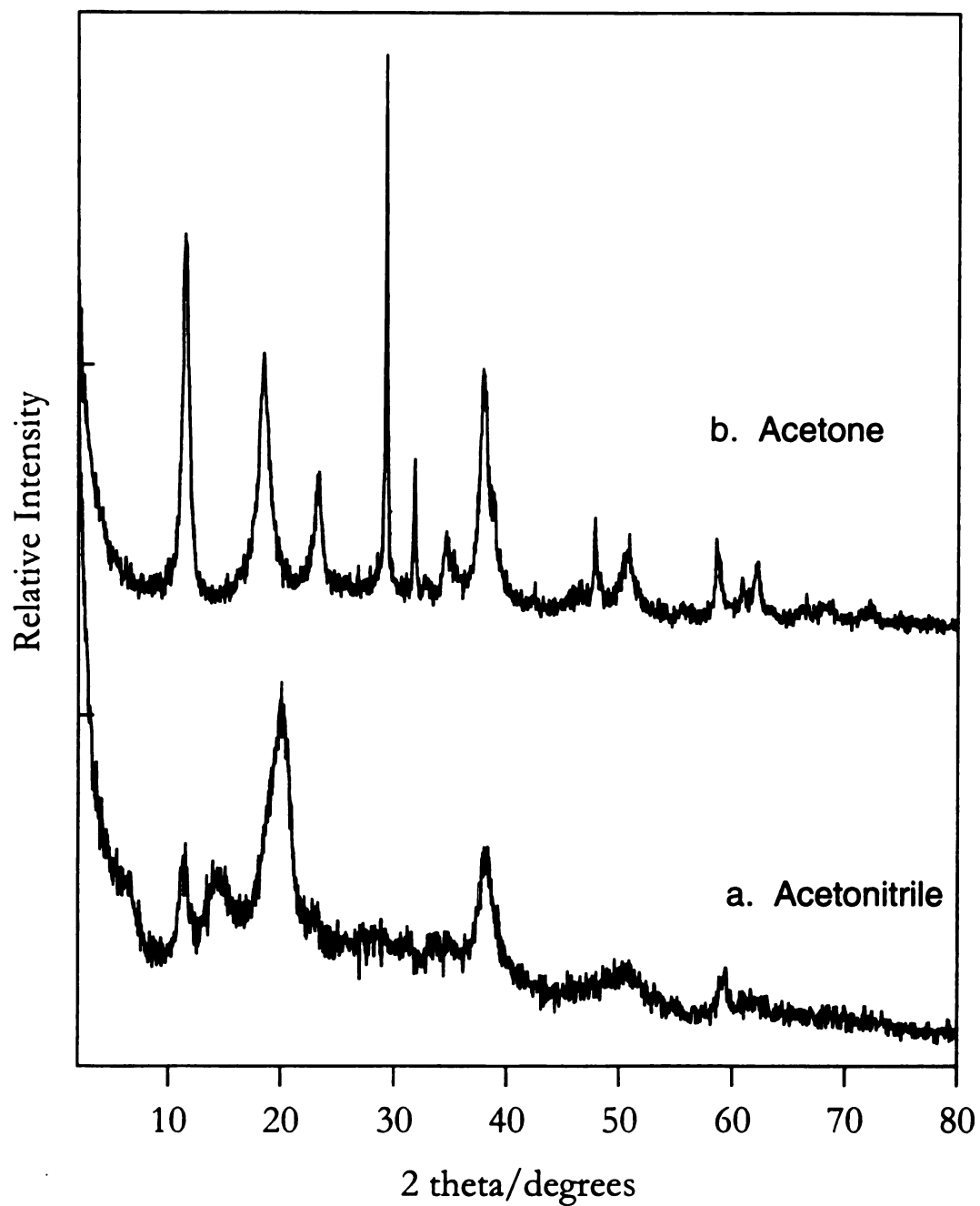


Figure 4-1. X ray diffraction pattern of products prepared in the reaction of a.  $\text{Mg}(\text{NO}_3)_2$ ,  $\text{Al}(\text{NO}_3)_3$ , and  $\text{NaOH}$  in acetonitrile and b. acetone. Synthesis of LDHs in acetone and acetonitrile by standard coprecipitation methods is unsatisfactory due to the insolubility of the Mg and Al salts in these solvents.

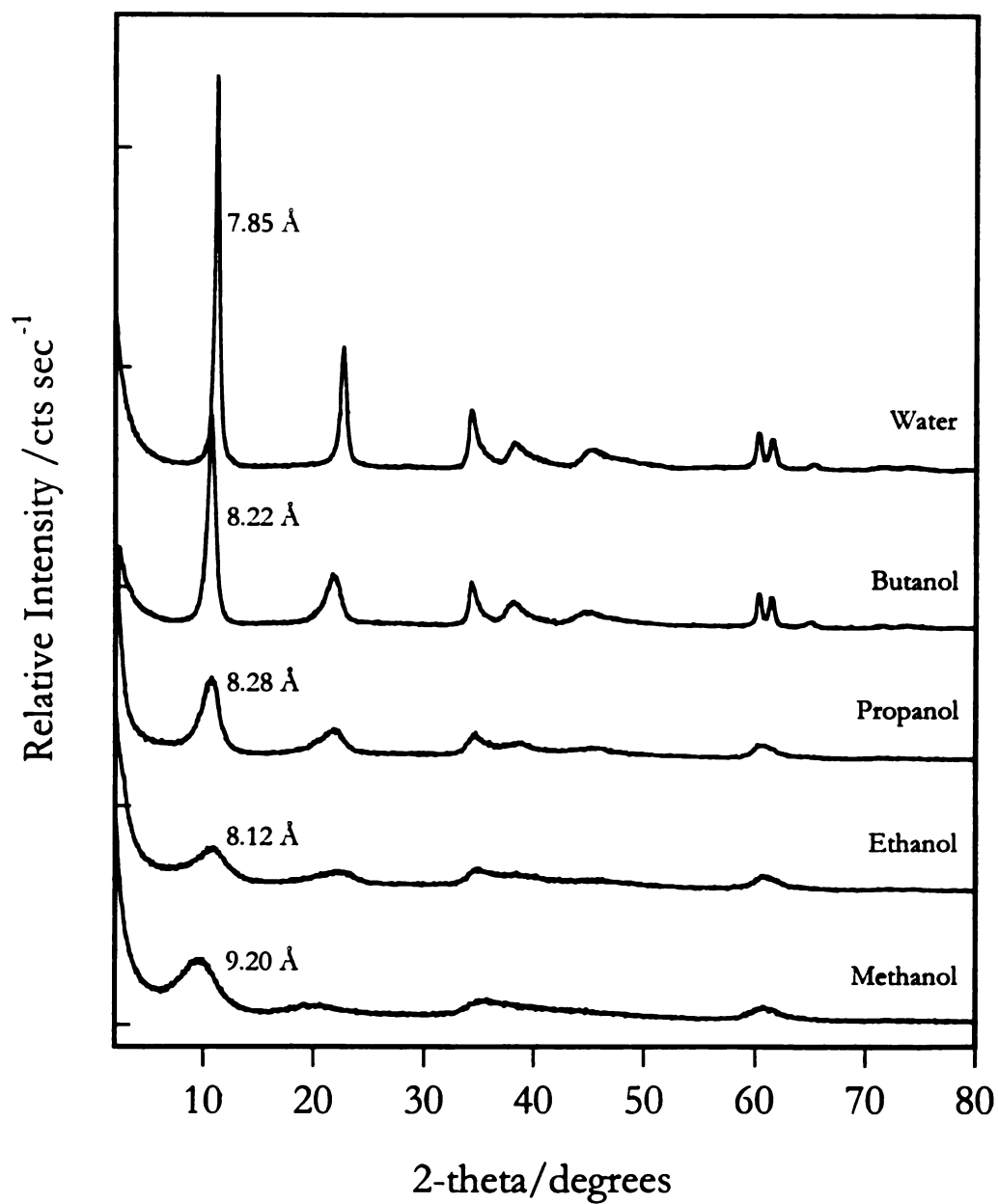


Figure 4-2. Powder X-ray diffraction patterns for LDHs and LDH precursor products precipitated from various organic solvents and water. The LDHs synthesized in propanol and butanol were washed with methanol to remove the remaining  $\text{NaNO}_3$  salt byproduct

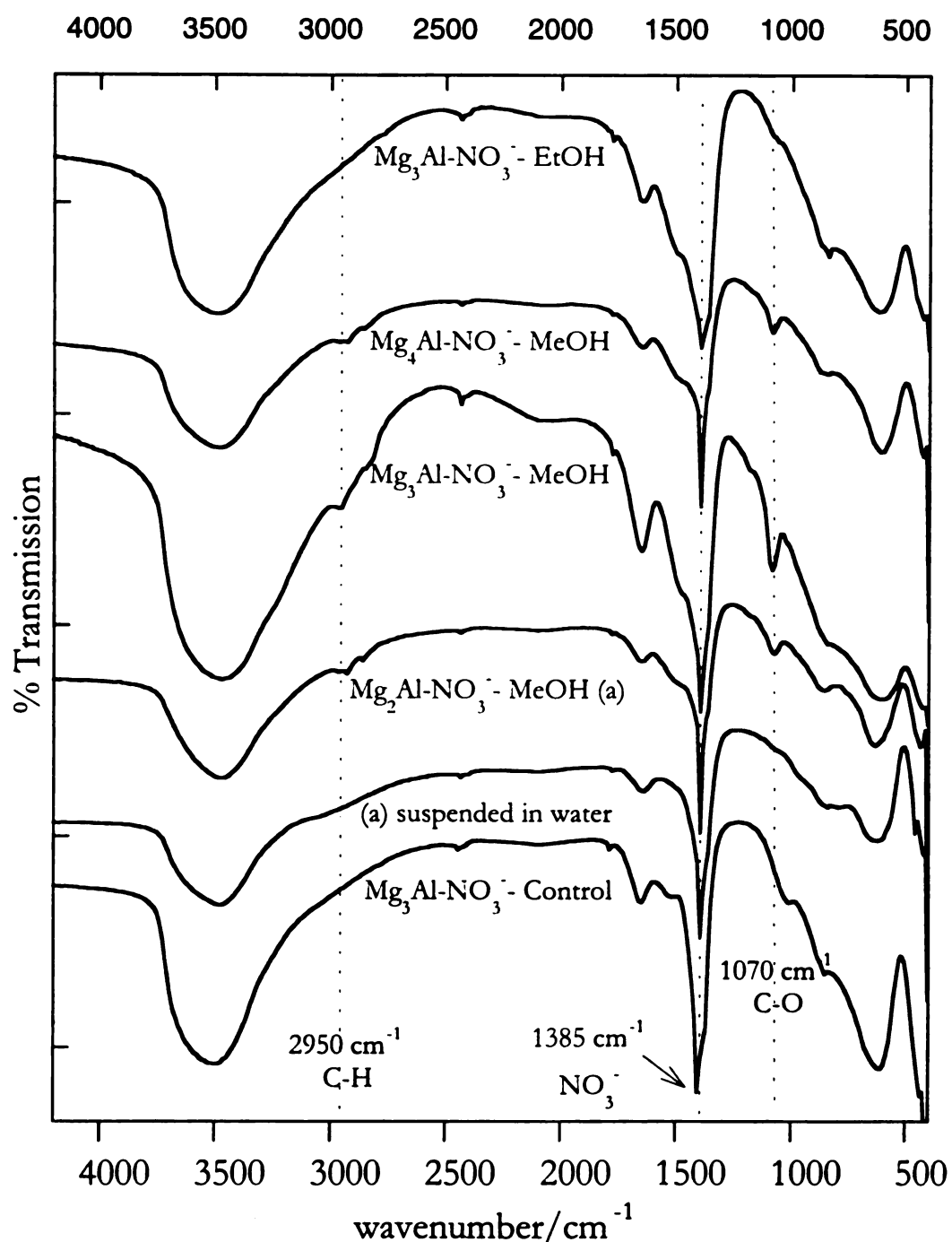


Figure 4-3. Infrared Spectra of  $\text{Mg}_x\text{Al-NO}_3^-$ , synthesized in ethanol, methanol, and water. From top to bottom: A  $\text{Mg}_3\text{Al-NO}_3^-$  synthesized in ethanol; the  $\text{Mg}_4\text{Al-NO}_3^-$ ,  $\text{Mg}_3\text{Al-NO}_3^-$ , and  $\text{Mg}_2\text{Al-NO}_3^-$  product from precipitation in methanol; the  $\text{Mg}_2\text{Al-NO}_3^-$  precipitation product after suspension in water and an LDH formed by traditional coprecipitation.

ROH in the interlayer region. The  $d$  spacing of 8.2 Å is a little higher than the water control, but suggests that the gallery anions are water solvated. The water can come from the metal salts used in the reaction or from the air.

The FT-IR spectra for a  $Mg_3Al$  precipitation product as synthesized in ethanol and for  $Mg_4Al$ -,  $Mg_3Al$ -,  $Mg_2Al$ -LDHs as synthesized in methanol are shown in Figure 4-3. The intergallery anion for the LDHs synthesized in ethanol and water is  $NO_3^-$ , ( $1385\text{ cm}^{-1}$ ). Even though it was expected that contamination by  $CO_3^{2-}$  ( $1355\text{ cm}^{-1}$ ) would be eliminated due to the low solubility of air in organic solvents, apparently maintaining an elevated temperature throughout the synthesis is enough to eliminate most dissolved  $CO_2$ . There is some water present in all the LDHs synthesized in organic solvents as evidenced by the absorption at  $1640\text{ cm}^{-1}$ , characteristic of coordinated water. In addition to the coordinated water, an organic species is present in the  $Mg_xAl-NO_3^-$  product synthesized in methanol. The absorptions at  $2950\text{ cm}^{-1}$  are C-H stretching vibrations and the absorption at  $1070\text{ cm}^{-1}$  is characteristic of the C-O stretch of an alcohol. These absorptions are absent in the LDH synthesized ethanol.

### **M-LDHs**

Even though the powder diffraction pattern of the product precipitated from methanol has low broad reflections, there are no crystalline impurity phases present. The low broad diffraction peaks of the product precipitated from methanol could be evidence of a polycrystalline material with poor inter particle interactions due to the limited H-bonding available with MeOH as the solvent. As a test, the precipitate was centrifuged and the pellet suspended in

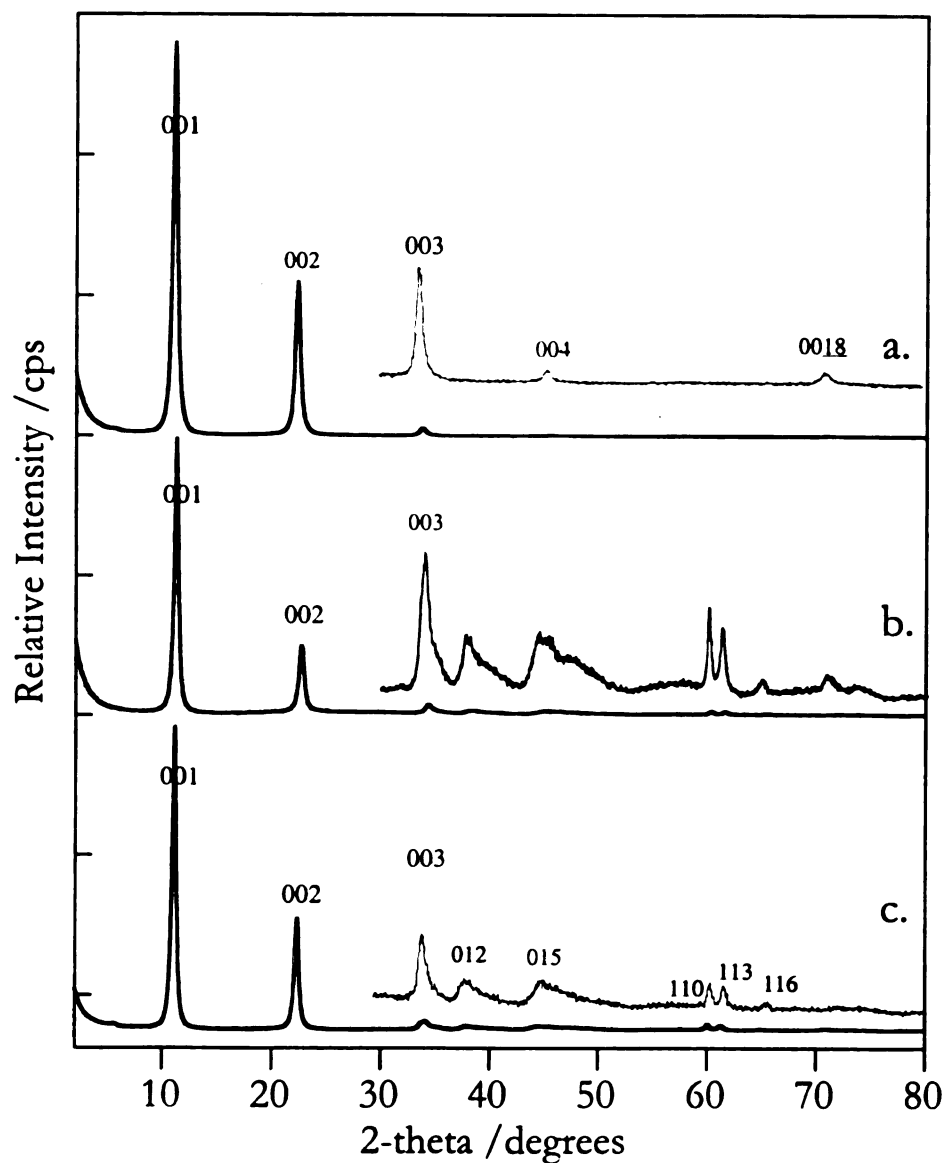


Figure 4-4. The X-ray diffraction pattern of an oriented thin films of  $Mg_3Al-NO_3$  a. product prepared by coprecipitation of an in methanol and subsequent hydrolysis in water, 0.030 mole  $Mg(NO_3)_2$  and 0.010 mol  $Al(NO_3)_3$  in 100 ml methanol are dripped into a solution of 0.09 mol NaOH in 100 ml methanol and stirred for 3 days at 55 °C. b.. LDH product prepared by coprecipitation in water at 55 °C under conditions analogous to the synthesis in methanol. The orientation of the LDH layers in pattern a. is evident from the complete lack of in-plane reflections for the M-LDH . c. A less oriented powder pattern of the M-LDH product. The presence of the in-plane reflections verify that the M-LDH is an authentic layered double hydroxide.

water. After standing overnight, the resulting suspension was nearly transparent and remained in suspension after being centrifuged at 8,000 rpm for 20 minutes. When the suspension was allowed to dry on a glass slide, a transparent film formed. The X-ray diffraction pattern of the transparent film is shown in Figure 4-4a. Figure 4-4c shows the less oriented powder X-ray diffraction pattern of the same material shown in Figure 4-4a and is the diffraction pattern of an authentic LDH (hereafter designated M-LDH). The intense (00 $l$ ) peaks and the absence of any in-plane reflections ( $h,k \neq 0$ ) in Figure 4-4a are evidence of an extremely well oriented sample. In addition, the (004) reflection is present in the oriented thin film, whereas in the X-ray diffraction pattern of the water control, the (004) reflection is buried under the broad asymmetric (015) reflection with in-plane components (Figure 4-4b). Applying the Scherrer equation (1) to the (002) reflections of Figure 4-4a. and Figure 4-4c. gives a particle size of 80 Å in the c direction.

$$L = \lambda K / B \cos \theta \quad (1)$$

where L is the mean crystallite dimension in Å, K is a constant taken to be near unity, B is the peak width at half height in radians. The mean particle size of the colloidal M-LDH is 66 nm, measured by light scattering.

The surface area for a small particle LDH should be very high. The surface area of the Mg<sub>3</sub>Al-NO<sub>3</sub><sup>-</sup> precipitate is very high when dried under vacuum at 150 °C is 600 m<sup>2</sup>/g. The surface area of the M-LDH or the Mg<sub>x</sub>Al-NO<sub>3</sub><sup>-</sup> precipitate dried under ambient conditions decreases to only 2-69 m<sup>2</sup>/g, in the range of a traditional LDH. The tendency for the LDH particles to form stacked aggregates is seen in the reduction of the surface area for the M-LDH.

Film thickness measurements were taken from SEM micrographs of the cross sections of both a self-supported Mg<sub>3</sub>Al-NO<sub>3</sub><sup>-</sup> and a supported Mg<sub>2</sub>Al-Cl-

film of an M-LDH. Figure 4:6a. shows the cross section of a 20 mm thick self supporting film with no substrate. This film was made by drying the aqueous suspension of a  $Mg_2Al-Cl^-$  M-LDH on a sheet of Teflon. Figure 4:6b shows the SEM micrograph of a cross section of a 0.3 mm thick  $Mg_3Al-NO_3^-$  film deposited on a glass microscope slide. The film was made by diluting the aqueous suspension of colloidal M-LDH by a factor of 10 and depositing two ml of the suspension on a standard glass microscope slide. The M-LDH was slowly dried over a 3-5 day time period. While the magnification is too low for the individual particles to be discerned, the horizontal orientation of the plates is evident.

Figure 4:6 compares the film surface of the  $Mg_3Al-NO_3^-$  film from Figure 4-5a to a 30 mm film of the water control. As can be seen in the micrograph of the water control (Figure 4:6d), storing the LDH as a slurry eliminates the aggregation of particles generally seen in LDH films, but Figure 4:6c shows the further improvement possible when a colloidal M-LDH is used in making the film.

The electron micrographs make it clear that pre-drying an LDH reduces the quality of the final LDH film. This is true for the M-LDHs as well. If the as synthesized or water suspended M-LDH is dried under ambient conditions, it will not resuspend in water as a colloidal suspension.

The M-LDHs exhibit the same thermal behavior as LDHs synthesized by traditional methods. Figure 4-7 shows the diffraction pattern of the mixed metal solution that forms when an LDH is calcined at a temperature at or below 500 °C. When the mixed metal oxide solution is stirred in water, the LDH reforms as seen in the upper XRD pattern in Figure 4-7. The TGA for 4:1, 3:1 and 2:1 M-LDH and the water control are shown in Figure 4-8. The M-LDHs have TGA profiles with two transition stages. The first is the loss of gallery and

physisorbed water and occurs between 97 and 300 °C. The second stage is the dehydroxylation of the  $\text{Mg}^{2+}$  and  $\text{Al}^{3+}$ . The  $\text{Al}^{3+}$  tends to dehydroxylate at a slightly lower temperature than the  $\text{Mg}^{2+}$ . The two steps for  $\text{Al}^{3+}$  and  $\text{Mg}^{2+}$  are clearer in the water control than in the M-LDHs. The only other remarkable difference is that the M-LDHs tend to lose slightly more (2-5%) gallery and sorbed water, which is advantageous for applications as fire retardants.

As discussed earlier, LDHs are very versatile materials. The  $\text{M}^{2+}/\text{M}^{3+}$  ratio, the intergallery anions, and the framework cations can all be easily varied in LDHs. In many of the methods for synthesizing an LDH, the ratio of  $\text{M}^{2+}/\text{M}^{3+}$  in the LDH product reflects the ratio of cations added to the reaction. In addition to  $\text{Mg}_3\text{Al-NO}_3^-$ , M-LDHs with Mg:Al reaction ratios of 2:1 and 4:1 were synthesized. The XRD of these LDHs shown in Figure 4-9 have essentially the same d spacing (8.0 Å) even though the layer spacing should change with charge.

There are two ways the gallery anion can affect the d spacing when only the layer charge changes. When the layer charge increases, the attraction between the opposite charges of the layers and the anions is increased and the d spacing decreases. This is a well studied phenomenon in  $\text{MgAl-CO}_3^{2-}$  LDHs.<sup>9</sup> The d spacing for MgAl-carbonates decreases from 8.0 Å for a 4:1  $\text{MgAl-CO}_3^{2-}$  to 7.6 Å for a 2:1  $\text{MgAl-CO}_3^{2-}$  LDH. The second effect on layer spacing comes from the orientation of the gallery anion. In  $\text{Mg}_2\text{Al-CO}_3^{2-}$  LDHs, the gallery carbonate lies parallel to the layers. While nitrate is isostructural to carbonate, it is monovalent and twice as many charge balancing nitrate anions as are required. In a 2:1  $\text{Zn}_2\text{Al-NO}_3^-$ , the d spacing increases to 9.0 Å, indicating that the nitrates are tilted relative to the layers. The d spacing for the  $\text{Mg}_2\text{Al-NO}_3^-$  is 8 Å, too small for a 2:1 LDH nitrate.

Figure 4-5 Scanning electron micrographs of; a. A 20 mm self supporting  $\text{Mg}_3\text{Al-NO}_3^+$  M-LDH film. b. A 0.3 mm  $\text{Mg}_2\text{Al-Cl}^-$  film supported on glass.

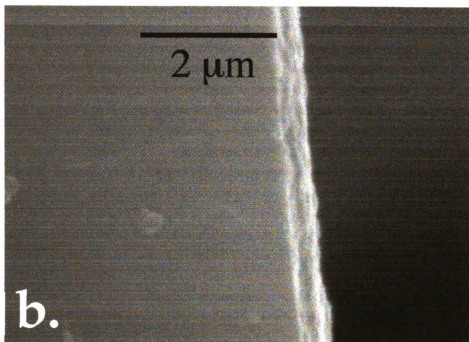
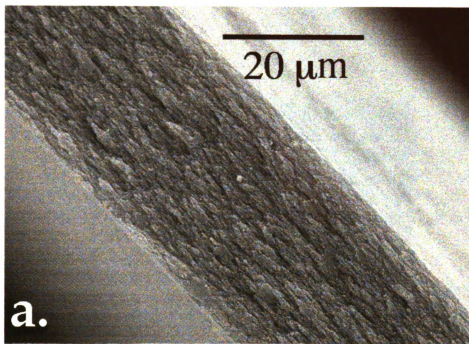
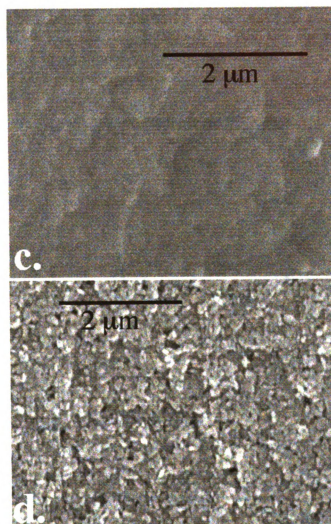


Figure 4:6. Scanning electron micrographs of c. The surface of the  $\text{Mg}_3\text{Al-NO}_3^-$  M-LDH film. d. The surface of a 30 mm film of the  $\text{Mg}_3\text{Al-NO}_3^-$  control synthesized in water.



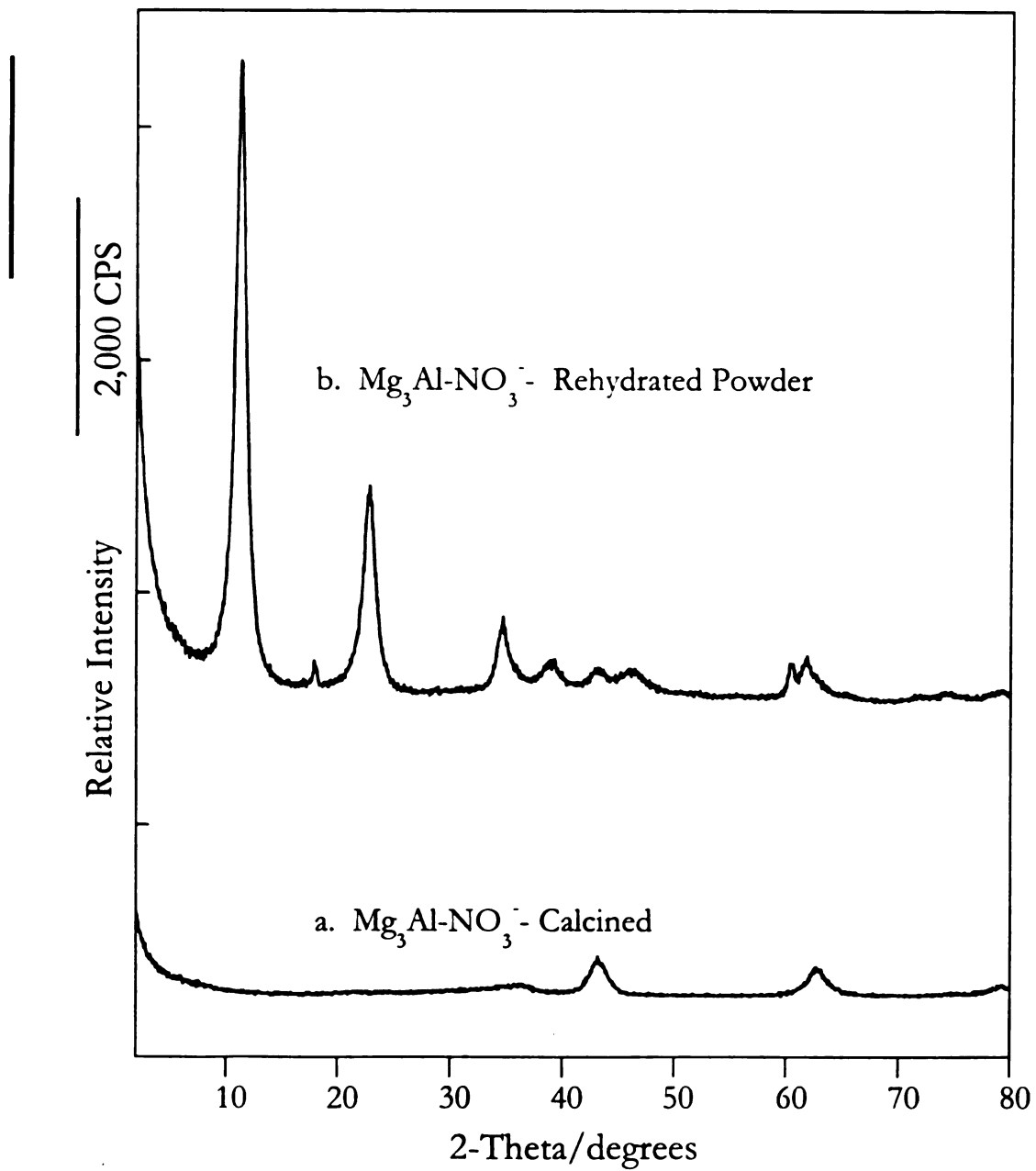


Figure 4-7. a. X ray diffraction pattern of an M-LDH calcined at 500 °C. b. the same material after being reconstituted in water to reform the LDH.

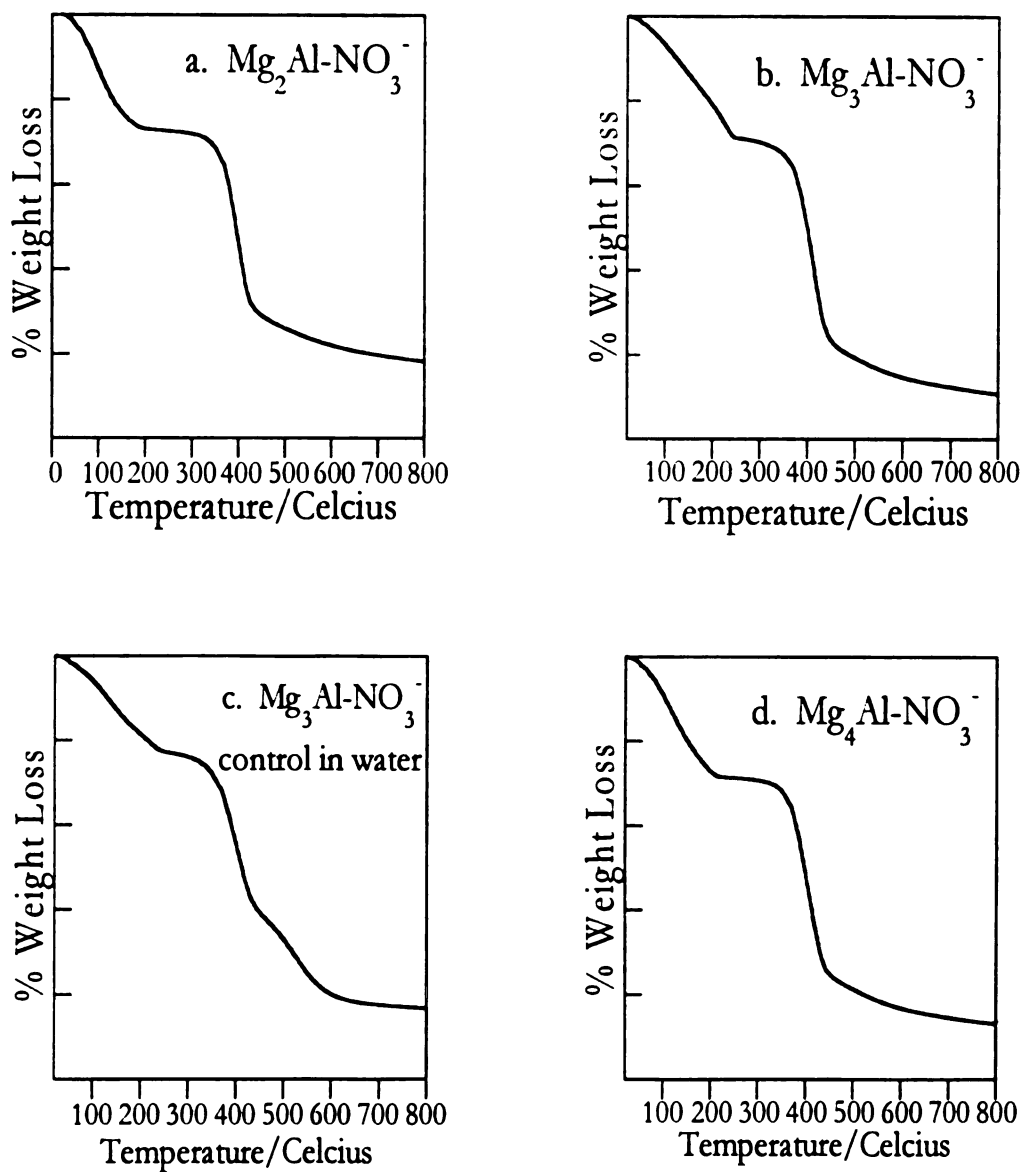


Figure 4-8. Thermogravimetric analysis of  $Mg_xAl-NO_3^-$  M-LDH a. M-LDH with a 2:1 Mg:Al ratio. b. M-LDH with a 3:1 Mg:Al ratio. c.  $Mg_3Al-NO_3^-$  made by coprecipitation in water. d. M-LDH with 4:1 Mg:Al ratio

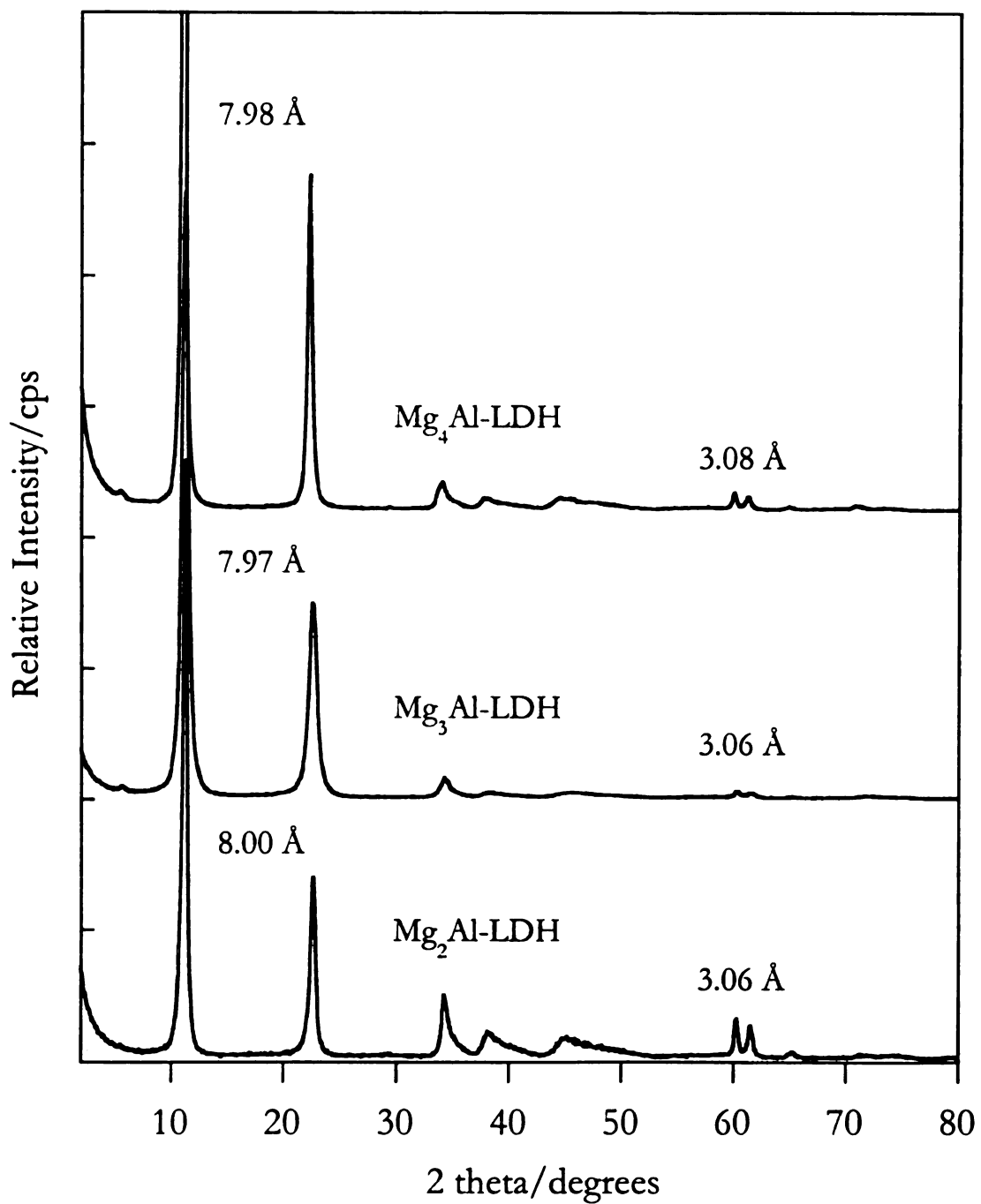


Figure 4-9. X-ray diffraction patterns of M-LDHs with theoretical 4:1 (4.0:1.0), 3:1 (3.2:1.0), and 2:1 (3.0:1.0) Mg:Al ratios. The actual ratios are in parentheses.

As discussed in the introduction, the lattice parameters of the  $a,b$  plane of an LDH are not affected by the gallery anion. Again, the effect of varying the layer charge on the in plane crystal parameters has been thoroughly studied for  $Mg_xAl-CO_3^{2-}$  LDHs. The crystal parameter  $a$  is equal to two times the  $d$  spacing of the (110) reflection. As the fraction of aluminum substitution increases, the lattice parameter  $a$  decreases from 3.07 Å for a 4:1 to 3.06 Å for a 3:1 to finally, 3.04 for a 2:1  $Mg_2Al-CO_3^{2-}$  LDH. The values of the lattice parameter  $a$  for the M-LDHs with varying Mg/Al ratio are listed in Figure 4-9. A unit cell value of 3.08 Å and 3.06 Å for the ratios of 4:1 and 3:1 M-LDH respectively, indicate that the composition of the LDH reflects the ratio of the reactants. The 2:1 M-LDH unit cell dimension of 3.06 Å, suggests that the product ratio is 3:1. Analysis by ICP verified these results. The Mg/Al ratios were 4.1, 3.2, and 3.0 for the 4:1, 3:1, and 2:1 initial ratios respectively. The M-LDH products are slightly enriched in magnesium and do not form an LDH with a ratio of 2:1 under these conditions.

The methanol synthesis was extended to other intergallery anions with the synthesis of  $MgAl-Cl^-$  and  $MgAl-SO_4^{2-}$  M-LDHs. The  $MgAl-Cl^-$  M-LDHs behaved similarly to the  $MgAl-NO_3^-$ , however attempts to produce  $MgAl-SO_4^{2-}$  resulted in poor products as judged by X-ray diffraction. The reactants were magnesium and aluminum sulfates, which are only sparingly soluble in methanol. Therefore, the solubility of the metal salts reactants is a limiting factor for the synthesis of LDHs in methanol. This can be circumvented by utilizing anion exchange reactions. Figure 4-10 shows the X-ray diffraction pattern of a  $Mg_3Al-Fe(CN)_6^{3-}$  made by an exchange reaction with a  $Mg_2Al-Cl^-$ .

Next, M-LDHs were made from cations other than Mg and Al. The trend here is less obvious. Magnesium, aluminum, nickel, and cobalt produce M-

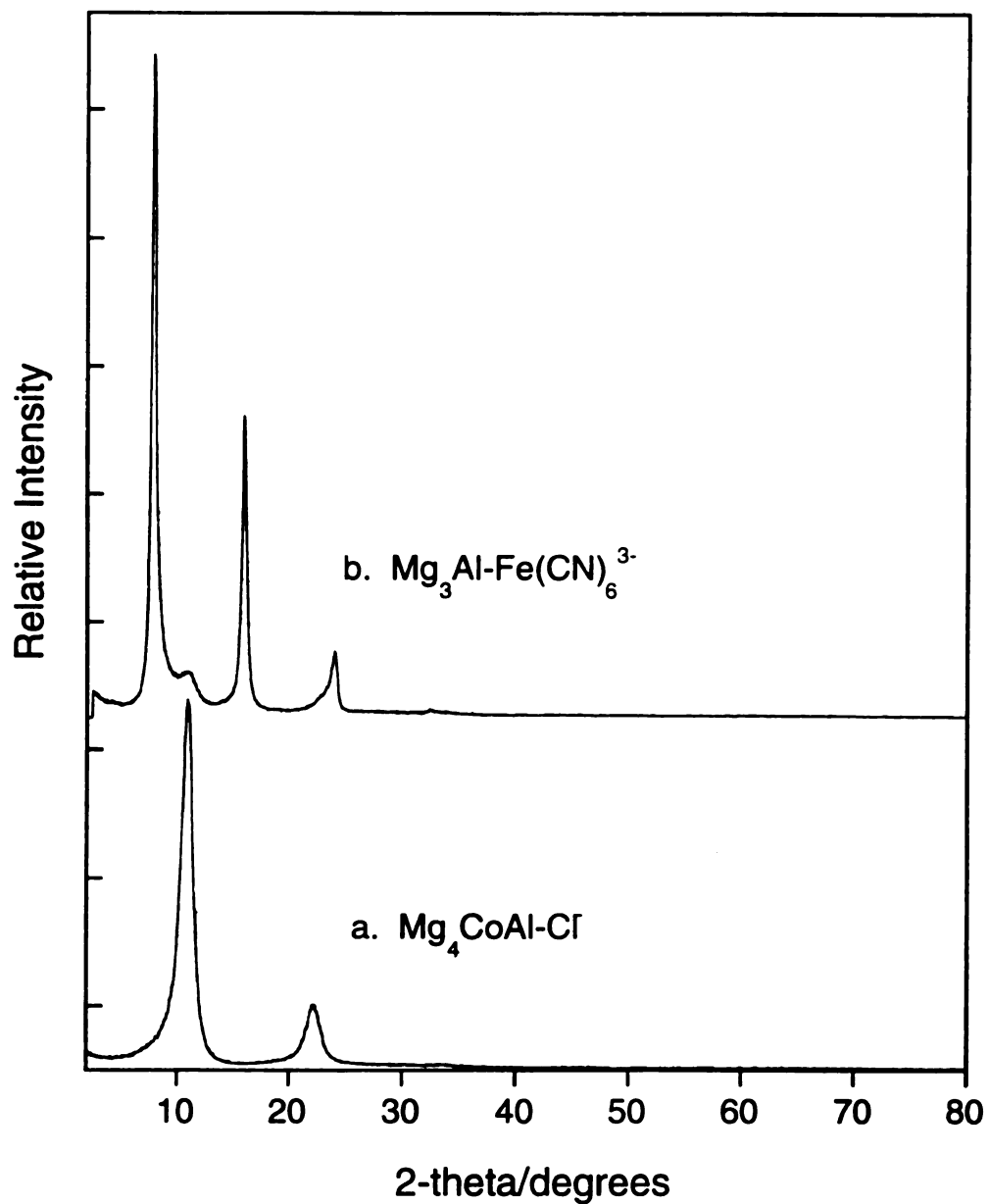


Figure 4-10. X ray diffraction patterns for a. M-LDH where the gallery anion of interest was intercalated via an exchange reaction. b. M-LDH where  $\text{Co}^{3+}$  cation of interest is present in a fractional substitution

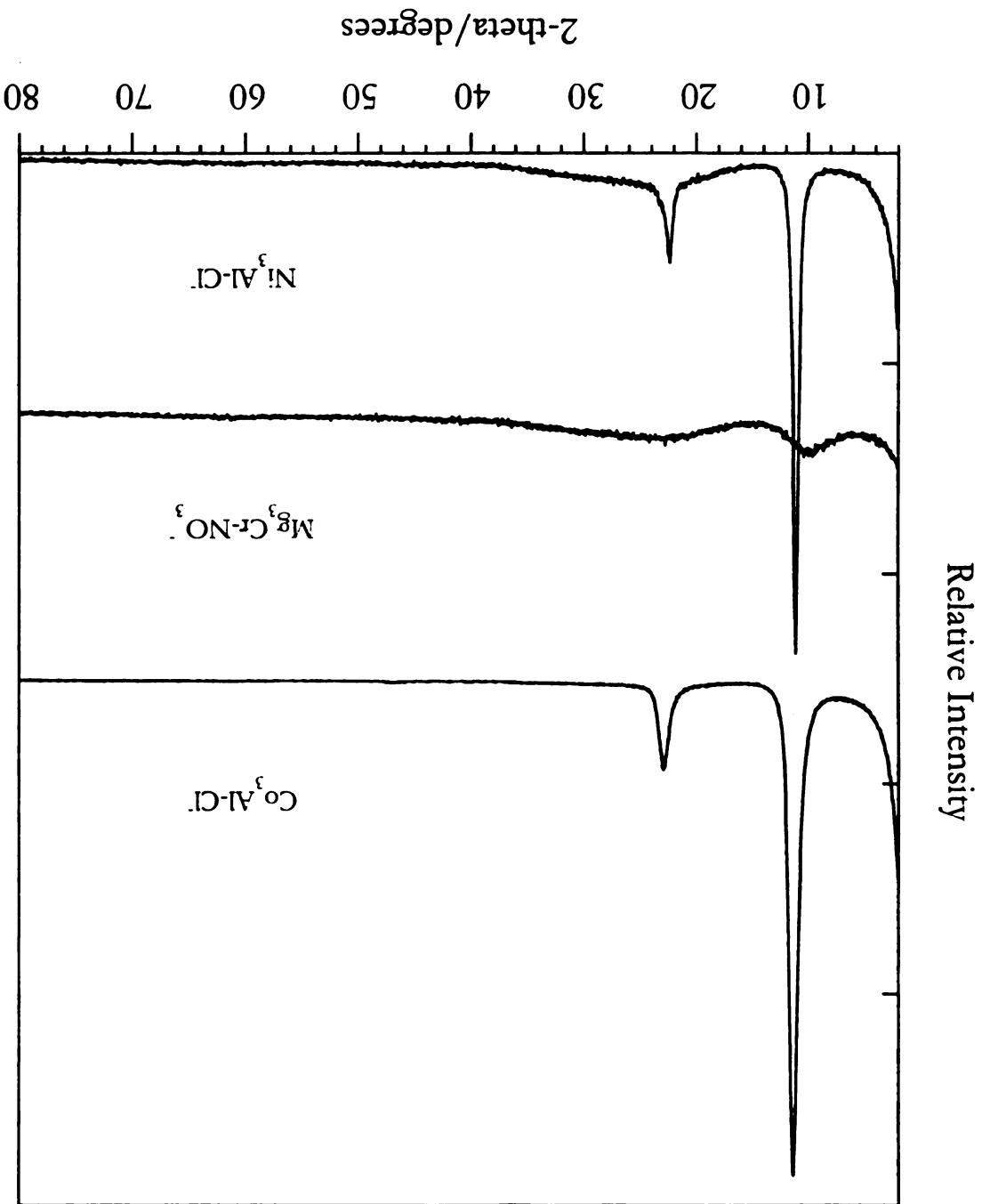


Figure 4-11. XRD of M-LDH with varying layer cations and anions.

LDHs which form colloidal suspensions in water. Chromium forms a very poorly crystalline M-LDHs, even when suspended in water, and zinc will not form an LDH at all. All these metals will result in a reasonable LDH when synthesized in water. This problem can be circumvented by substituting only a small fraction of the desired cation. The x-ray diffraction pattern of CoAl-, MgCr-, and NiAl-M-LDHs are shown in Figure 4-11. Figure 4-10 shows a Mg<sub>2</sub>CoAl-Cl- with only a small fraction of Co.

### **The Precipitate from Methanol**

The infrared and X-ray diffraction data indicate that only the precipitate synthesized in methanol is solvated by or coordinated to the organic solvent. Although the LDHs synthesized in the remaining alcohols (especially ethanol) also form oriented films when suspended in water, the best films are made from the LDHs formed by the precipitation of a MgAl-NO<sub>3</sub><sup>-</sup> product from methanol, followed by hydrolysis in water. When the product of the precipitation of MgAl-A<sup>n-</sup> is suspended in water, the result is an authentic LDH and this is a reasonably general method for the synthesis of LDHs. However, the precipitate as formed in methanol is not indisputably an LDH. The first two reflections in the X ray diffraction pattern of the MgAl-NO<sub>3</sub><sup>-</sup> product of coprecipitation from methanol are ordered reflections characteristic of a layered material, but the d spacing is 2.5 Å greater than the LDH coprecipitated from water. The third peak is not a third order reflection, although it is so broad that it does encompass the third order reflection and the (015) reflections of an LDH. The product could be an LDH with methanol solvating the gallery anions. It is also possible that the product of precipitation from methanol is a layered magnesium aluminum alkoxide hydroxide.

Analysis for HCN verifies that nitrate is present in the precipitate formed in methanol supporting the argument for an anionic layered material. In addition, the nitrate can be substituted by other anions and a variety of metals can be substituted for the magnesium and aluminum. Hydrotalcite must be the parent structure.

Only the intensity of the peaks in the FTIR of the  $\text{Mg}_3\text{Al-NO}_3^-$  precipitate changes when it is dried under vacuum at 150 °C (

Figure 4-12). It would be expected that any methanol solvating the gallery or coordinated to the surface would be volatilized under these conditions. The continued presence of a methanol derivative supports the argument that the  $\text{Mg}_x\text{Al-NO}_3^-$  precipitate is a MgAl-methoxy hydroxide.

The weight percent of Al, Mg, (ICP) and H, C, N was used to calculate the molecular formula for a 3:1  $\text{MgAl-NO}_3^-$ , and show the percent of methoxy substitution in the precipitate as formed in methanol. The formula is  $[\text{Mg}_{3.6}\text{Al}(\text{OH})_{7.2}(\text{OCH}_3)](\text{CO}_3)_{0.3}(\text{NO}_3)_{0.4}$ . The Mg/Al ratio for this synthesis was higher than usual, but the results of the elemental analysis do indicate the relative amount of methoxylation of the precipitate from methanol.

## Conclusions

Layered double hydroxides can be synthesized by coprecipitation in primary alcohols ( $n=2-4$ ) without significant contamination by carbonate. An LDH precursor synthesized in methanol and followed by hydrolysis in water results in a crystalline LDH which is distinctly different from that synthesized in water under the same conditions. When the precipitate formed in methanol is transferred to water, it becomes a transparent colloidal LDH suspension from

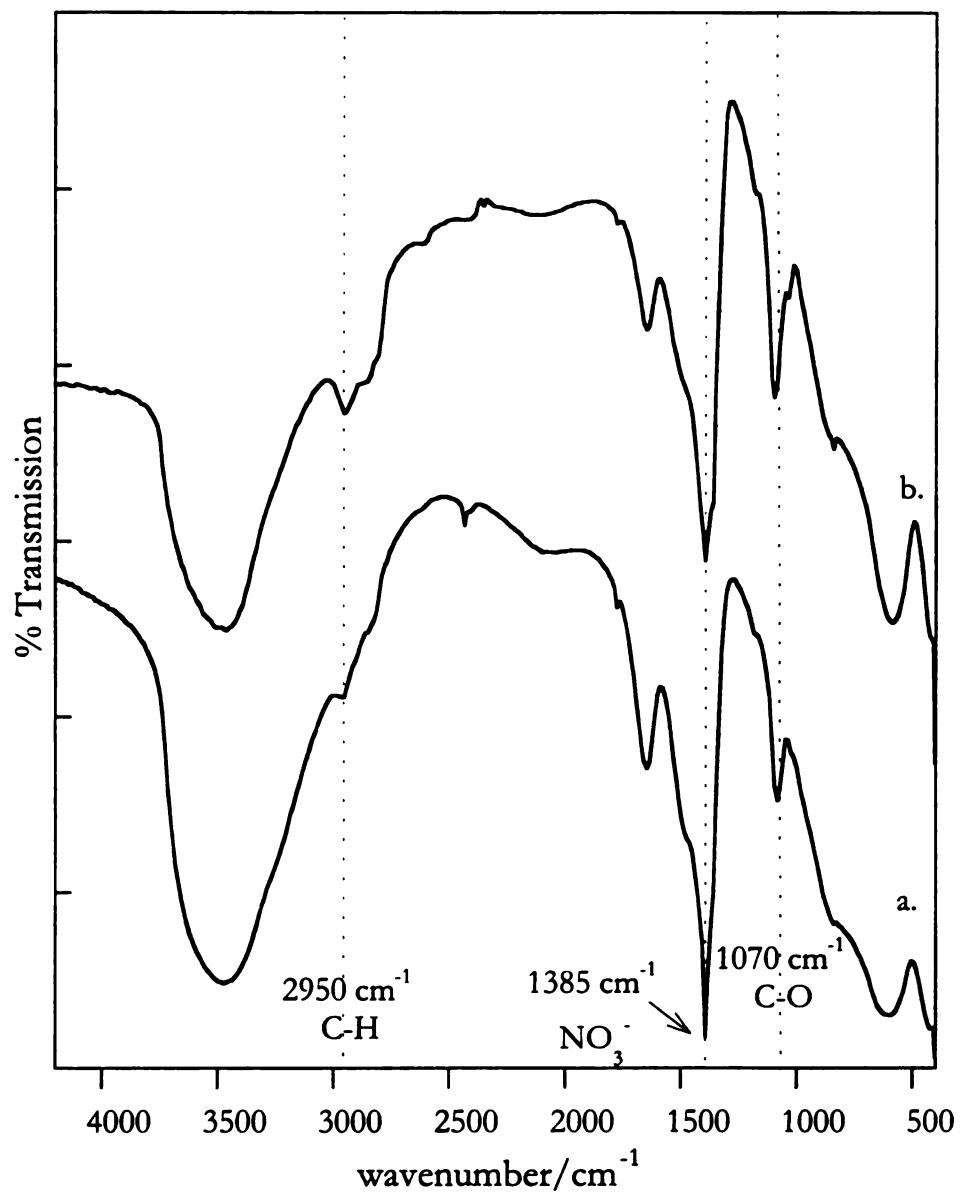


Figure 4-12. FTIR of a.  $\text{Mg}_3\text{Al-NO}_3^-$  dried under ambient conditions. b.  $\text{Mg}_3\text{Al-NO}_3^-$  dried under vacuum at 150 °C.

which very well oriented transparent thin films can be formed. It is important to note that these M-LDHs were not dried prior to being made into films. Similar to results reported by Pinnavaia<sup>109</sup> and Clearfield for anion exchange reactions, the best films are made when the LDH is maintained as a suspension prior to use.

M-LDHs with a variety of layer charges, intergallery anions and framework cations have been made, demonstrating that this is a reasonably general method. The gallery anions are limited by the solubility of the starting materials, but this can be circumvented by anion exchange reactions. The trends for incorporating cations into the layers have not been determined.

The lack of a good method for making thin films of LDHs has been a limiting factor in their utility as sensors and membranes. The development of a facile method for the synthesis of oriented continuous thin films may well prove to be the keystone advance enabling the practical application of these materials as membranes, sensors, and devices and in the area of fire retardant materials.

## Experimental Methods

### *Synthesis of $[Mg_{(1-x)}Al_x(OH)_2]NO_3$ in methanol*

NaOH (3.6-4.0 g, 0.09-0.10 mole) was dissolved in 100 mL CH<sub>3</sub>OH solvent and heated with stirring to 55 °C. A mixed metal solution of Mg(NO<sub>3</sub>)<sub>2</sub>·6H<sub>2</sub>O and Al(NO<sub>3</sub>)<sub>3</sub>·6H<sub>2</sub>O (0.04 M in total metal ion concentration, with ratios of Mg:Al of 2-4) in 100 mL of CH<sub>3</sub>OH was slowly dripped into the sodium hydroxide solution and stirred for 3 days at 55° C. The solid product was rinsed at least 4 times by centrifuging and resuspending in MeOH, until NaNO<sub>3</sub> was not evident in the powder x-ray diffraction pattern and the pH of

the decantate was below 8 as judged by Hydrion pH paper. The product was stored as a slurry in 150 mL MeOH.

MgAl-NO<sub>3</sub><sup>-</sup> LDHs, MgAl-Cl<sup>-</sup> and MgAl-SO<sub>4</sub><sup>2-</sup> LDHs were made by substituting the metal chlorides or sulfates for the Mg and Al nitrates.

Ethanol, propanol, butanol, acetone, and acetonitrile were also used to synthesize Mg<sub>3</sub>Al-NO<sub>3</sub><sup>-</sup> LDHs. However at 55 °, NaOH reacts with propanol and butanol, so better results are obtained when solid sodium hydroxide is added to the mixed metal solution (0.02 M, 200 mL) at 55 °C.

Portions of the LDH slurry were centrifuged and the pellet suspended in water at a concentration of approximately half the initial concentration. After standing overnight, the cloudy suspension would generally become clear. When centrifuged at 8,000 rpm for 20 min., the LDH remained in suspension.

## **II. CATALYSIS BY INTERCALATED POLYOXOMETALATES**

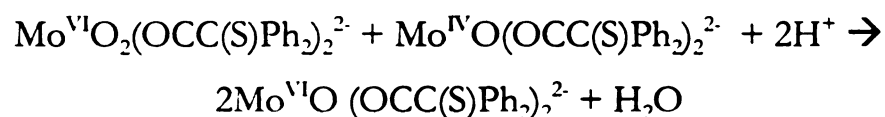
## Chapter 5. Layered Double Hydroxides Pillared with Polyoxometalate Catalysts

From large volume manufacture to laboratory synthesis, oxidative transformations of organic functional groups are basic to synthetic chemistry<sup>110</sup> Due to economic and environmental pressures, there is an increased interest in developing catalysts which can simplify the stoichiometric reagents needed in liquid phase oxidation reactions, especially those run at ambient temperatures and pressures. While many of the promising catalytic systems are molecular homogeneous catalysts, there are several factors driving the development of heterogeneous analogs. Because they are easily removed from the reaction mixture and recycled, non-labile supported catalysts are environmentally sound and economically attractive. There are many well documented homogeneous catalysts that can be supported on a solid surface, such as alumina-supported molybdate.<sup>111</sup> These hybrid catalysts combine the known catalytic properties of homogeneous catalysts with the advantages of a heterogeneous catalyst. If the support is a layered or porous material into which the catalyst may be intercalated, the additional benefits of size and chemical selectivity may be achieved. Size selectivity is accomplished through manipulation of the pore size of the material. Fine tuning of the chemical environment inside the pores increases substrate selectivity.

Catalysis by anions intercalated into a layered material implies that the catalysts are also functioning as pillars. In order for a substrate to reach catalyst centers deep within the layers, intercalation of the catalysts must cause a

significant layer separation and an equally significant lateral separation of the catalysts.

Many of the catalysts employed in the oxidation of organic substrates are anionic. Layered double hydroxides are the only general class of inorganic host materials into which anionic catalysts can be intercalated by ion exchange. Anionic catalysts that function as pillars upon intercalation into LDHs and retained their catalytic activity include metal porphyrins and organometallic complexes. The LDH supported Co(II) phthalocyanine tetrasulphonate is twice as active and has a greater longevity than the homogeneous catalyst.<sup>112</sup> Another example is the intercalation of sterically hindered metal complex  $[\text{Mo(VI)O}_2(\text{O}_2\text{CC(S)Ph}_2)]^{2-}$ .<sup>113</sup> Constraining the catalyst in an LDH eliminates the formation of inactive  $\text{Mo}^{\text{V}}$  through the comproportionation reaction,



eliminating the need for bulky organic ligands. Another important advantage is that water can be used as a solvent in this system.

Pillaring is another example of the utility of LDHs as materials by design. Potential applications of pillared LDHs include:

1. heterogeneous and supported homogeneous catalysis: acid, base, redox, enzymatic, photocatalysis
2. processing of selective nanoreactors
3. separation and membrane technology: separation by adsorption, by optically active isomers, and by adsorption-desorption cycles,
4. membrane technology: membrane materials for filtration, permeation, ion selectivity and heating and cooling systems,
5. scavenging and controlled release: pollutant scavenging and waste management, controlled drug or pesticide delivery for environmental, agricultural, or pharmaceutical applications

6. electroactive materials - electrodes, dielectrics, electrolytes for batteries, microelectronic and microionic devices, and sensors
7. photoactive materials - pigments, photocatalysts, luminescent materials, and optical devices

Polyoxometalates are a large class of anionic catalysts that hold great promise for intercalation into LDHs. Layered double hydroxides pillared with POM anions have substantial potential for applications in industrial and environmental catalysis.

### **Polyoxometalates**

Polyoxometalates are inorganic metal oxygen clusters which contain symmetrical core assemblies of  $\text{MO}_x$  units ( $\text{M} = \text{V}, \text{W}, \text{and Mo}$ ). Polyoxometalates form a class of inorganic compounds that is unmatched in terms of molecular and electronic structural versatility, reactivity, and relevance to analytical and clinical chemistry, catalysis, biology, medicine, geochemistry, materials chemistry, and topology.<sup>114</sup> Underlying all aspects of the chemistry of polyoxometalates is their extreme thermal robustness and stability against oxidation. Significant general properties of POMs are their solubility in solvents with polarity ranging from dimethyl sulfoxide to benzene (with the proper cation), their extreme stability, their completely inorganic composition, and most important, their ability to undergo reversible multiple electron reductions.

An extensive and highly regarded review of POMs was written by Pope<sup>114</sup> in 1984, followed by a second review in 1991.<sup>114</sup> More recent reviews include an entire issue of *Chem. Rev.* **1998**, vol. 98 no. 1, *Journal of Molecular Catalysis A:Chemical*, **1998**, vol. 144, C. L. Hill, ed. A review by Hill and Prosser-McCarthy<sup>115</sup> focuses mainly on mixed addenda and transition metal substituted polyoxometalates (TSMP).

## Applications

The applications of POMs are centered primarily on their redox properties, photochemical response, ionic charge, conductivity, and ionic weights. About 80 - 85% of the patent and applied literature concentrates on the catalytic activity of POMs. The remaining 15-20% can be grouped in the categories listed in Table 5-1.<sup>116</sup> The divisions are based on the material form of the POM or on a particular value-adding property of the POM;<sup>116</sup>

1. metal oxide like
2. large size (6-25 Å in diameter)
3. discrete size and/or structure (confined geometric factors)
4. anionic charge form -3 to -14
5. high ionic weight ( $10^3$ - $10^4$ )
6. fully oxidized compounds are reducible
7. variable oxidation number for the addenda atoms ( $E_{1/2} = 0.5$  to  $-1.0$  V vs. SCE)
8. color of oxidized forms different from color of reduced forms
9. photoreducible
10. Arrhenius acids ( $pK_a < 0$ )
11. processing advantages
  - a. air and water stable
  - b. incorporate over 70 elements and from large number of structures
  - c. acid forms very soluble in water and other oxygen carrying solvents (ethers, alcohols, and ketones)
  - d. soluble or transferable to nonpolar solvents
  - e. hydrolyzable to form deficient structures
  - f. low toxicity

## Catalysis by polyoxometalates

Polyoxometalates are multi-functional catalysts. They are very strong Brønsted acids, approaching the superacid region, and more applicable to POMs

**Table 5-1. Applications for Polyoxometalates, Excluding Catalysis and Medicine**

1. Pharmaceuticals
2. Clinical analysis
3. Coatings
4. Analytical Chemistry
5. Processing radioactive waste
6. Separations
7. Sorbents of gases
8. Membranes
9. Sensors
10. Dyes and pigments
11. Electrooptics
12. Electrochemistry and electrodes
13. Capacitors
14. Dopants in nonconductive polymers
15. Dopants in conductive polymers
16. Dopants in sol-gel matrices
17. Flammability control
18. Food Chemistry

supported on LDHs, they are efficient oxidants with fast, reversible multi-electron redox transformations under mild conditions. Their redox properties can be varied over a wide range by changing the chemical composition.

Polyoxometalates are remarkable because they function as reversible oxidants under mild conditions. In liquid phase oxidation by heteropolyanions, an addenda atom must be substituted by vanadium or one or more of redox active transition metal such as  $\text{Fe}^{3+}$ ,  $\text{Mn}^{3+}$ ,  $\text{Co}^{3+}$ , or  $\text{Cu}^{3+}$ .<sup>117</sup> Examples of oxidative catalysis by Keggin ions include the oxidation of alkanes, phenols and olefins, C-C bond cleavage of *vic*- diols, the epoxidation of alkenes, allylic acetoxylation, forming glycerol from allylic alcohols, gluteraldehyde from cyclopentene,<sup>118</sup> and oxidative bromination of aromatics.<sup>119</sup>

Tungsten and molybdenum catalysts are known to be efficient catalysts for oxidation by peroxides. Polyoxometalates with tungsten and molybdenum addenda atoms have been used to catalyze the oxidation of various organic substrates by hydrogen peroxide. Peroxo polyoxometalates are the active intermediate in the peroxidation of olefins, the oxidation of alcohols, glycols, and phenols in homogeneous or two-phase reactions.<sup>117</sup> The oxygen transfer mechanism in alkene epoxidation by transition metal complexes is still under debate. Sharpless has proposed a mechanism via a three center transition state where the alkene coordinates to one of the peroxo oxygens on the peroxo POM.<sup>120</sup> Experimental data from mononuclear peroxo complexes support the Sharpless mechanism,<sup>121</sup> but there is no direct information on the peroxo polyoxometalates.

Venturello designed the first polyoxometalate catalyzed peroxide oxidation in a biphasic  $\text{CHCl}_3$ - $\text{H}_2\text{O}$  system with 2-15%  $\text{H}_2\text{O}_2$  and tungstate and phosphate ions as the catalytic precursors to  $\{\text{PO}_4[\text{WO}(\text{O}_2)_2]_4\}^{3-}$ .<sup>122</sup> The epoxidation of 1-

octene with 15% H<sub>2</sub>O<sub>2</sub> in the presence of a quaternary salt of {PO<sub>4</sub>[WO(O<sub>2</sub>)<sub>2</sub>]<sub>4</sub>}<sup>3-</sup> resulted in 89% yield of epoxyoctane based on the initial H<sub>2</sub>O<sub>2</sub>.

In a similar system with 35% H<sub>2</sub>O<sub>2</sub> and tris-cetylpyridinium salts of PMo<sub>12</sub>O<sub>40</sub><sup>3-</sup> and PW<sub>12</sub>O<sub>40</sub><sup>3-</sup>, it was determined that the POM decomposed and the active catalysts were lower nuclearity peroxo species similar to the Veturello catalysts.<sup>123</sup> The anions BW<sub>12</sub>O<sub>40</sub><sup>5-</sup>, P<sub>2</sub>W<sub>18</sub>O<sub>62</sub><sup>6-</sup>, and SiW<sub>12</sub>O<sub>40</sub><sup>4+</sup> were inactive in these systems and did not change structure during the reaction, while H<sub>2</sub>WO<sub>4</sub> and H<sub>2</sub>W<sub>12</sub>O<sub>40</sub><sup>6-</sup> showed high activity for the epoxidation of 1-octene.<sup>124</sup>

Transition metal substituted polyoxometalates (TSMMP) such as [WM<sub>3</sub>(H<sub>2</sub>O)<sub>2</sub>(XW<sub>9</sub>O<sub>34</sub>)<sub>2</sub>]<sup>12-</sup> (X, M=Zn<sup>2+</sup>, Co<sup>2+</sup>, Mn<sup>3+</sup>, Fe<sup>2+</sup>, Fe<sup>3+</sup>, Ni<sup>2+</sup>, Cu<sup>2+</sup>, Pd<sup>2+</sup>, Pt<sup>2+</sup>, V<sup>4+</sup>, etc.) are stable to hydrolysis and also to degradation to H<sub>2</sub>O<sub>2</sub>. These anions are promising oxidation catalysts. The solvolytically stable disubstituted WZnMn<sub>2</sub>(H<sub>2</sub>O)<sub>2</sub>(ZnW<sub>9</sub>O<sub>34</sub>)<sub>2</sub><sup>12-</sup> is a highly active catalyst for the epoxidation of alkenes and for the oxidation of alcohols with thousands of turnovers and greater than 99% selectivity.<sup>125</sup> These catalysts have also been used to oxidize alkenols, diols, and amines.<sup>126</sup>

Mixed addenda POMs such as PW<sub>9</sub>V<sub>3</sub> and PW<sub>10</sub>V<sub>2</sub><sup>127</sup> and the TMSMP anions FePW<sub>11</sub>O<sub>39</sub><sup>4-</sup>,<sup>128</sup> and Ti<sub>2</sub>PW<sub>10</sub>O<sub>40</sub><sup>7-</sup>,<sup>129</sup> catalyze the peroxo oxidation of aromatics via an HO radical. Catalysis by PW<sub>10</sub>V<sub>2</sub> shows 92-98% selectivity for the peroxide oxidation of benzene to phenol and the catalyst structure and activity was maintained for over 576 hours. The FePW<sub>11</sub>O<sub>39</sub><sup>4-</sup> anion will also oxidize benzene to phenol although the decomposition of the H<sub>2</sub>O<sub>2</sub> is the major reaction.

{PO<sub>4</sub>[WO(O<sub>2</sub>)<sub>2</sub>]<sub>4</sub>}<sup>3-</sup> and WZnMn<sub>2</sub>(H<sub>2</sub>O)<sub>2</sub>(ZnW<sub>9</sub>O<sub>34</sub>)<sub>2</sub><sup>12-</sup> have been supported on silicate xerogels modified with phenyl and quaternary ammonium groups. The catalysts epoxidize alkenes at room temperature in the absence of an organic solvent.<sup>130</sup>

POM chemistry also can also be environmentally relevant, particularly when it is applied to non-polluting 'green technology' or to remediation methods to clean polluted segments of the environment. An example of an application to green technology is their use as a highly selective, multifunctional and reusable catalyst in production of wood pulp into paper.<sup>131</sup> The decontamination of water by the photocatalytic decomposition of organic pollutants, such as aromatic and chlorinated hydrocarbons by  $W_{10}O_{32}^{4-}$ ,  $PW_{12}O_{40}^{3-}$ , and  $SiW_{12}O_{40}^{4-}$ , is an example of their potential use for environmental remediation.<sup>132</sup> A range of POMs can be used in the efficient oxidation of  $H_2S$  to sulfur<sup>133</sup> and thioethers to sulfoxides and sulphones.<sup>134</sup>

Recent industrial applications of POMs in catalysis include the vapor phase oxidation of methacrolien to methacrylic acid<sup>135</sup> (at a volume of over 80,000 tons/year), the hydration of olefins, the polymerization tetrahydrofuran<sup>136</sup> and the oxidation of methane.<sup>137</sup>

Approximately two-thirds of the applied chemistry of POMs is based on  $H_3PMo_{12}O_{40}$ ,  $H_3PW_{12}O_{40}$ ,  $H_4SiMo_{12}O_{40}$ , and  $H_4SiW_{12}O_{40}$ . Their popularity is due to the large volume of literature describing their fundamental chemistry and their commercial availability. Given the enormous number of available POM complexes, it is obvious that plenty of opportunity exists for expanding the application of these materials. However, for these potentially promising reactions to be used in practice, complete recovery and recycling of POM catalysts is needed for catalyst design and scale up.<sup>117</sup>

## History

Berzelius<sup>138</sup> is credited for the discovery of polyoxoanions in 1826 when he mixed ammonium molybdate and phosphoric acid to form 12-molybdophosphate. Merignac followed with the discovery of tungstosilicic acid and its salts in 1862.<sup>139</sup>

The field developed rapidly, by the end of the century, sixty anions and hundreds of salts were known<sup>140</sup> and by the 1930s, hundreds of POMs were described in Gmelin.<sup>141</sup> The structures were harder to determine. Several theories on the structure of POMs were proposed, but the first structure was not solved until 1934, by Keggin.<sup>142</sup> By 1971 only a few structures were understood, but now X-ray diffraction and multinuclear NMR make structure determination much easier.

### Composition

Polyoxometalates (POMs) are inorganic metal-oxygen clusters of quasi-octahedral-coordinated metal oxides with the formula  $[M_mO_y]^p$  (isopolyanions) and  $[(XO_4)_xM_mO_y]^n$  ( $m > x$ ) (heteropolyanions). Generally  $M = V^V, Mo^{VI},$  or  $W^{VI}$  in the highest oxidation state, with only a few POMs formed from  $Nb^V, Ta^V,$  and  $Zr^{IV}$ . The  $M$  atoms defining the framework structure of a POM are called “addenda” atoms. More than one element can be present to form mixed-addenda POMs. The ability of an element to form a polyoxoanion is determined by ionic radius, charge, the ability to form  $d\pi-p\pi$  M-O bonds, and the capacity to accept variable coordination states. The metals must be able to fit in the holes of close-packed oxygen tetrahedra and octahedra and must be stable in the  $d^0$  oxidation state. The large number of polyoxoanions formed by  $V^V, Mo^{VI},$  and  $W^{VI}$  is due to their ability to take on variable coordination numbers, while  $Cr^{VI}$  is limited to POMs with  $Cr^{VI}$  in four coordination, and  $Nb^V$  and  $Ta^V$  to six coordination. In addition to the mixed addenda POMs, the heteroatom  $X$  (if present) can be from nearly any group of the periodic table except the noble gases.

In addition to the mixed addenda POMs, a fraction of the addenda atoms can be substituted by transition metals such as  $Fe^{2+,3+}, Mn^{2+}, Zn^{2+}, Co^{2+},$  or  $Cu^{2+}$ . These POMs are often designated Transition Metal Substituted Polyoxometalates (TSMMP).

## Structure

Polyoxometalate structures are governed by two general principles:<sup>114</sup>

1. Each metal atom occupies an  $\text{MO}_x$  polyhedron (most commonly an octahedron or square pyramid) in which the metal atoms are displaced, as a result of M-O  $\pi$  bonding, towards those polyhedral vertices that form the surface of the structure.
2. Structures with  $\text{MO}_6$  octahedra that contain three or more free vertices are not generally observed.<sup>143</sup>

The polyoxoanion ( $\text{MO}_n$ ) tetrahedral and octahedral building blocks are connected by corner and edge (octahedra only) linkages so that each polyhedra has one or two unshared oxygen vertices. The small highly charged addenda atoms polarize the exterior O atoms, causing the metal atoms to be displaced from the centers of their octahedra toward the external oxygen(s). Short M-O bonds are due to oxygen  $\pi$ -donation into the vacant d-orbitals of the metal. These oxygen atoms are relatively polarized and, therefore, they have a very weak attraction for  $\text{H}^+$ . There are three types of external oxygen atoms: terminal  $\text{M}=\text{O}$ , corner sharing M-O-M, and edge sharing M-O-M. The interior oxygens have cations on all sides and are not polarized in any one direction.

There are two types of polyoxometalates. Type 1 POMs have one terminal oxygen per addenda atom and can accommodate  $d^0$ ,  $d^1$ ,  $d^2$  metals. Type 1 POMs are able to undergo multiple electron reductions. Type 2 POMs have 2 terminal oxygens per metal center. The two mutually cis terminal oxygens of Type 2 POMs are restricted to  $d^0$  metals and they do not undergo reversible reductions.

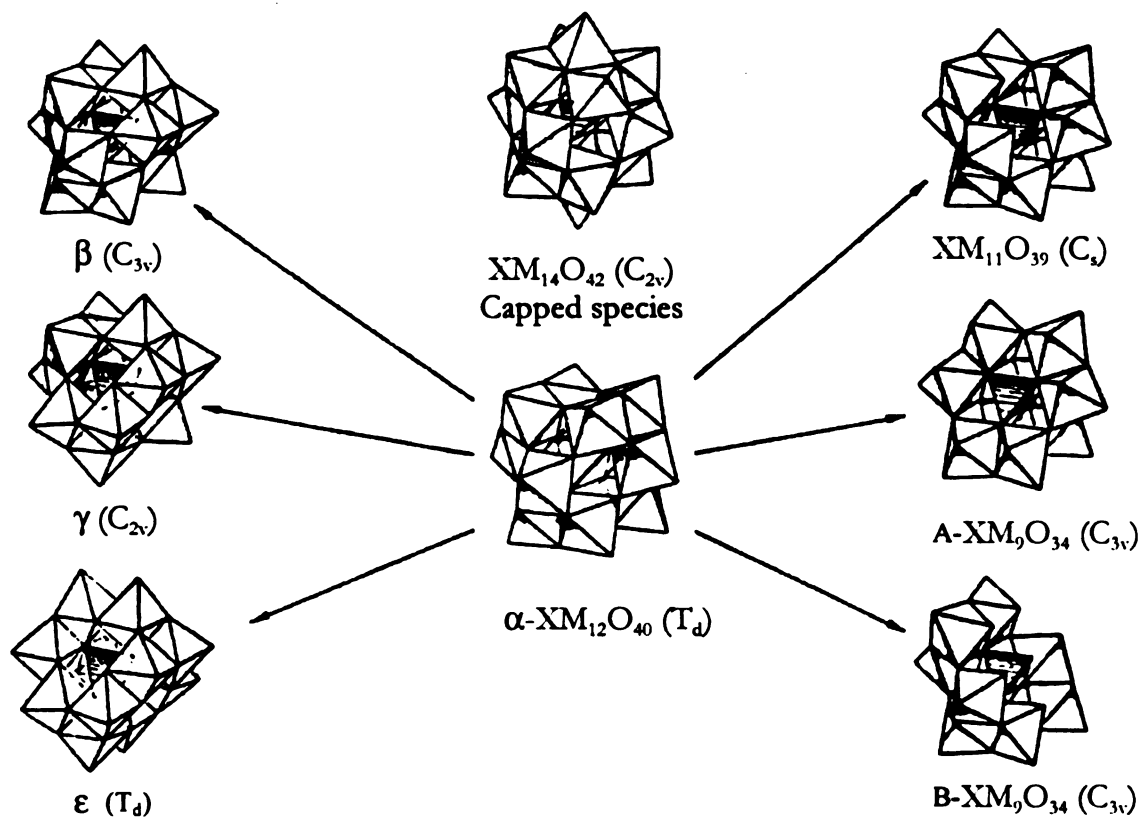


Figure 5-1. Schematic of the Keggin.<sup>114</sup> The  $\alpha$ - $XM_{12}O_{40}$  Keggin ion is shown with common derivatives. The left side shows the three isomers formed by the rotation of 1,2, or 4  $M_3$  triads. The lacunary ions on the right are formed by the dissociation of neutral  $MO_3$  octahedra. ( $H_2W_{12}O_{40}^{6-}$ ). The formula for the Keggin ion and its derivatives can be written as  $(XO_4)_nM_mO_{3m}$  where each Keggin ion (excepting  $H_2W_{12}O_{40}^{6-}$ ) has an internal  $XO_4$  tetrahedra and each addenda atom has one terminal oxygen. The Keggin anions are considered to be very weak bases with great softness.<sup>144</sup>

Most polyoxometalate structures can be derived from two parent structures. The  $\alpha$ - $\{(XO_4)(M_{12}O_{36})\}$  Keggin ion (Figure 5-1) is a common product of the self assembly of 12  $MO_3$  units which will occur even in the absence of a central tetrahedral  $XO_4$  unit.

Four isomers of the Keggin ion are possible. These are distinguished by a  $60^\circ$  rotation of 3 edge shared octahedra  $MO_3$  units, as illustrated on the left of Figure 5-1. Of the four possible isomeric structures, the existence of the  $\alpha$  and  $\beta$  have been verified. The lacunary anions shown on the right side of Figure 5-1 are formed by the removal of 1 or 3 adjacent  $MO_3$  groups. The dissociation of the neutral  $MO_3$  unit is facilitated by the strong trans effect of the terminal M-O bond. The resulting lacunary species can function as building blocks for multi-anion structures or as a reactive multi-dentate ligand. Transition metal substituted Keggin ions are formed when the lacunary ions coordinate the transition metal into the vacant octahedra. Larger ions form when two lacunary ions trap the transition metal to form a sandwich complex (Figure 5-3). Including heteroatoms, mixed addenda, and TSMPs, the number of isomers for Keggin ions is enormous.

The parent anion  $\{(XO_6)(M_{12}O_{32})\}$  shown in Figure 5-2 has not been observed as a discrete polyanion. All the derivatives of this structural type form Type 2 polyoxometalates with two terminal oxygens. They are based on edge sharing  $MO_6$  octahedra and may be considered fragments of cubic closest packing of oxygen. The  $M_7O_{24}$  POMs illustrated in Figure 5-2 are isomers. The planar bent structure is generally found for isopolyoxometalates as the central octahedra in the Anderson structure does not have any terminal M-O bonds. Internal  $MO_6$  are not generally observed for the addenda atoms. The Anderson structure is favored by heteropolyoxometalates.

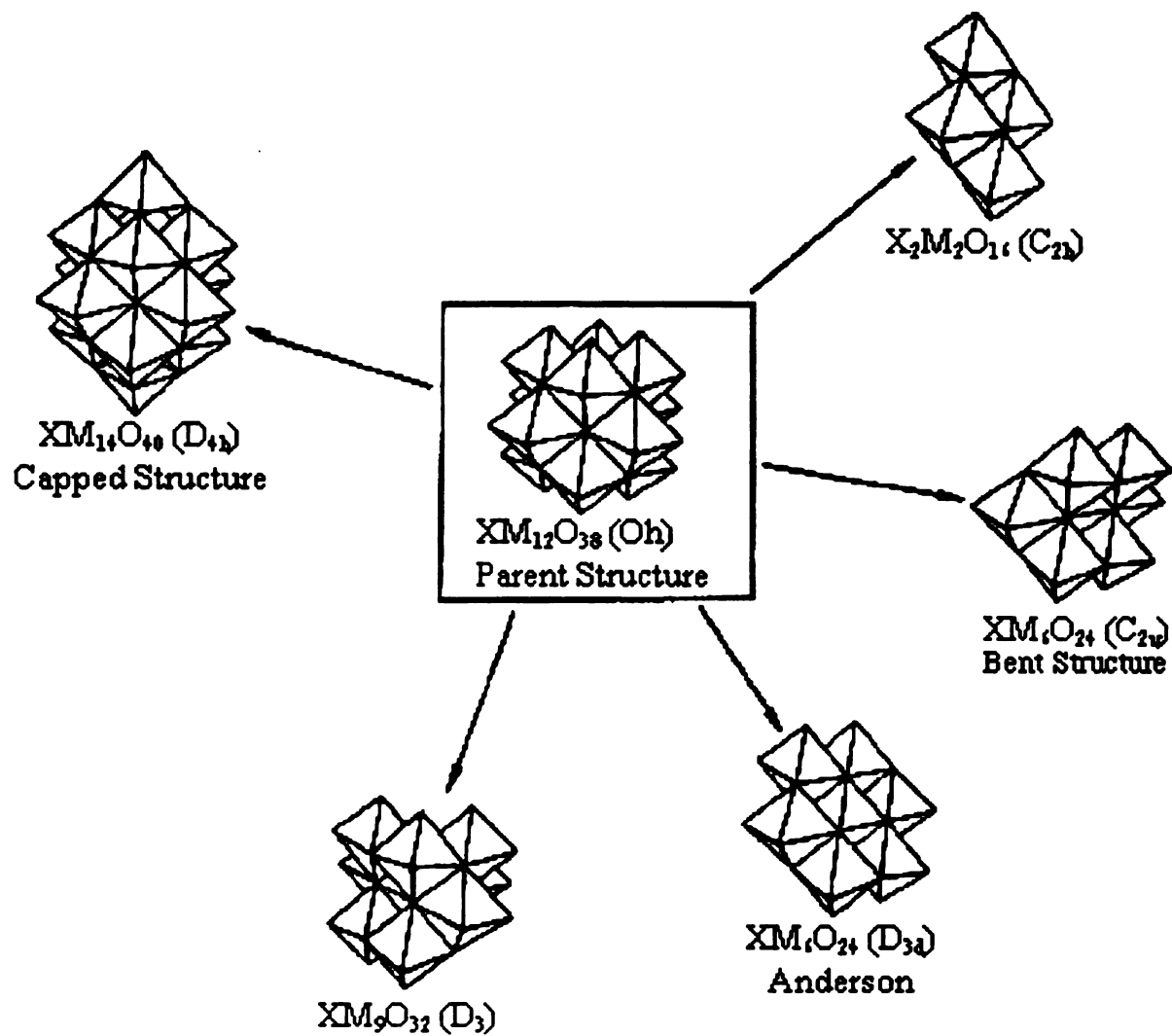


Figure 5-2. Examples of Type 2 structures where each addenda atom has two terminal oxygens.<sup>114</sup>

The structures  $\{(XO_{12})(M_{12}O_{30})\}$ ,  $\{M_6O_{19}\}$ , and  $\{(XO_4)_2M_5O_{15}\}$  are examples of less common polyoxometalate structures.

Recently, there has been considerable research involving macropolyoxometalates. These include the  $\{(XO_4)_2M_{18}O_{54}\}^{n-}$  Dawson and  $\{X_4M_{30}Z_4(H_2O)^2O_{112}\}^{n-}$  doubled Dawson,  $\{Z_4(H_2O)_2(XM_9O_{34})_2\}^{n-}$  (Figure 5-3) Finke and polyoxocryptates such as  $NaP_5W_{30}O_{110}^{14-}$  (Z = transition metal). The Dawson ion is formed by the fusion of two Keggin fragments formed spontaneously from  $Mo^{VI}$  and  $W^{IV}$  phosphates and arsenates. Isomers are formed from rotation of edge shared triads or the rotation of two half groups. A derivative of the Keggin ion, the Dawson structure incorporates internal  $XO_4$   $T_d$  attached by bridging oxygens and has single terminal oxygen for each addenda atom. The doubled Dawson is formed from a ring of four transition metals in oxide octahedra sandwiched between two lacunary Dawson ions. The Finke ion is similar to the doubled Dawson ion, with four transition metal cations sandwiched between lacunary Keggin ions.

The polyoxocryptate,  $NaP_5W_{30}O_{110}^{14-}$ , (Figure 5-3) is called the PJP anion after Preyssler,<sup>145</sup> Jeanin, and Pope.<sup>146</sup> It is composed of five  $(PO_4)W_6O_{18}^{3-}$  fragments with a rare 5-fold symmetry. The  $D_5$  symmetry is lowered to  $C_5$  due to the displacement of the Na atom to the center of one of the rings of ten W octahedra.

### *Synthesis*

Conversion of aqueous metalates to polyoxoanions is an equilibrium strongly dependent upon the ionic strength of the metal, the nature of the countercation, kinetics, and temperature. A thorough compilation of synthetic methods has been done by Tytko and Glemse<sup>147</sup> in 1990. The most common method of POM synthesis is through acidification of aqueous solutions of the

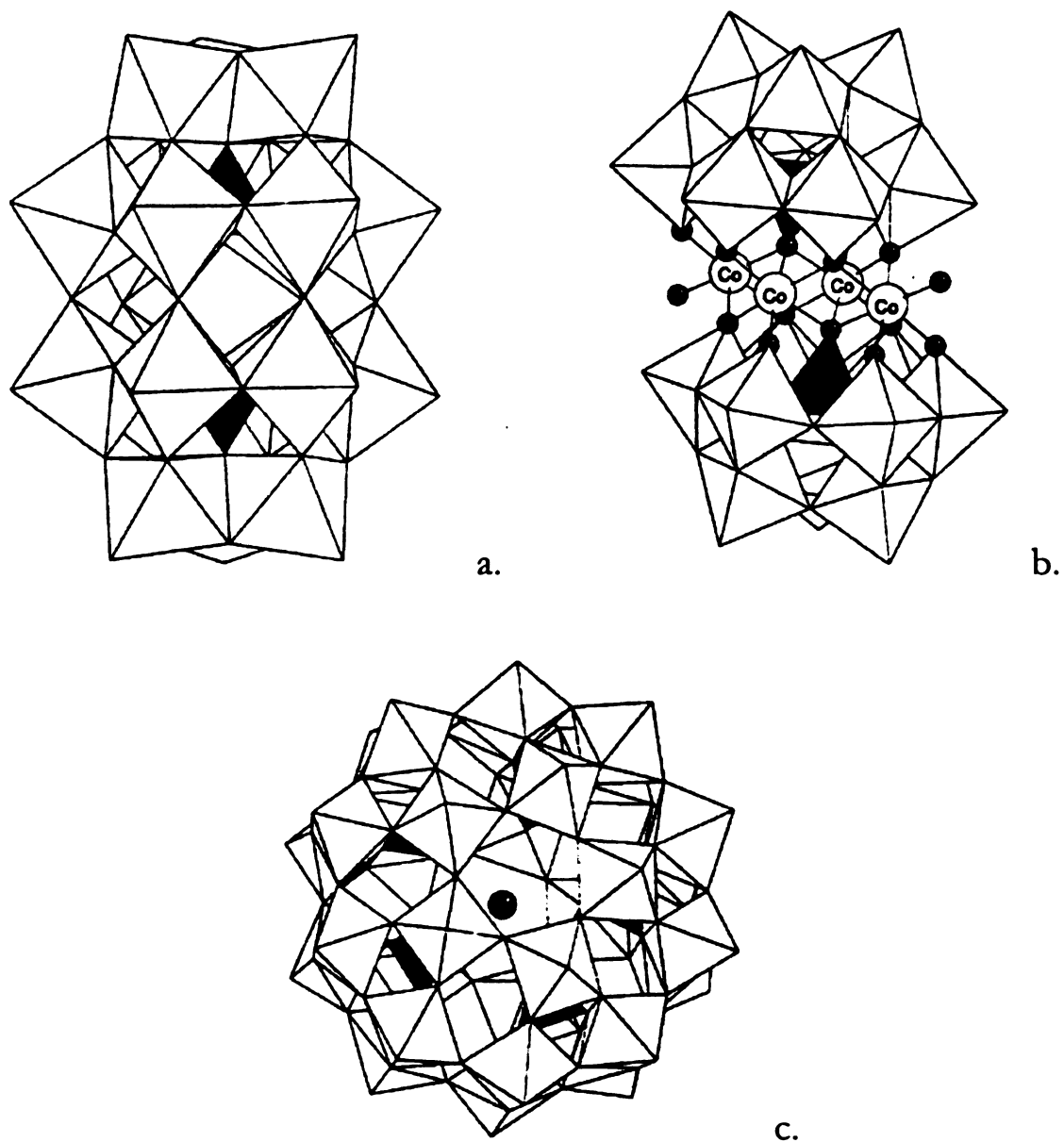
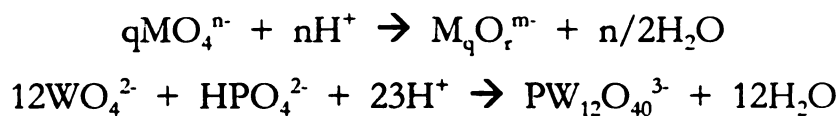


Figure 5-3. Schematic of some representative macropolyanions. a. A Dawson ion made from two  $M_9O_{31}$  Keggin lacunary ions. b. A Dawson TSMP complex sandwiching four planar Co octahdra. c. A PJP anion,  $NaP_5W_{30}O_{110}^{14-}$ . The Na cation is displaced from the center of the disk shaped anion.

mononuclear oxoanions and necessary heteroatoms. POMs can often be crystallized from stoichiometric mixtures of the components.



Several species may be in equilibrium and the predominant species may not be the compound isolated in crystalline form. In some cases, careful control of temperature or pH, sequence of addition, or specific catalysts may be necessary.

### *Isopolyanions*

Of Group 5 elements, only V<sup>V</sup> forms a significant range of isopolyanions. At pH > 6, tetrahedral [V<sub>2</sub>O<sub>7</sub>]<sup>4-</sup> is the dominant species. In the acidic region, six-coordinate decavanadates [H<sub>x</sub>V<sub>10</sub>O<sub>28</sub>]<sup>6-x-</sup> predominate. Other anions form in non-aqueous solvents or are metastable aqueous species. Niobium and Tantalum are limited to hexametalates [M<sub>6</sub>O<sub>19</sub>]<sup>6-</sup>.

Chromium from group 6 forms POMs based on tetrahedral CrO<sub>4</sub>, which are limited to [Cr<sub>2</sub>O<sub>7</sub>]<sup>2-</sup> and [Cr<sub>3</sub>O<sub>10</sub>]<sup>2-</sup>. Six coordinate molybdenum and tungsten form many isopolyanions. At pH = 5, paramolybdate and paratungstate [M<sub>7</sub>O<sub>24</sub>]<sup>6-</sup> are formed. In subsequent hydrolysis Mo and W form different structures, with tungsten ultimately converted to the Keggin structure, although other kinetically stable structures are known. In nonaqueous solvents it is possible to synthesize other structures.

### *Heteropolyanions*

The formation of a heteropoly complex involves the polymerization of addenda atoms around a heteroatom through a mechanism involving the attachment of protons to oxygens. The stereochemical requirements of the

heteroatom that control the architecture of the heteropolyanions. The strong polarization of the exterior layers of oxygens terminates further polymerization.<sup>148</sup>

### **Polyoxometalate Intercalated Layered Double Hydroxides**

There are several important considerations relevant to the intercalation of POMs into the gallery of an LDH. The pH stability of the POMs and LDHs, the reaction temperature, the swelling properties of the LDH, and the charge compensation between the LDH layers and the POM all affect the final product. The uniformity of the layer charge of the LDH effects the purity and crystallinity of the final product. In all examples of LDH-POM synthesis, there is an accompanying impurity phase present.

#### *Synthesis*

The only method for synthesizing LDHs that has not been used to synthesize LDH-POMs is the high temperature hydrothermal method (see Chapter 1). Table 5-2 lists the many polyoxometalates that have been intercalated into different LDH frameworks. The first preparation of an LDH polyoxometalate intercalate was reported by Woltermann.<sup>149</sup> However, the only evidence of the successful intercalation of the POMs into LDHs was the surface area of the calcined samples. The first authenticated crystalline LDH-POM was achieved through an anion exchange reaction of decavanadate ( $V_{10}O_{28}^{6-}$ ) and Keggin ions ( $XM_{12}O_{40}^{n-}$ ) with  $Zn_2Al-NO_3^-$ .<sup>150</sup> Since then several strategies for the intercalation of POMs have been advanced. In the method developed by Drezdron,<sup>76</sup> large organic ions were used to separate the layers, facilitating POM exchange. Chibwe and Jones<sup>151</sup> used a calcined  $Mg_2Al-CO_3^{2-}$  to form a metal oxide precursor which was rehydrated to form meixnerite, a  $Mg_2Al$  LDH

intercalated with OH<sup>-</sup>. This was followed by anion exchange with the desired POM. Narita et al. later showed this to be a general method<sup>152</sup> and in 1990, Dimotakis<sup>71</sup> showed that meixnerite could be swelled with glycols to facilitate POM anion exchange reactions. Direct synthesis of LDH-POMs<sup>153</sup> was followed by the intercalation of larger POMs such as Dawson and Finke ions into glycol solvated MgAl-adipate LDHs by Sang and Pinnavaia.<sup>154</sup> A direct coprecipitation method by Clearfield<sup>91</sup> used the hydrolysis of the urea to control the gradual increase in pH and avoid local changes in pH.

A novel *chimie douce*, or soft chemistry method was used by Delmas<sup>155</sup> to prevent fluctuation in chemical composition caused by the reaction of the acidic POMs with the basic LDH. A solid Na<sub>2</sub>Ni<sub>(1-x)</sub>Co<sub>x</sub>O<sub>2</sub> was formed through a high temperature synthesis to form a solid product with a d spacing of 5.18 Å. An oxidizing hydrolysis reaction with NaClO and KOH resulted in the insertion of K<sup>+</sup>, 7.08 Å, and was followed by reduction in an H<sub>2</sub>O<sub>2</sub>/NH<sub>4</sub>VO<sub>3</sub> solution. The intercalate was a polymeric metavanadate (VO<sub>3</sub>)<sub>n</sub><sup>n-</sup>.

Serwicka<sup>156</sup> intercalated PMo<sub>12</sub>O<sub>40</sub><sup>3-</sup> via electrochemical reduction of POM. The reduced Keggin ion is less acidic which aided in reducing, but not eliminating, the decomposition which occurs upon reaction with the basic LDH. Finally, very large macropolyanions such as the doubled-Dawson and PJP anions were intercalated into Mg<sub>3</sub>Al-OH<sup>-</sup> and Zn<sub>2</sub>Al-NO<sub>3</sub><sup>-</sup> through anion exchange reactions.<sup>3</sup>

Ulibarri<sup>157</sup> surveyed the various routes to intercalate POMs. The main effect of the different routes was in the pore size distribution. The use of large organic ions as pre-swelling agents creates stable pores with a narrow size distribution and minimizes the formation of impurity phases.

At the present time, anion exchange is the most common method for synthesizing LDH-POMs. Several techniques can be used to facilitate the most

difficult exchange reaction. One approach is to sonicate the LDH during the exchange reaction.<sup>158</sup> The reaction is aided by partial delamination of the LDH. Kooli and Jones<sup>159</sup> found that exchange reactions done at pH 4.5 did not need to be kept under N<sub>2</sub>. The low pH eliminated carbonate formation and its subsequent intercalation into the LDH phase. They also identified the pH needed for successful anion exchange of different LDH cation compositions.<sup>162</sup>

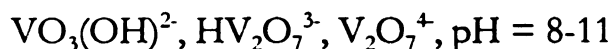
**Layered Double Hydroxides Intercalated with Isopolyoxometalates**

*Molybdates*

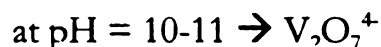
Heptamolybdate ( $\text{Mo}_7\text{O}_{24}^{6-}$ ) which is the predominant solution species between pH 6-4, has been the major isopolymolybdate to be intercalated into LDHs. Drezdzon<sup>76</sup> claimed that the  $\text{MgAl-Mo}_7\text{O}_{24}^{6-}$  was stable to 400 °C, however this conclusion was based exclusively on morphology of the calcined LDH-POM. Twu and Dutta<sup>160</sup> used Raman and XRD to study  $\text{MgAl-Mo}_7\text{O}_{24}^{6-}$  intercalates and found that the  $\text{MgAl-LDH}$  layers decomposed at 120 °C, but that the  $\text{Mo}_7\text{O}_{24}^{6-}$  anion was stable to 350 °C. The XRD was not extended to the range where the LDH in plane reflection would appear and the Raman spectrum was not recorded in the range where polymeric Mo-O-Mo bonds would appear. Hibino and Tsumashima saw a loss of the XRD pattern when  $\text{MgAl-Mo}_7\text{O}_{24}^{6-}$  was dried at 80 °C, but the heptamolybdate intercalate was reconstituted in water.<sup>161</sup> They also performed anion exchange reactions in a 50:50 MeOH/water solvent mixture and saw a difference in the physical properties of the exchanged product, however, the XRD patterns were not significantly different from the product produced by Drezdzon's *in situ* hydrolysis method.<sup>76</sup>

### *Vanadates*

There have been many studies on isopolyvanadate intercalated LDHs. There are several isopolyvanadates species present in the pH range 12-4.



The first crystalline LDH-POM was a  $V_{10}O_{28}^{6-}$  intercalated into ZnAl-, NiAl-, and ZnCr-LDHs by anion exchange at pH = 4.5. The d spacing of the product was 11.9 Å.<sup>103</sup> Battacharyya<sup>168</sup> and Besse<sup>169</sup> both used careful regulation of the reaction pH to control the nuclearity of intercalated species. On the basis of Battacharyya's studies of MgAl and MgZnAl LDHs and the work of Besse on CrCu LDH systems, the following relationship between pH and the vanadate intercalate has been established:



Besse used a large organic anion as swelling agents to facilitate anion exchange and found that the size of the precursor anion favored the intercalation of a vanadate with similar size.

Similar studies with MgCr and NiCr LDHs verified the importance of using a hydrated LDH as a precursor, but the layer cation determined the optimal pH for intercalation. The optimal pH for intercalation of decavanadate into a MgCr LDH was 6.5 for and 5.5 for a NiCr LDH.<sup>162</sup>

## *Tungstates*

The isopolytungstate intercalates have not been as thoroughly studied as the molybdates and vanadates, although they are commonly used for catalytic activity studies. Along with heptatungstate, two isomers of dodecatungstate, namely metatungstate and paratungstate A,<sup>163</sup> have been intercalated into MgAl- and ZnAl-LDHs.

### **LDHs Intercalated with Heteropolyoxometalates**

Kwon and Pinnavaia<sup>163</sup> intercalated a variety of Keggin anions with varying charges into ZnAl-LDHs. The intercalation of a Keggin ion was limited by the charge on the ion. Keggin ions with a charge less than 6- did not intercalate into Zn<sub>2</sub>Al-LDHs. This is due to the area needed by the Keggin ion, diameter = 9.8 Å, area = 83 Å<sup>2</sup>. The charge density of 2:1 LDH is 16.6 Å<sup>2</sup>/e. The surface area for Zn<sub>2</sub>Al- $\alpha$ -[SiV<sub>3</sub>W<sub>9</sub>O<sub>40</sub>]<sup>7-</sup> was 155 m<sup>2</sup>/g, compared to 26 m<sup>2</sup>/g for the Zn<sub>2</sub>Al-NO<sub>3</sub><sup>-</sup> precursor. Wang et al. intercalated PW<sub>12</sub>O<sub>40</sub><sup>3-</sup> into MgAl-LDHs with a d spacing of 12 Å. The low d spacing (compared to 14.6 for Keggin ions) was explained as being an effect of the partial dissolution of the divalent cation in the acidic media. This results in partial removal of hydroxyl groups and leads to vacancies where the Keggin ions could fit. This would lead to lower d spacings than expected and also explains the intercalation of a 3- Keggin ion.<sup>173</sup> Studies with NiAl-CO<sub>3</sub><sup>2-</sup> LDH precursor showed that exchange only occurred when the NiAl-LDH was maintained in aqueous suspension and not allowed to dry prior to anion exchange.<sup>164,165</sup>

Keggin ions are treated as spherical anions, whereas Dawson and Finke anions are cylindrical. The d spacing for an LDH intercalated with a Keggin ion has been shown experimentally to be 14.6-14.8 Å. Studies involving <sup>31</sup>P and <sup>27</sup>Al MAS-NMR have been used to determine that Keggin ions are oriented with

**Table 5-2. Summary of Polyoxometalate Intercalated Layered Double Hydroxides**

Polyoxometalate	LDH Framework	Method	pH	d spacing Å	Ref.
<b>Isopolyoxometalates</b>					
$\text{Mo}_7\text{O}_{24}^{6-}$	$\text{Mg}_3\text{Al}, \text{Mg}_2\text{Al}, \text{Zn}_2\text{Al}$	anion exchange swell/exchange reconstruction	4.4- amb.	9.9-12.2	161,76 166,2 7
$\text{W}_7\text{O}_{24}^{6-}$	$\text{Mg}_2\text{Al}, \text{Zn}_2\text{Al}$	swell/exchange	4.4	12.2	2
$\text{H}_2\text{W}_{12}\text{O}_{40}^{6-}$	$\text{Zn}_2\text{Al}, \text{Mg}_x\text{Al}$ $x=2,3$	anion exchange reconstruction swell/exchange	4.4- amb.	14.6	163,71 178,179 167,2
$\text{H}_2\text{W}_{12}\text{O}_{42}^{10-}$	$\text{Mg}_3\text{Al}, \text{Zn}_2\text{Al}$	anion exchange swell/exchange	4.4- amb.	12.2-14.8	163 7
$\text{HV}_2\text{O}_7^{3-}$	$\text{Mg}_2\text{Al}$	coprecipitation	8.8	9.4	168
$\text{V}_2\text{O}_7^{4-}$	$\text{Mg}_2\text{Al}, \text{Mg}_2\text{Zn}_2\text{Al}, \text{Cu}_2\text{Cr}$	coprecipitation	10-11	10.5	168 169
$\text{V}_4\text{O}_{12}^{4-}$	$\text{Mg}_2\text{Al}, \text{Mg}_2\text{Zn}_2\text{Al}, \text{Cu}_2\text{Cr}$	Coprecipitation	6-8	9-10	168 169
$\text{V}_{10}\text{O}_{28}^{6-}$	$\text{Mg}_2\text{Al}, \text{Zn}_2\text{Al}, \text{Zn}_2\text{Cr}, \text{Ni}_3\text{Al}, \text{CuCr}, \text{MgCr}, \text{NiCr}$	anion exchange swell/exchange reconstruction	4-6.5	11.9	76 161 166 150,171
<b>Hetero-polyoxometalates</b>					
$\alpha\text{-SiW}_{12}\text{O}_{40}^{4-}$	$\text{Zn}_2\text{Al}$	anion exchange		14.6	163
$\alpha\text{-PW}_{12}\text{O}_{40}^{3-}$	$\text{Zn}_2\text{Al}$	anion exchange		14.6	163
$\alpha, \beta\text{-SiW}_{11}\text{O}_{39}^{8-}$	$\text{Mg}_3\text{Al}, \text{Zn}_2\text{Al}$	reconstruction/ swell reconstruction coprecipitation	6.0	14.6-14.8	72 152 153
$\text{PW}_{11}\text{O}_{39}^{7-}$	$\text{Mg}_x\text{Al}, \text{Mg}_x\text{Ga}$ $x=2-4$	swell/exchange	5-6	14.6-14.8	170
$\text{BW}_{11}\text{O}_{39}^{9-}$	$\text{Mg}_3\text{Al}, \text{Zn}_2\text{Al}$	swell/exchange	amb.	14.5	179
$\text{PW}_9\text{O}_{34}^{9-}$	$\text{Mg}_3\text{Al}, \text{Zn}_2\text{Al}$	swell/exchange	amb.	14.5	179
$\text{V}_2\text{W}_4\text{O}_{19}^{4-}$	$\text{Mg}_2\text{Al}, \text{Zn}_2\text{Al}$	ion exchange coprecipitation	<7	12	171
$\text{HV}_4\text{W}_8\text{PO}_{40}^{6-}$	$\text{Mg}_2\text{Al}$	ion exchange coprecipitation	<7	14.7	171

Polyoxometalate	LDH Framework	Method	pH	d spacing Å	Ref.
$\alpha$ -SiV <sub>3</sub> W <sub>9</sub> O <sub>40</sub> <sup>7-</sup>	ZnAl	anion exchange reconstruction		14.6-14.8	163,152 179
PVW <sub>11</sub> O <sub>40</sub> <sup>4-</sup>	Zn <sub>2</sub> Al	anion exchange		14.5-14.8	172 175 179
PV <sub>n</sub> W <sub>(12-n)</sub> O <sub>40</sub> <sup>(3+n)-</sup> (n=0-4)	Mg <sub>x</sub> Al, Ni <sub>x</sub> Al, Zn <sub>x</sub> Al, x=2,5	anion exchange	4-7	11.4-12.2	173 174
PV <sub>3</sub> W <sub>9</sub> O <sub>40</sub> <sup>6-</sup>	Cu <sub>2</sub> Al, Ni <sub>5</sub> Al	coprecipitation	7-11	11-12	68
BVW <sub>11</sub> O <sub>40</sub> <sup>7-</sup>	Mg <sub>3</sub> Al, Zn <sub>2</sub> Al	swell/exchange	6-amb.	14.1	179
PCu(H <sub>2</sub> O)W <sub>11</sub> O <sub>39</sub> <sup>5-</sup>	ZnAl	anion exchange		14.8	163
PCr(H <sub>2</sub> O)W <sub>11</sub> O <sub>39</sub> <sup>4-</sup>	ZnAl	anion exchange		14.6	175
PTiW <sub>11</sub> O <sub>40</sub> <sup>5-</sup>	ZnAl	anion exchange		14.6	175
SiCo(H <sub>2</sub> O)W <sub>11</sub> O <sub>39</sub> <sup>6-</sup>	ZnAl	sonication/exchange		14.7	176
[XZ(H <sub>2</sub> O)W <sub>11</sub> O <sub>39</sub> ] <sup>n-</sup> (x=Si; Z= Co, Ni, Cu, Al)	Zn <sub>2</sub> Al	anion exchange	amb.	14.5	172
[Ln(XW <sub>11</sub> O <sub>39</sub> ) <sub>2</sub> ] <sup>n-</sup> (Ln=La, Ce <sup>III</sup> ; X=Si, P, B)	Zn <sub>2</sub> Al	anion exchange	amb.	14.4	172
SiX(H <sub>2</sub> O)W <sub>11</sub> O <sub>39</sub> <sup>6-</sup> (X=Co, Mn)	MgAl	anion exchange		15.2	177
$\alpha$ -P <sub>2</sub> W <sub>18</sub> O <sub>62</sub> <sup>6-</sup>	Mg <sub>3</sub> Al	anion exchange reconstruction	amb.	17.4-19.3	178
Co <sub>4</sub> (H <sub>2</sub> O) <sub>2</sub> (PW <sub>9</sub> O <sub>34</sub> ) <sub>2</sub> <sup>10-</sup>	Mg <sub>3</sub> Al	anion exchange reconstruction	amb.	17.7	178
$\alpha$ -P <sub>2</sub> W <sub>17</sub> O <sub>62</sub> <sup>10-</sup>	Mg <sub>3</sub> Al, Zn <sub>2</sub> Al	anion exchange reconstruction	amb.	17.4	2
Nb <sub>x</sub> W <sub>(6-x)</sub> O <sub>19</sub> <sup>(x+2)-</sup>	Mg <sub>x</sub> Al, Zn <sub>x</sub> Al x < 2	anion exchange coprecipitation	5.8-11.6	14.7	171
Ti <sub>2</sub> W <sub>10</sub> O <sub>40</sub> <sup>7-</sup>	Mg <sub>x</sub> Al, Zn <sub>x</sub> Al x < 2	anion exchange coprecipitation	7.6	14.7	74
SiFe(III)(SO <sub>3</sub> )W <sub>11</sub> O <sub>39</sub> <sup>7-</sup>	Mg <sub>3</sub> Al, Zn <sub>3</sub> Al	swell/exchange	amb.	14.7	179
PMo <sub>2</sub> W <sub>9</sub> O <sub>39</sub> <sup>7-</sup>	Mg <sub>3</sub> Al, Zn <sub>3</sub> Al	swell/exchange	amb.	14.5	179
BCo(II)W <sub>11</sub> O <sub>39</sub> <sup>7-</sup>	Mg <sub>3</sub> Al, Zn <sub>2</sub> Al	swell/exchange	amb.	14.3	179
BCu(II)W <sub>11</sub> O <sub>39</sub> <sup>7-</sup>	Mg <sub>3</sub> Al, Zn <sub>2</sub> Al	swell/exchange	amb.	14.4	179,179
P <sub>4</sub> W <sub>30</sub> Zn <sub>4</sub> (H <sub>2</sub> O) <sub>2</sub> O <sub>112</sub> <sup>16-</sup>	Mg <sub>3</sub> Al, Zn <sub>2</sub> Al	anion exchange swell/exchange	amp	16.3	3
NaSb <sub>8</sub> W <sub>21</sub> O <sub>86</sub> <sup>18-</sup>	Mg <sub>3</sub> Al, Zn <sub>2</sub> Al	anion exchange swell/exchange	amb.	17.6	3
NaAs <sub>4</sub> W <sub>40</sub> O <sub>140</sub> <sup>27-</sup>	Mg <sub>3</sub> Al, Zn <sub>2</sub> Al	anion exchange swell/exchange	amb.	14.7	3
NaP <sub>5</sub> W <sub>30</sub> O <sub>110</sub> <sup>14-</sup>	Mg <sub>3</sub> Al, Zn <sub>2</sub> Al		"amb.	21-22	3

their  $C_2$  axis perpendicular to the LDH layers.<sup>172</sup> Two orientations are possible for Dawson and Finke transition metal substituted polyoxometalates. The Dawson ions can be intercalated with either the long  $C_3$  axis perpendicular (19.3 Å) or parallel (17.4 Å) to the LDH layers. The parallel orientation, obtained at higher temperature, is the most stable orientation. Intercalation of Finke ions always results in the more stable orientation with the long axis parallel to the LDH layers.<sup>178</sup>

### *Macropolyoxometalates*

There are only a few reports of LDH-macropolyoxometalates. The first large polyoxometalates intercalated into LDHs by anion exchange were reported in a patent by Pinnavaia et al.,<sup>179</sup> one of which was the PJP anion. Evans et al. used extended X-ray absorption fine structure (EXAFS) to characterize a  $Zn_{1.3}Al$ -PJP. The EXAFS derived structural parameters did not give any evidence for the formation of mixed salts or for the polyoxometalate fitting into defects in the LDH layers. Wang et al., intercalated  $P_2W_{18}O_{62}^{6-}$  and the PJP anion into  $Ni_5Al$ -LDHs for the catalytic conversion of isopropanol to propylene and acetone. Recently, macropolyoxometalates including the Dawson ion,  $\alpha$ - $P_2W_{17}O_{61}^{10-}$ , two Finke ions,  $Zn_4(H_2O)_2(AsW_9O_{34})_2^{10-}$  and  $WZn_3(H_2O)_2(ZnW_9O_{34})_2^{12-}$ , a double Dawson,  $P_4W_{30}Zn_4(H_2O)O_{112}^{16-}$  and the inorganic cryptates, and  $NaSb_9W_{21}O_{86}^{18-}$  have been intercalated into  $MgAl$ - and  $ZnAl$ -LDHs.<sup>3</sup> These LDH-POMs can be defined as pillared LDHs, even though the surface area is less than expected from theoretical calculations.

**Table 0-3. Oxidation Reactions with Intercalated Polyoxometalate Catalysts**

Polyoxometalate	LDH	Oxygen Source	Substrate	Product	Effect of Intercalation	Ref.
$V_{10}O_{28}^{6-}$	$Zn_2Al$	$O_2$	isopropanol	acetone	increased photo-activity	62
$PV_3W_9O_{40}^{6-}$ , $PW_{12}O_{40}^{3-}$	$Ni_5Al$		isopropanol	acetone, propylene	increased selectivity for propylene	70
$Mo_7O_{24}^{6-}$ $H_2W_{12}O_{40}^{6-}$ $W_{12}O_{41}^{10-}$	$Mg_2Al$ $Zn_2Al$	$H_2O_2$	2-hexene, cyclohexene, $\beta$ -methylstyrene	oxide, diol	size selectivity	7.2
$SiW_{11}O_{39}^{8-}$ $SiZ(H_2O)W_{11}O_{39}^{6-}$ Z = $Co^{2+}$ , $Ni^{2+}$ , $Cu^{2+}$	$ZnAl$	$H_2O_2$	benzaldehyde	benzoic acid	increased activity	77
$XZ(H_2O)W_{11}O_{39}$ X = P, Si; Z = $Mn^{2+}$ , $Fe^{2+}$ , $Co^{2+}$ , $Cu^{2+}$		$O_2$	cyclohexene		tuning of catalytic site	78
$SiCo(H_2O)W_{11}O_{39}^{6-}$	$ZnAl$	$H_2O_2$	benzaldehyde	benzoic acid	increased activity	72
$SiW_{12}O_{42}^{8-}$	$ZnAl$		isobutene with butene	alkylation	bifunctional acid-base catalyst	79
$PW_{10}O_{39}^{15-}$ $SiW_{12}O_{40}^{4-}$	$MgAl$		propylene oxide + ethanol	2-ethoxy-1-propanol, 1-ethoxy-2-propanol	acid versus base catalysis	80

## Applications

Table 5-3 lists many of the polyoxometalate intercalated LDHs which have been used in oxidation reactions. One of the first examples of catalysis by LDH-POMs was photocatalysis of isopropanol to acetone by  $\text{Zn}_2\text{Al-H}_2\text{W}_{12}\text{O}_{40}^{6-}$ ,  $\text{BVW}_{11}\text{O}_{40}^{7-}$ , and  $\text{SiV}_3\text{W}_9\text{O}_{40}^{7-}$ .<sup>184</sup> This was followed by Tatsumi's<sup>7</sup> report of size selective oxidation of olefins by  $\text{MgAl-Mo}_7\text{O}_{24}^{6-}$  and  $-\text{H}_2\text{W}_{12}\text{O}_{40}^{6-}$ .

The Keggin ions,  $\text{SiW}_{12}\text{O}_{42}^{8-}$  and  $\text{PW}_{12}\text{O}_{42}^{7-}$  were used for the alkylation of iso-butene with butene.<sup>182</sup> The calcined LDH-POM (300 °C) had a higher butene conversion as well as a higher  $\text{C}_{12}$  and  $\text{C}_{16}$  product selectivity. Wang et al. used TSMP Keggin ions intercalated into a variety of LDH supports as catalysts for the conversion of isopropanol to acetone and propene.<sup>173</sup> Lopez-Salinas<sup>177</sup> found that the coordinatively unsaturated X centers in  $\text{LDH-SiX(H}_2\text{O)W}_{11}\text{O}_{39}^{6-}$  ( $\text{X}=\text{Co, Mo}$ ) can reversibly absorb small molecules such as water methanol, ethanol or ammonia, while larger molecules like pyridine or tetrahydrofuran cannot access the interlayer Keggin anion. The variation acid/base functionality of  $\text{MgAl-H}_2\text{W}_{12}\text{O}_{40}^{6-}$  as determined through the dehydration/cleavage reaction of 2-methyl-3-butyn-2-ol as a reactive probe, was attributed to the differences in porosity obtained by the various LDH-POM synthetic methods.<sup>167</sup> Kayuga and Jones correlated the catalytic activity of  $\text{MgAl-SiW}_{12}\text{O}_{40}^{4-}$  to the surface area and basic sites in the aldol condensation of acetaldehyde. The catalytic activity is directly related to the surface area and the selectivity is related to the number and strength of the basic sites of the LDH support.

## Chapter 6. Polyoxometalates and Their Intercalation into Layered Double Hydroxides

### Introduction

Considerable effort has been invested in the design of layered double hydroxides (LDHs) intercalated with robust POMs for applications in shape-selective adsorption and catalysis. In practice however, polyoxometalate intercalated LDHs have not yet reached their anticipated potential as heterogeneous catalysts. Substrate size and shape selectivity implies a pillared LDH, which would allow the substrate access to POM catalysts buried deep within the LDH layers. The intercalation of large, highly-charged polyoxometalate anions into LDHs fulfills the requirement of a pillared material as a result of the increase in the layer separation and the lateral separation of the anions as calculated from the charge per unit area of the POM and the LDH. However, the observed microporous surface areas are not as high as the theoretical values calculated from the gallery heights and charge densities of the intercalated POM anions. Access to the microporous galleries may be limited by POM salt impurities deposited on the edges of the particles. These impurities are present in all polyoxometalate intercalated layered double hydroxides reported to date. As a result, two different approaches to the immobilization of catalytic anions on LDH supports have emerged. One approach is to immobilize the catalysts on the external LDH surface without intercalation. In

this case, selectivity is introduced through the basic nature of the LDH framework and the hydrophilic/hydrophobic properties of the gallery anion.<sup>185</sup> The second approach is to intercalate an anionic catalyst in order to control the selectivity. Several pillared LDH-POM derivatives have been shown to be active catalysts for the oxidation of cyclohexene with molecular oxygen by transition metal substituted Keggin ions,<sup>181</sup> the epoxidation of alkenes by lower nuclearity peroxotungsten compounds,<sup>1</sup> as well as other oxidation reactions.<sup>186</sup> But in all these examples, it has not been possible to separate the catalytic activity of the intercalated anion from that of the ever present impurity phase. So far, only one study has been reported concerning shape selectivity for an LDH-POM catalytic reaction.

Tatsumi et al.,<sup>7</sup> were the first to suggest substrate shape selectivity for LDH catalysts interlayered by polyoxomolybdate and tungstate anions. The active phases were identified as Mg<sub>2</sub>Al-LDHs of heptamolybdate, [Mg<sub>12</sub>Al<sub>6</sub>(OH)<sub>36</sub>]Mo<sub>7</sub>O<sub>24</sub>·mH<sub>2</sub>O, (d spacing = 9.9 Å) and paratungstate B (dodecatungstate), [Mg<sub>20</sub>Al<sub>10</sub>(OH)<sub>60</sub>]H<sub>2</sub>W<sub>12</sub>O<sub>42</sub>·mH<sub>2</sub>O (d spacing = 12.2 Å). Both intercalates were better catalysts for the oxygenation of 2-hexene than the unsupported POMs. More importantly, for the epoxidation of 2-hexene and cyclohexene, the intercalated POMs were 4-6 times more selective in favor of the smaller 2-hexene substrate than the homogeneous catalysts.

In light of the substrate selectivity effects reported by Tatsumi et al., the present study was initiated with the intent of extending the selective oxidation catalysis of LDH-POM to include acidic Zn<sub>2</sub>Al-LDH hosts. In contrast to basic Mg<sub>2</sub>Al-POMs, Zn<sub>2</sub>Al-LDH derivatives can be formed at acidic pH values where many POM anions are stable. Consequently, hydrolysis reactions between the POM and LDH host are less likely to occur. However, the synthetic method used to prepare the original catalysts affords products that are much more

complex that previously realized. The results to be presented here indicate that the relevant  $\text{Mg}_2\text{Al-LDH}$  phases are structurally unstable even under relatively mild conditions. In contrast, the acidic  $\text{Zn}_2\text{Al-LDH}$  phases are more stable, particularly when the gallery anion is the relatively robust  $\text{H}_2\text{W}_{12}\text{O}_{40}^{6-}$  Keggin ion. Even in this latter case, substrate shape selectivity is precluded by the lack of intracrystalline microporosity under condensed phase reaction conditions. Thus, the selectivity reported by Tatsumi cannot be attributed to shape selectivity effects.

Next, a stable  $\text{Zn}_2\text{Al-P}_5\text{W}_{30}\text{O}_{110}^{14-}$  intercalate LDH-POM with a d spacing of 21.5 Å was selected for study as a catalyst for the oxidation of cyclohexene. The expectation was that in the case of  $\text{Zn}_2\text{Al-P}_5\text{W}_{30}\text{O}_{110}^{14-}$ , the partial blocking of the pores by the impurity salt would not be sufficient to restrict access of organic substrates to the intergallery catalysts. The results of the catalytic studies show that while access to the intergallery  $\text{P}_5\text{W}_{30}\text{O}_{110}^{14-}$  catalyst remains a limitation, the LDH support is vital to the catalytic activity and product selectivity.

## Results and Discussion

### Catalyst Synthesis and Characterization

The substrate-selective LDH-POM catalysts<sup>7</sup> were prepared, according to Tatsumi, by *in situ* hydrolysis of  $\text{MO}_4^{2-}$  followed by anion exchange, a method originally developed by Drezdson.<sup>76</sup> A  $\text{Mg}_2\text{Al-Terephthalate}$  (TA) was synthesized by coprecipitation and added to a solution of  $\text{MO}_4^{2-}$ . The pH of the solution is lowered with the addition of  $\text{HNO}_3$ , the isopolyoxometalate forms, and undergoes ion exchange reaction with the LDH-TA. As shown by the X-ray diffraction patterns in Figure 6-1, the XRD of a thin film sample of  $\text{Mg}_2\text{Al-}$

# $\text{Mg}_2\text{Al-Mo}_7\text{O}_{24}^{6-}$ System

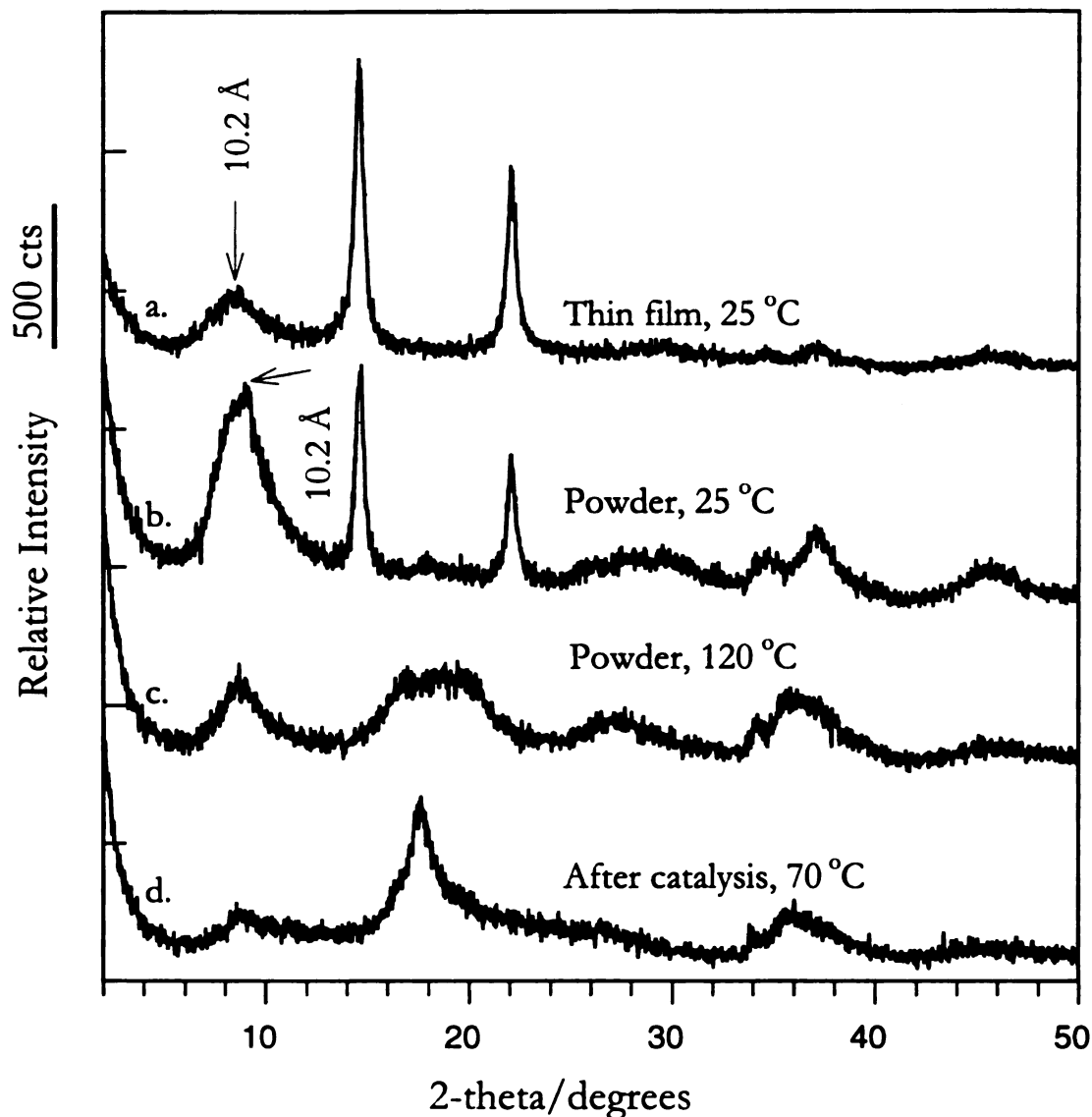


Figure 6-1. X-ray diffraction patterns of the mixed phase product formed by in situ hydrolysis of  $\text{Na}_2\text{WO}_4$  in the presence of a  $\text{Mg}_2\text{Al}$ -terephthalate: a. thin film sample dried under ambient conditions; the sharp reflections are (001) lines of  $[\text{Mg}_{12}\text{Al}_6(\text{OH})_{36}](\text{Mo}_7\text{O}_{24})^{6-}$  with a basal spacing of 12.2 Å, whereas the broad lines are due to a salt-like impurity phase with a spacing of 10.2 Å. b. powder sample, dried under ambient conditions, showing a marked reduction in the intensity of the LDH phase; c. powder sample dried overnight at 120 °C showing the loss of the  $\text{Mg}_2\text{Al-Mo}_7\text{O}_{24}^{6-}$  phase; d. thin film of sample after use as a catalyst in the oxidation of cyclohexene.

$\text{Mo}_7\text{O}_{24}^{6-}$  dried at room temperature has sharp 00l reflections characteristic of the 12.2 Å phase of  $\text{Mg}_2\text{Al-Mo}_7\text{O}_{24}^{6-}$ , although they are of very low intensity. The 001 reflection is buried under a broad impurity peak at  $\sim 10.2$  Å. The XRD pattern is consistent with a mixture of an authentic  $\text{Mg}_2\text{Al-Mo}_7\text{O}_{24}^{6-}$  LDH phase and a salt-like  $\text{Mg}^{2+}$ - or  $\text{Al}^{3+}$ -POM impurity phase. When the XRD pattern of the reaction product is obtained for an unoriented powder sample (Figure 6-1b) rather than a film, the impurity phase reflection increases greatly relative to the LDH phase. That is, the preferred orientations of the LDH platelets in a thin film sample masks the salt-like impurity. The ratio of Mg:Al:Mo by ICP analysis is 1.7:1.0:0.82, whereas the expected ratio is 2.00:1.00:1.17. These values do not give an accurate indication of the Mg:Al:Mo ratio in the LDH phase, because the impurity also adds to the total metal content.

In the catalytic oxidation studies reported by Tatsumi, the  $\text{Mg}_2\text{Al-Mo}_7\text{O}_{24}^{6-}$  catalyst was dried at 120 °C before use. The X-ray diffraction pattern of the  $\text{Mg}_2\text{Al-Mo}_7\text{O}_{24}^{6-}$  LDH dried at 120 °C shows an unexpected result (Figure 6-1c). The heptamolybdate intercalated LDH component undergoes decomposition at this temperature, as indicated by the disappearance of the 002 and 003 reflections, whereas the salt-like impurity phase is unaffected by heating at 120 °C.

Raman spectroscopy was used to identify the intercalated anion and the impurity salt obtained as the major components of the  $\text{Mg}_2\text{Al-Mo}_7\text{O}_{24}^{6-}$  reaction products (Figure 6-2). Previous work<sup>187</sup> has shown that as the pH of a  $\text{MoO}_4^{2-}$  solution is reduced from an initial value of 11.0 to 4.2, the anion is progressively converted to heptamolybdate as the only other POM species in solution. The  $\text{MoO}_4^{2-}$  anion exhibits a Raman  $\text{Mo=O}_t$  stretching frequency at 898  $\text{cm}^{-1}$  and a  $\text{Mo=O}$  bending frequency at 320  $\text{cm}^{-1}$ . Heptamolybdate is readily distinguished from molybdate by a  $\text{Mo=O}_t$  symmetric stretch at 947  $\text{cm}^{-1}$ , a  $\text{Mo=O}_t$  bend at

## Raman Spectra

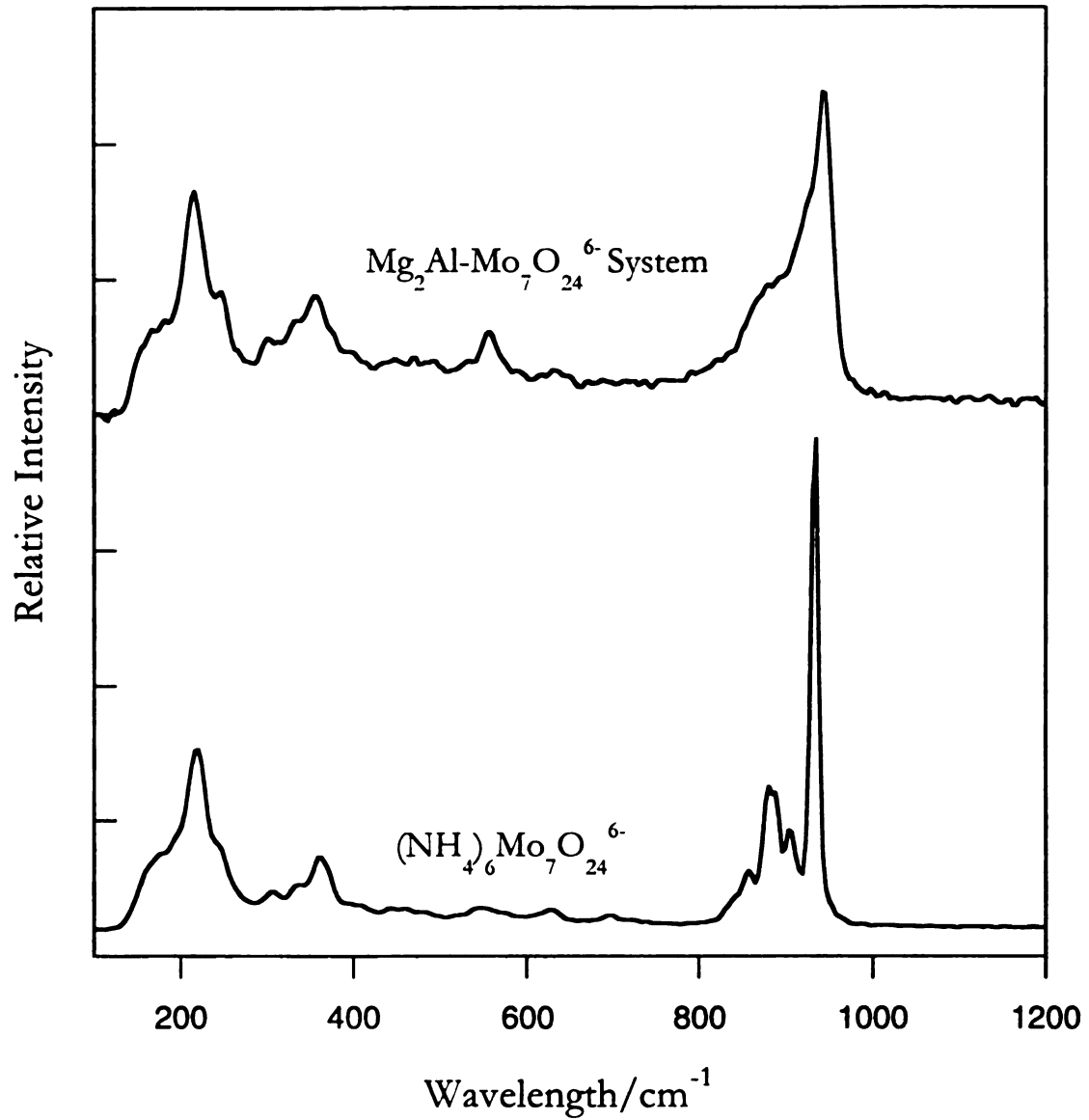


Figure 6-2. Raman spectra of  $(\text{NH}_4)_6\text{Mo}_7\text{O}_{24}^{6-}$  and the  $\text{Mg}_2\text{Al-Mo}_7\text{O}_{24}^{6-}$  product formed by in situ hydrolysis of  $\text{MoO}_4^{2-}$  and ion exchange with a  $\text{Mg}_2\text{Al}$ -terephthalate LDH.

340  $\text{cm}^{-1}$ , and a Mo-O-Mo deformation at 220  $\text{cm}^{-1}$ . The Raman spectrum of the reaction product formed by *in situ*  $\text{MoO}_4^{2-}$  hydrolysis and exchange reaction with  $\text{Mg}_2\text{Al-TA}$  matched closely the spectrum of solid  $(\text{NH}_4)\text{Mo}_7\text{O}_{24}$ . The presence of heptamolybdate as the only Raman-identifiable POM suggests that the relatively large fraction of the impurity phase formed in the  $\text{Mg}_2\text{Al-Mo}_7\text{O}_{24}^{6-}$  reaction system is a magnesium/aluminum salt of  $\text{Mo}_7\text{O}_{24}^{6-}$ .

The *in situ* hydrolysis method also was used to prepare a paratungstate B pillared LDH,  $(\text{Mg}_2\text{Al-H}_2\text{W}_{12}\text{O}_{42}^{10-})$  LDH intercalate, for the peroxide oxidation of olefins. As shown by the XRD patterns in Figure 6-3, however, the product by this reaction route is a mixture of two phases with XRD properties very similar to those found for the analogous molybdate product (cf., Figure 6-1). The d spacing of the minor  $\text{Mg}_2\text{Al-LDH}$  component is 12.1 Å, and the salt-like impurity phase gives a peak at 10.1 Å. The observed Mg:Al:W molar ratio of 1.8:1.0:0.74 is close to the calculated ratio of 2.0:1.0:0.83, but, again, the elemental ratio is not an accurate indication of the LDH composition due to the large amount of impurity present. The 12.1 Å d spacing for the  $\text{Mg}_2\text{Al}$ -isopolytungstate phase is not consistent with the previously reported literature value of 14.6 Å for  $\text{H}_2\text{W}_{12}\text{O}_{42}^{10-}$  intercalated into an LDH.<sup>188</sup> Drying the isopolytungstate catalyst at 120 °C results in the decomposition of the LDH component (see Figure 6-3c). This result also is incompatible with a  $\text{H}_2\text{W}_{12}\text{O}_{42}^{10-}$  intercalated LDH phase, because such intercalates have been previously shown to be stable to 220 °C.<sup>188</sup>

The hydrolysis reactions of  $\text{WO}_4^{2-}$  are known to be considerably more complex than those of  $\text{MoO}_4^{2-}$ .<sup>189</sup> At least three species are present in solution over the pH range 11.0 to 4.2. At pH 9, the predominant species is  $\text{WO}_4^{2-}$ . As the solution is acidified,  $\text{W}_7\text{O}_{24}^{6-}$  is rapidly formed at pH 5 to 6. The  $\text{W}_7\text{O}_{24}^{6-}$  ion, which is in equilibrium with  $\text{H}_2\text{W}_{12}\text{O}_{42}^{10-}$  is converted primarily to  $\text{H}_2\text{W}_{12}\text{O}_{42}^{10-}$  at

$\text{Mg}_2\text{Al-W}_7\text{O}_{24}^{6-}$  System

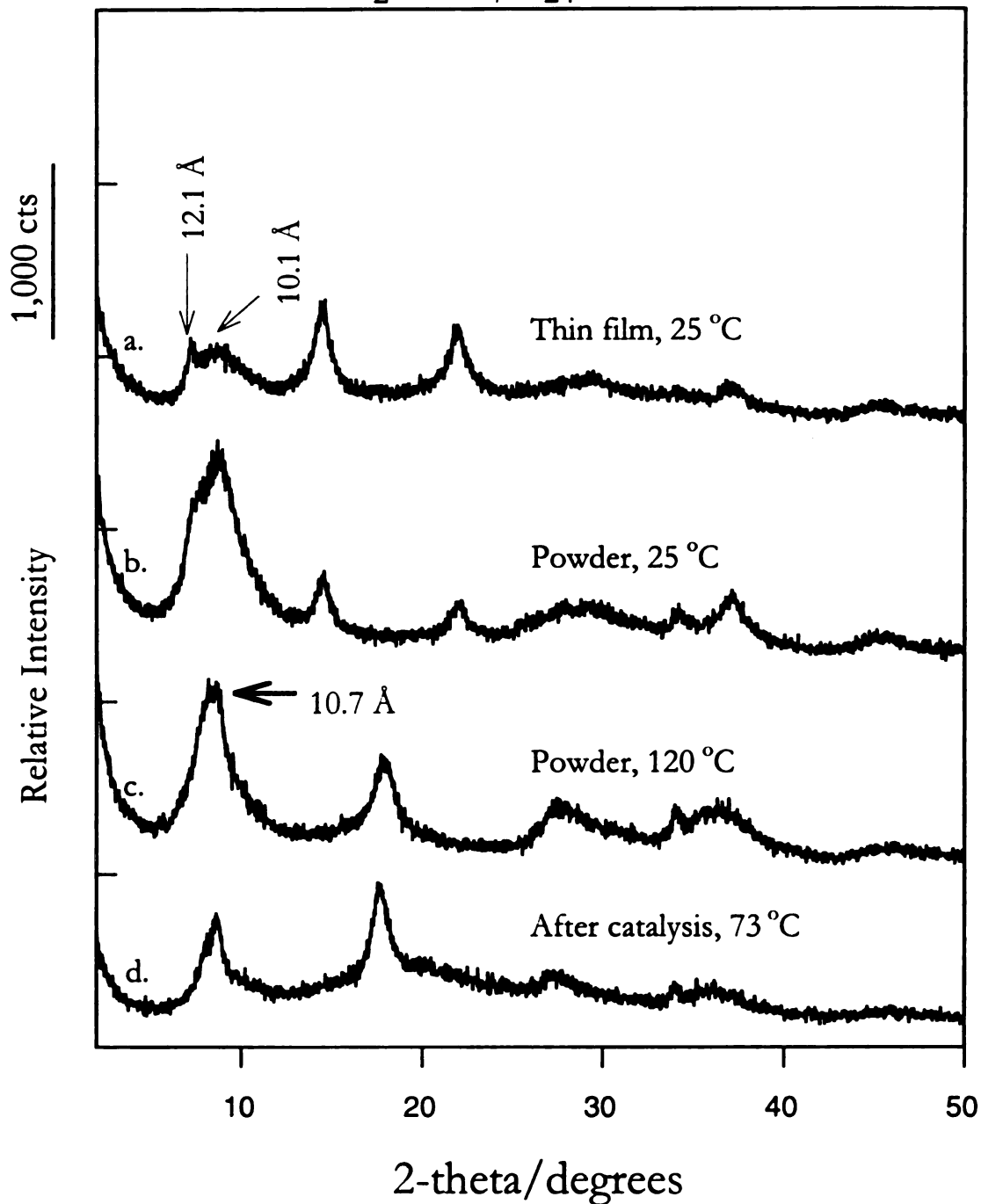


Figure 6-3 X-ray diffraction patterns of the mixed phase product formed by in situ hydrolysis of  $\text{Na}_2\text{WO}_4$  in the presence of  $\text{Mg}_2\text{Al}$ -terephthalate. Parts a-d are analogous to those given in Figure 6-1 for the corresponding molybdate system.

pH 4.4. It was not possible to distinguish between these isopolytungstate possibilities by Raman spectroscopy, the X-ray spacing of 12.1 Å (cf. Figure 6-3) suggests that  $W_7O_{24}^{6-}$  is the intercalated anion in the  $Mg_2Al$ -tungstate formed by *in situ* hydrolysis. Apparently, the  $W_7O_{24}^{6-}$  anion rapidly exchanges with the  $Mg_2Al$ -TA as soon as it is formed in the *in situ* hydrolysis reaction and is stabilized in the LDH galleries at a pH where  $H_2W_{12}O_{42}^{10-}$  would normally form. By further analogy to the molybdate system, the impurity phase was assigned as a salt of the  $W_7O_{24}^{6-}$  anion.

From the above results, it is clear that neither the  $Mo_7O_{24}^{6-}$  nor the  $H_2W_{12}O_{42}^{10-}$  are the active catalyst in the size selective epoxidation studies. Instead, the initial catalysts consist of salt-like  $Mo_7O_{24}^{6-}$  phases that are present as an initial impurity and a decomposition product that forms as a result of the thermal decomposition of the LDH component when dried at 120 °C. In order to obtain stable LDH systems, authentic  $Zn_2Al$ -POMs were synthesized, wherein the layered host is acidic and less likely to hydrolyze the intercalated POM. Well crystallized  $Zn_2Al$ - $Mo_7O_{24}^{6-}$  and  $-H_2W_{12}O_{40}^{6-}$  LDH intercalates were prepared by anion exchange of the ammonium polyoxometalate salt with  $Zn_2Al$ - $NO_3^-$ ,<sup>102</sup> using the method developed by Kwon and Pinnavaia,<sup>188</sup> with only slight modifications. The  $Zn_2Al$ - $NO_3^-$  suspension was formed at 95 °C and the anion exchange reaction was conducted at the ambient pH of the aqueous polyoxometalate solution. The product was digested for 18 h digestion period at 80 °C. The digestion was especially helpful for promoting the  $Mo_7O_{24}^{6-}$  exchange. In general, the digestion step is desirable because it helps in producing consistently well-ordered intercalated products as judged by XRD. A 12.1 Å d spacing for  $Zn_2Al$ - $Mo_7O_{24}^{6-}$  was obtained by averaging the values from five orders of (00 $l$ ) reflections. (Figure 6-4a). Analysis by ICP gave the ratio of Zn:Al:Mo as 2.0:1.0:1.1, very close to the expected ratio of 2.00:1.00:1.17.

## $Zn_2Al-Mo_7O_{24}^{6-}$ System

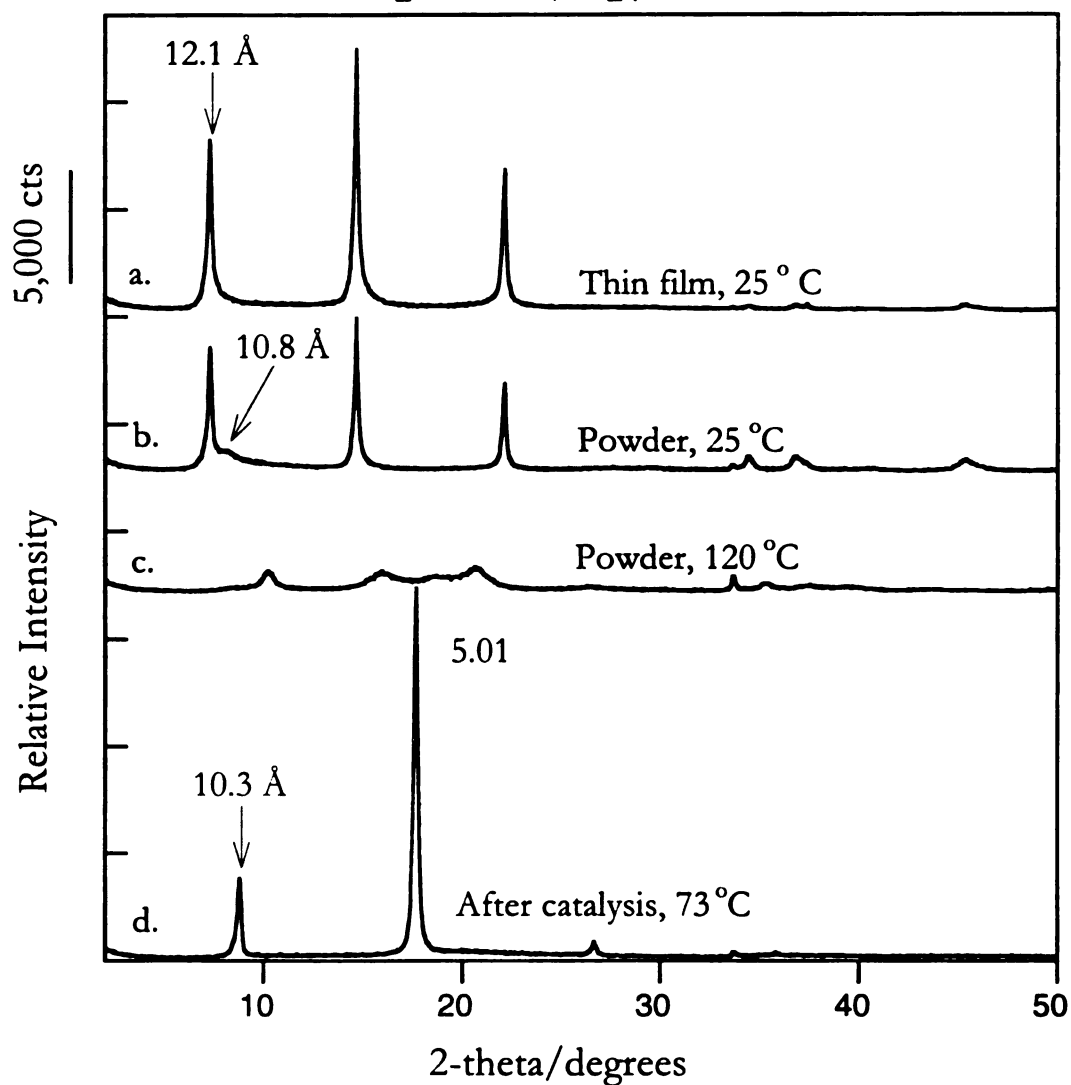


Figure 6-4. X-ray diffraction patterns of  $[Zn_{12}Al_6(OH)_{36}](Mo_7O_{24})mH_2O$  prepared by ion exchange of the corresponding LDH-nitrate with  $Mo_7O_{24}^{6-}$ ; a. thin film sample dried under ambient conditions; b. powder sample dried under ambient conditions; c. powder sample dried overnight at 120 °C showing the loss of the LDH phase; d. thin film sample after use as a catalyst in the oxidation of cyclohexene. The broad weak reflection at 10.8 Å in spectrum (b) is due to a salt-like impurity phase.

**Table 6-1. Raman Bands ( $\text{cm}^{-1}$ ) of Isopolymolybdates**

Sample	d spacing ( $\text{\AA}$ )	$\nu_{\text{sym}}(\text{M}=\text{O}_t)$	Bend ( $\text{M}=\text{O}_t$ )	Def (M-O-M)
$\text{MoO}_4^{2-}(\text{aq})^a$		898	320	-
$(\text{NH}_4)_6\text{Mo}_7\text{O}_{24}$		947	340	208
$\text{PMo}_{12}\text{O}_{40}^{3-}(\text{aq})^a$		995	251	-
$\text{Zn}_2\text{Al-Mo}_7\text{O}_{24}^{6-}$ (25) <sup>b</sup>	12.1	950	360	220
$\text{Zn}_2\text{Al-Mo}_7\text{O}_{24}^{6-}$ (105)	10.6	950(919)	360(317)	222
$\text{Zn}_2\text{Al-Mo}_7\text{O}_{24}^{6-}$ (220)	7.8	936	341	206
$\text{Zn}_2\text{Al-Mo}_7\text{O}_{24}^{6-}$ (25) <sup>c</sup> , rehydrated	9.6	922	333	213

a. Values for the aqueous POMs were taken from Payen et al.<sup>iv</sup>

b. Values in parenthesis are the temperatures at which the LDHs were heated prior to the recording of the Raman spectra.

c. The  $\text{Zn}_2\text{Al-Mo}_7\text{O}_{24}^{6-}$  dried at 220 °C, was rehydrated by slurring in water at 25 °C and air drying.

The Raman spectrum of the  $\text{Zn}_2\text{Al-Mo}_7\text{O}_{24}^{6-}$  LDH product showed the presence of bands at 950, 360 and  $220\text{ cm}^{-1}$  (Table 6-1), in good agreement with the Raman spectrum of crystalline  $(\text{NH}_4)\text{Mo}_7\text{O}_{24}$ . The Raman data, together with the ICP and X-ray diffraction measurements) are consistent with a well defined intercalated product. In fact, the X-ray diffraction pattern of the oriented thin film of  $\text{Zn}_2\text{Al-Mo}_7\text{O}_{24}^{6-}$  (Figure 5:4a) is a textbook example of an LDH diffraction pattern with sharp, intense (00/) peaks. However, the XRD pattern of a less oriented powder sample shows a small impurity peak, though relatively weak in intensity, at a d spacing of  $10.8\text{ \AA}$ . (Figure 6-4b) Thus, as emphasized earlier, thin film samples can mask the presence of an impurity phase by enhancing the (00/) reflections of the LDH phase through preferred orientation of the platy crystallites. Although the X-ray diffraction pattern, ICP elemental analyses, and Raman spectrum for the  $\text{Zn}_2\text{Al-Mo}_7\text{O}_{24}^{6-}$  intercalate verified that the initial gallery anion is heptamolybdate, this intercalate also decomposes when dried at  $120\text{ }^\circ\text{C}$  (Figure 5:4c).

The change in d spacing for the  $\text{Mg}_2\text{Al-}$  and  $\text{Zn}_2\text{Al-Mo}_7\text{O}_{24}^{6-}$  LDHs upon drying at  $120\text{ }^\circ\text{C}$  could be due to the loss of water in the gallery or due to a decomposition of the  $\text{Mo}_7\text{O}_{24}^{6-}$ . A Raman study was carried out for the thermal decomposition for the relatively pure  $\text{Zn}_2\text{Al-Mo}_7\text{O}_{24}^{6-}$  LDH phase (Figure 6-4) because the Raman features could be attributed to an authentic LDH-POM and not a artifact of the impurity salt. The important Raman features, given in Table 6-1, are the  $(\text{M}=\text{O})\nu_{\text{sym}}$  band above  $900\text{ cm}^{-1}$ , the polymeric Mo-O-Mo deformation band at  $220\text{ cm}^{-1}$ . The spectrum of  $\text{Zn}_2\text{Al-Mo}_7\text{O}_{24}^{6-}$  dried at  $105\text{ }^\circ\text{C}$  shows a splitting of the  $(\text{M}=\text{O})\nu_{\text{sym}}$  stretch ( $950, 919\text{ cm}^{-1}$ ) and the  $(\text{M}=\text{O})$  bend ( $360, 317\text{ cm}^{-1}$ ), respectively. The Mo-O-Mo deformation frequency does not change significantly in wavelength or intensity. By  $220\text{ }^\circ\text{C}$ , the bands have shifted to  $936, 341, \text{ and } 206\text{ cm}^{-1}$ .

## Raman Spectra of $\text{Zn}_2\text{Al-Mo}_7\text{O}_{24}^{6-}$ LDH

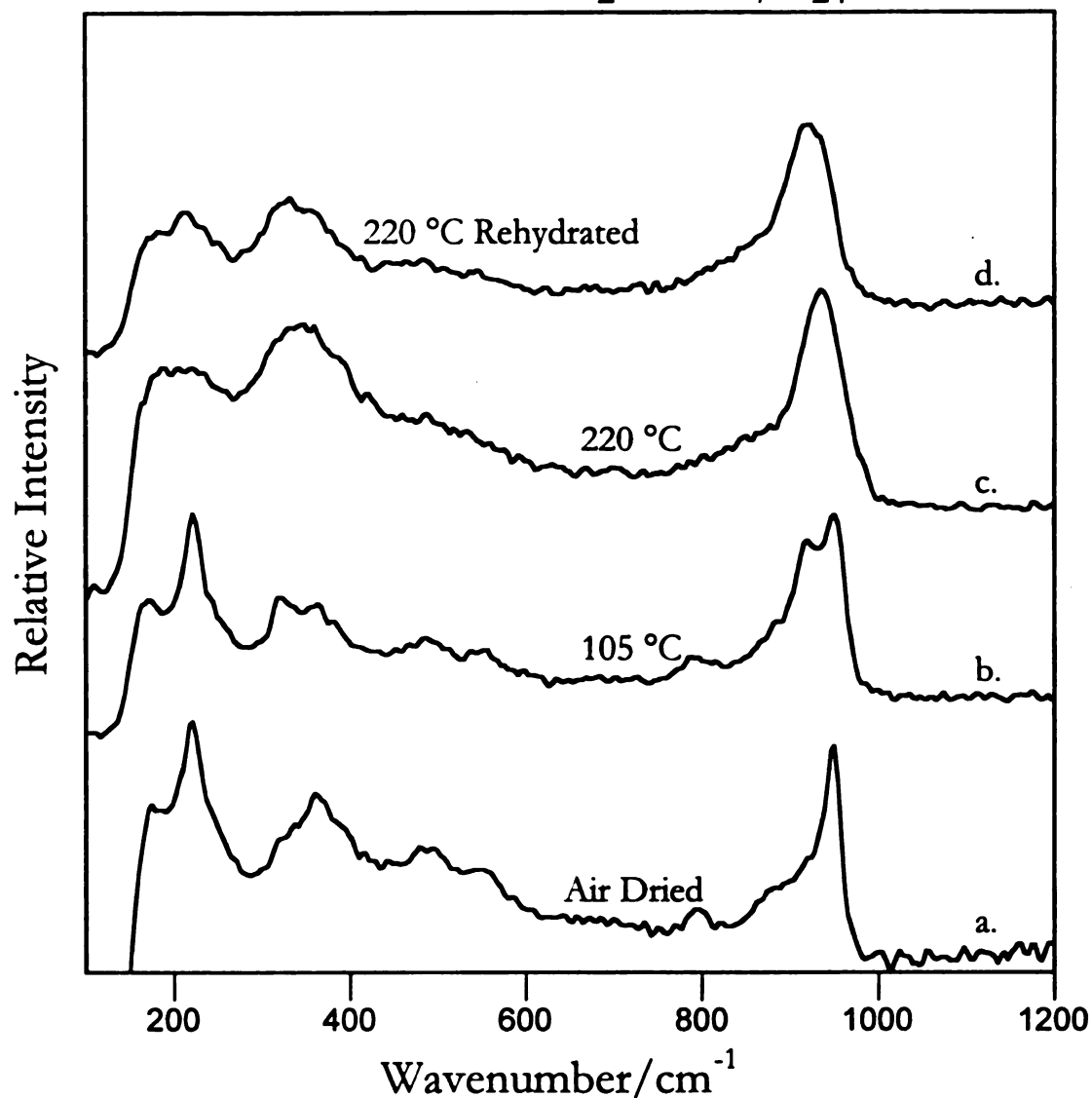


Figure 0-5 Raman spectra of  $\text{Zn}_2\text{Al-Mo}_7\text{O}_{24}^{6-}$  after heating to various temperatures: a. the air sample, showing bands analogous to those in ammonium heptamolybdate; b. After drying at 105 °C, showing the splitting of the terminal Mo=O band at 950 cm<sup>-1</sup>; c. After heating to 220 °C, the terminal Mo=O band at 936 cm<sup>-1</sup> and the Mo-O-Mo polymeric band at 220 cm<sup>-1</sup> decreased in intensity similar to the band for Mo-O-Al in alumina supported molybdate d. The sample dried at 220 °C and then slurried in distilled water, showing the further shift in the terminal Mo-O band to 922 cm<sup>-1</sup>.

The polymeric Mo-O-Mo band at  $206\text{ cm}^{-1}$  has broadened and decreased in intensity. This is similar to the effect seen in alumina supported  $\text{Mo}_7\text{O}_{24}^{6-}$  and has been attributed to a Mo-O-Al deformation band. The sample dried at  $220\text{ }^\circ\text{C}$  was slurried in water to determine if rehydration would return the layer spacing to that of the original LDH intercalate. Ordered reflections for a layered material with a d spacing of  $9.6\text{ \AA}$  were observed. The Raman spectrum of the rehydrated product has the most intense band at  $922\text{ cm}^{-1}$  and low intensity, broad bands near  $320$  and  $200\text{ cm}^{-1}$ . The spectrum is similar to those reported for the Raman bands arising from the Al-O-Mo linkages in rehydrated  $\text{MoO}_3$  supported on alumina or a protonated molybdate,<sup>190</sup> which suggests that the decomposition product contains similar linkages. There is no evidence for the survival or reformation of the heptamolybdate anion. Thus, the changes in XRD properties upon heating to  $220\text{ }^\circ\text{C}$  are not due simply to the loss of gallery water, but to the transformation of the LDH- POM structure itself. In a related Raman study of LDH heptamolybdates, Twu and Dutta<sup>160</sup> concluded that the LDH layers degraded at  $200\text{ }^\circ\text{C}$ , while the integrity of the heptamolybdate was maintained to  $400\text{ }^\circ\text{C}$ . However, they did not confirm this result by examining the polymeric Mo-O-Mo  $320\text{ cm}^{-1}$  Raman band or the in plane reflection of an LDH layer at  $60^\circ$  2-theta. There is not enough evidence to support their claim.

A Keggin ion intercalated  $\text{Zn}_2\text{Al-H}_2\text{W}_{12}\text{O}_{40}^{6-}$  LDH also was prepared by the same general ion exchange reaction between the POM salt and a  $\text{Zn}_2\text{Al-NO}_3^-$  LDH precursor. The molar Zn:Al:W ratio for the reaction product was 2.1:1.0:2.2, close to the expected 2.0:1.0:2.0 ratio, but still with some impurity present. The d-spacing for the LDH was  $14.6\text{ \AA}$ , in good agreement with the sum of  $4.8\text{ \AA}$  or an LDH layer and  $9.8\text{ \AA}$  for a Keggin ion (Figure 6-6a). However, a

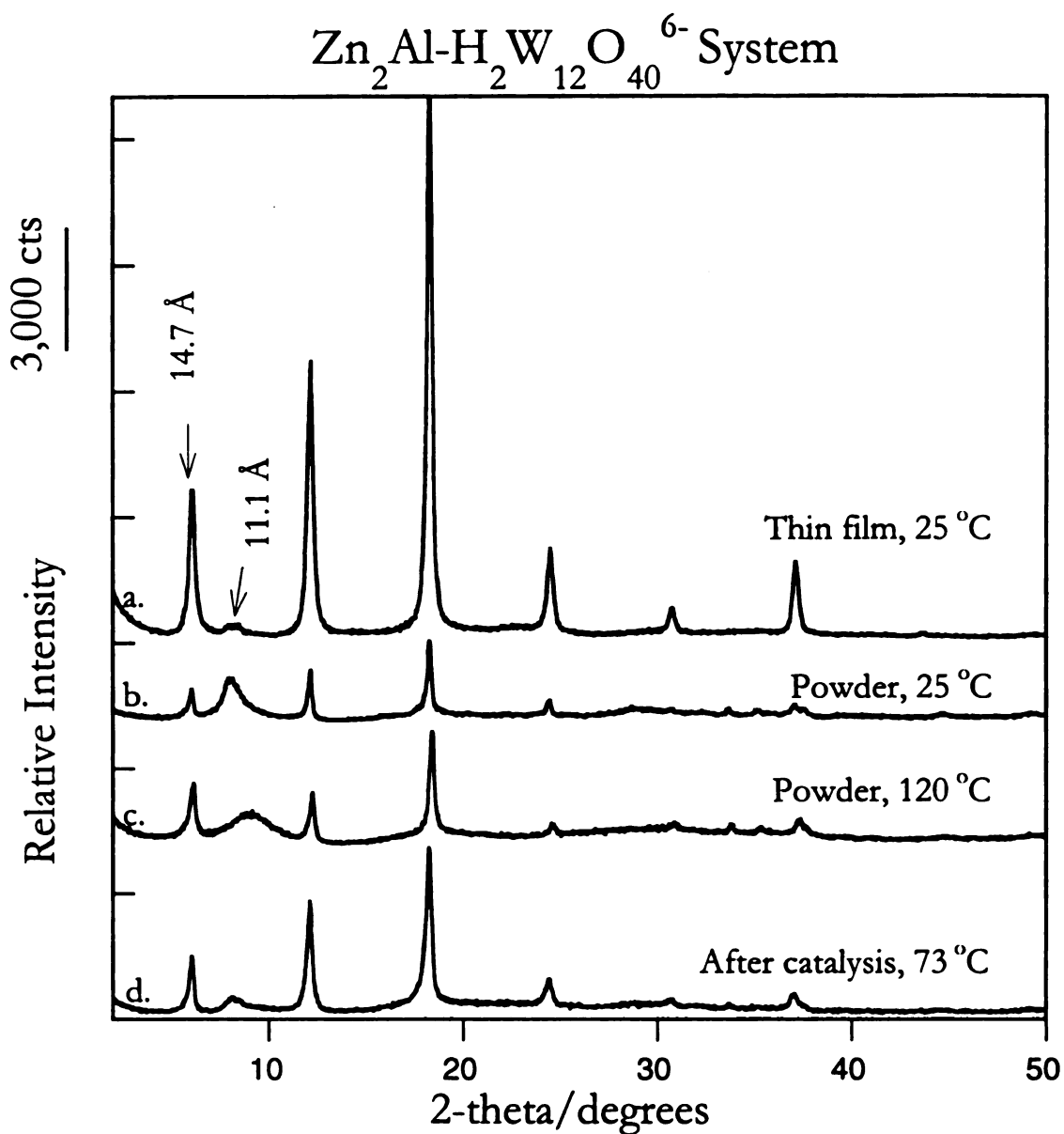


Figure 6-6 X-ray diffraction patterns of  $[\text{Zn}_{12}\text{Al}_6(\text{OH})_{36}](\text{H}_2\text{W}_{12}\text{O}_{40})_m\text{H}_2\text{O}$  prepared by ion exchange of the corresponding LDH-nitrate with  $\text{H}_2\text{W}_{12}\text{O}_{40}^{6-}$ : a. thin film sample dried under ambient conditions; b. powder sample dried under ambient conditions; c. powder sample dried overnight at 120 °C; d. thin film sample after use as a catalyst in the oxidation of cyclohexene. The broad line at 11.1 Å is due to a salt-like POM impurity phase.

salt-like impurity also was present, as indicated by the broad peak at 11.1 Å. For this LDH intercalate, there is no change in the diffraction pattern when it is dried at 120 °C (Figure 6-6b, c). The identification of the intercalate as an  $\text{H}_2\text{W}_{12}\text{O}_{40}^{6-}$  anion, was based on the ICP elemental analysis, the d spacing, and the thermal stability, all of which are in agreement with previous literature results.<sup>188</sup>

In the present work only the  $\text{Zn}_2\text{Al-H}_2\text{W}_{12}\text{O}_{40}^{6-}$  LDH intercalate was stable when dried at 120 °C. Although the LDH structure is retained, the intragallery POM anions are not accessible for reaction with olefinic substrates in solution. Not even  $\text{N}_2$  is capable of accessing the space between the solvated gallery anions, as judged by the absence of microporosity and low surface area when the LDH is dried at the catalytically relevant temperature of 70 °C. The BET surface area for  $\text{Zn}_2\text{Al-H}_2\text{W}_{12}\text{O}_{40}^{6-}$  was 10  $\text{m}^2/\text{g}$ , compared to  $\text{Mg}_2\text{Al-W}_7\text{O}_{24}^{6-}$  with a surface area of 44  $\text{m}^2/\text{g}$ . Both materials exhibit isotherms characteristic of non-porous (solvated) structures. It should be noted, however, that  $\text{Zn}_2\text{Al-H}_2\text{W}_{12}\text{O}_{40}^{6-}$  is microporous, indeed pillared, when outgassed under vacuum at 150 °C, in accord with the results of previously reported studies.<sup>71,188</sup>

### **Catalytic Properties $\text{Mg}_2\text{Al-}$ and $\text{Zn}_2\text{Al-POMs}$**

As shown by the results given in Table 6-2, we have verified that the  $\text{Mg}_2\text{Al-LDH}$  catalysts precursors as prepared by the *in situ* hydrolysis method of Tatsumi et al. are indeed active for the peroxide oxidation of cyclohexene to the corresponding epoxide and diol in  $(\text{BuO})_3\text{PO}$  solution. The results for the  $\text{Zn}_2\text{Al-LDH}$  derivatives prepared by direct ion exchange of  $\text{Zn}_2\text{Al-NO}_3^-$  the

**Table 6-2. Peroxide Oxidation of Cyclohexene Over Polyoxometalate Catalysts**

Catalyst Precursor	% Conversion <sup>a</sup>	
	epoxide	diol
<u>Controls</u>		
$(\text{NH}_4)_6\text{Mo}_7\text{O}_{24}$	0	21
$(\text{NH}_4)_6\text{H}_2\text{W}_{12}\text{O}_{40}^{6-}$	12	60
$\text{Mg}_2\text{Al-CO}_3^{2-}$	0	0
<u>LDH-Heptamolybdates<sup>b</sup></u>		
$\text{Zn}_2\text{Al-Mo}_7\text{O}_{24}^{6-}$	1.9	3.2
$\text{Mg}_2\text{Al-Mo}_7\text{O}_{24}^{6-}$	0	4.0
<u>LDH-Tungstates<sup>b</sup></u>		
$\text{Zn}_2\text{Al-H}_2\text{W}_{12}\text{O}_{40}^{6-}$	0	22
$\text{Zn}_2\text{Al-H}_2\text{W}_{12}\text{O}_{40}^{6-}$ , recycled,	0	26
$\text{Mg}_2\text{Al-W}_7\text{O}_{24}^{6-}$	17	0
<u>Al-POM Salt<sup>c</sup></u>		
$\text{Al-H}_2\text{W}_{12}\text{O}_{40}^{6-}$	0	5.8

- Reaction conditions: 100 mmol of 10%  $\text{H}_2\text{O}_2$  in  $(\text{BuO})_3\text{PO}$  was allowed to react with 100 mmol of cyclohexene in the presence of 1 mmol of metal (Mo or W) at 73 °C for 3 hrs. The  $\text{Mg}_2\text{Al-POMs}$  were dried at 120 °C and the  $\text{Zn}_2\text{Al-POMs}$  were dried at 25 °C prior to use as catalysts.
- The  $\text{Mg}_2\text{Al-LDH}$  phases were prepared by *in situ* hydrolysis of  $\text{MoO}_4^{2-}$  or  $\text{WO}_4^{2-}$  in the presence of  $\text{Mg}_2\text{Al-TA}$ , whereas the  $\text{Zn}_2\text{Al-LDH}$  phases were prepared by ion-exchange reaction of the POM with  $\text{Zn}_2\text{Al-NO}_3^-$  LDH. All of the heptametalate LDH intercalates are unstable under reaction conditions and are transformed into lower nuclearity species on the LDH surface. Only the  $\text{Zn}_2\text{Al-H}_2\text{W}_{12}\text{O}_{40}^{6-}$  intercalate is stable under reaction conditions.
- The Al-POM salt was made by reaction of  $\text{Al}(\text{NO}_3)_3$  and  $(\text{NH}_4)_6\text{H}_2\text{W}_{12}\text{O}_{40}$  under conditions analogous to those used to prepare  $\text{Zn}_2\text{Al-H}_2\text{W}_{12}\text{O}_{40}^{6-}$  LDH.

unsupported catalyst precursors,  $(\text{NH}_4)_6\text{Mo}_7\text{O}_{24}$  and  $(\text{NH}_4)_6\text{H}_2\text{W}_{12}\text{O}_{40}$  as well  $\text{Mg}_2\text{Al-CO}_3^{2-}$  are also shown in Table 6-2. No olefin oxidation products were detected in the absence of a POM catalyst or in the presence of a  $\text{Mg}_2\text{Al}$  LDH in which carbonate is the gallery anion.

The results given in Table 6-2 show that the LDH intercalates are far less reactive than the unsupported catalysts. This is consistent with the inaccessibility of the gallery POM centers under reaction conditions. It is highly unlikely that the activities observed for the LDH catalysts are due to leaching of POM ions into solution. LDH intercalates have virtually no solubility in  $(\text{BuO})_3\text{PO}$  and no anions are generated in the oxidation reaction for displacing POM ions from the LDH surfaces.

On the basis of the X-ray powder diffraction results described above, the  $\text{Mg}_2\text{Al-Mo}_7\text{O}_{24}^{6-}$  and  $\text{Mg}_2\text{Al-W}_7\text{O}_{24}^{6-}$  LDH precursors decompose when heated to 120 °C. The decomposition products are not substantially altered under reaction conditions (see parts c and d in Figure 6-1 and Figure 6-3). Because the original catalysts were dried at 120 °C prior to use for olefin oxidation in  $(\text{BuO})_3\text{PO}$  solution, it was concluded that the LDH decomposition products and not the initial  $\text{Mg}_2\text{Al-POM}$  LDH phases that were responsible for favoring 2-hexene oxidation over cyclohexene oxidation relative to the unsupported POMs. Drying the  $\text{Mg}_2\text{Al-LDH}$  precursors at room temperature instead of 120 °C does not preserve the LDH structure under catalytic reaction conditions. In fact, when air-dried  $\text{Mg}_2\text{Al-Mo}_7\text{O}_{24}^{6-}$  was merely stirred in cyclohexene at 75 °C for three hours, the result was a loss of ordered reflections for the  $\text{Mg}_2\text{Al-Mo}_7\text{O}_{24}^{6-}$  LDH phase. The phase formed under the conditions of catalytic oxidation is uncertain, but the X-ray powder pattern, shown in Figure 6-4d, is consistent with a layered structure, perhaps a  $\text{MoO}_4^{2-}$  LDH intercalate. However, this layered

$Zn_2Al_2H_2W_{12}O_{40}^{6-}$  and Salts

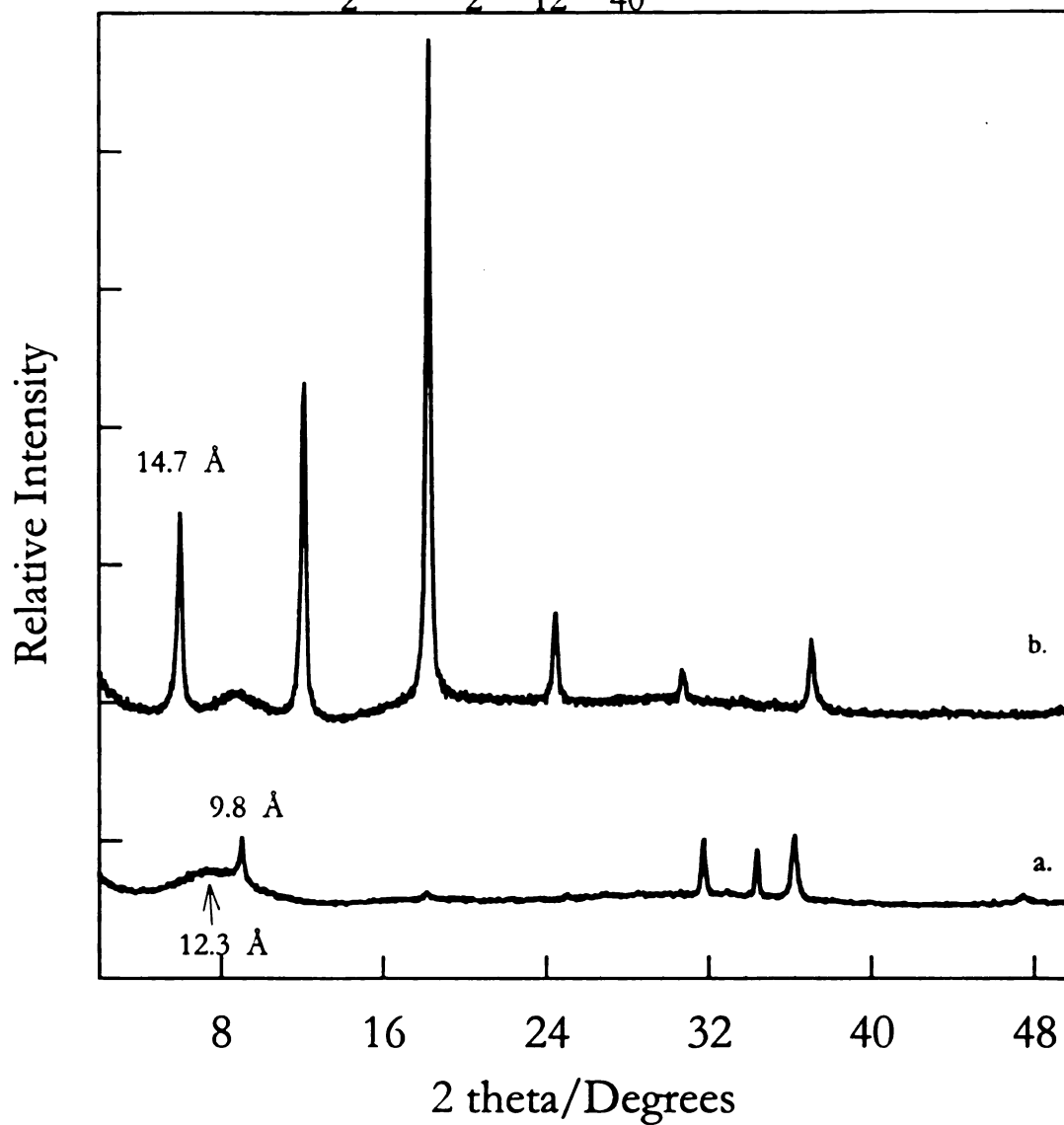


Figure 6-7 a. XRD pattern of a physical mixture of  $Zn-H_2W_{12}O_{40}^{6-}$  salt and  $Al-H_2W_{12}O_{40}^{6-}$  salts b. XRD pattern of a physical mixture of  $Zn-Mo_7O_{24}^{6-}$  salt and  $Al-Mo_7O_{24}^{6-}$  salts.

phase is no more reactive for cyclohexene oxidation than the decomposition product obtained from the corresponding  $Mg_2Al$ -LDH precursor (cf., Table 6-2). In the present work only the  $Zn_2Al-H_2W_{12}O_{40}^{6-}$  LDH derivative was stable toward both to drying at 120 °C and to olefin oxidation conditions (see Figure 6-6c and d). Although most of the intercalated POM anions in this intercalate are inaccessible to the substrate under catalytic reaction conditions, significant activity is observed. This suggests that the accessible POM sites at the outer LDH surfaces are more reactive than unsupported POMs. But even this catalyst in as-synthesized form contained a salt-like impurity phase that was observable by XRD. The salt-like impurity cannot be ignored as a potential olefin oxidation catalyst. In an effort to demonstrate the possible role this impurity phase in the catalytic process, aluminum and zinc salts of  $H_2W_{12}O_{40}^{6-}$  were prepared by a precipitation reaction of  $Al(NO_3)_3$  or  $Zn(NO_3)_2$  and  $(NH_4)_6H_2W_{12}O_{40}^{6-}$  under conditions analogous to the LDH-POM synthesis. The diffraction pattern of a physical mixture of the Al- And  $Zn-H_2W_{12}O_{40}^{6-}$  is shown in Figure 6-7. The precipitate of the Al-POM salts gave an x-ray diffraction pattern similar to the impurity phase found in  $Zn_2Al$ -POMs, while the  $Zn-H_2W_{12}O_{40}^{6-}$  salt is more crystalline. Table 6-2 shows that the  $Al-H_2W_{12}O_{40}^{6-}$  salt is reactive for the oxidation of cyclohexene to the corresponding diol. Consequently, the role of the salt-like impurity phases as contributors to the catalytic properties cannot be discounted, particularly for the  $Mg_2Al$  systems where these impurity phases are an abundant component.

### **Catalytic Oxidation of Cyclohexene by $Zn_2Al$ -PJP**

Recently, large macropolyoxometalates have been intercalated into LDHs.<sup>3</sup> A Dawson ion,  $\alpha-P_2W_{17}O_{61}^{10-}$ , two Finke ions,  $Zn_4(H_2O)_2(AsW_9O_{34})_2^{10-}$  and  $WZn_3(H_2O)_2(ZnW_9O_{34})_2^{12-}$ , a double Dawson,  $P_4W_{30}Zn_4(H_2O)O_{112}^{16-}$  and the

inorganic cryptates,  $\text{NaP}_5\text{W}_{30}\text{O}_{110}^{14-}$  and  $\text{NaSb}_9\text{W}_{21}\text{O}_{86}^{18-}$  were intercalated into MgAl- and ZnAl-LDHs. A stable LDH-POM with a high surface area,  $\text{NaP}_5\text{W}_{30}\text{O}_{110}^{14-}$  was selected to repeat the oxidation of cyclohexene experiments in the expectation that the partial blocking of the pores by the impurity salt would not be sufficient to restrict the access of organic substrates to the intergallery catalysts. The results of the catalytic studies show that while access to the intergallery  $\text{NaP}_5\text{W}_{30}\text{O}_{110}^{14-}$  catalyst is still a limitation, the presence of the LDH support is vital to the selectivity and catalytic rate.

### **$\text{Zn}_2\text{Al-NaP}_5\text{W}_{30}\text{O}_{110}^{14-}$**

The catalytic results for LHD- $\text{Mo}_7\text{O}_{24}^{6-}$  and  $-\text{H}_2\text{W}_{12}\text{O}_{40}^{6-}$  show that there are two factors that need to be taken into consideration when discussing the catalytic activity of LDH-POM catalysts, namely, the stability of the intercalated polyoxometalate anion and the impurity phase present in all syntheses of LDH supported polyoxometalates. The PJP anion,  $\text{NaP}_5\text{W}_{30}\text{O}_{110}^{14-}$ , named after Preyssler, Jeanin, and Pope, is a good candidate for catalytic oxidation studies where the stability of the intercalate is important. The remarkable robustness of  $\text{NaP}_5\text{W}_{30}\text{O}_{110}^{14-}$  has been utilized in other studies of catalysis by polyoxometalates,<sup>191</sup> the most notable of which is the aerobic oxidation of hydrogen sulfide to sulfur.<sup>192</sup> After 14 days under reaction conditions there was little or no degradation of the homogeneous  $\text{NaP}_5\text{W}_{30}\text{O}_{110}^{14-}$  catalyst, as judged by  $^{31}\text{P}$  NMR. Another aspect of the PJP anion which makes it very compatible with LDH chemistry is its stability to basic pH. The PJP anion has been reported stable in a pH range of 0 to 11 at 25 °C.<sup>193</sup>

The PJP anion was first intercalated into  $\text{Zn}_2\text{Al-LDHs}$  by Pinnavaia et al. in 1992 by anion exchange. The XRD pattern exhibits six orders of (00/ ) reflections corresponding to a gallery height of 16.3 Å (Figure 6-8b). This POM

anion lies with its  $C_5$  axis perpendicular to the  $c$  axis of the LDH. This orientation is stabilized by H-bonding interactions with the host layer hydroxyls. The  $Zn_2Al-NaP_5W_{30}O_{110}^{14-}$  was dried at 200 °C without change in the XRD pattern.

The five equivalent phosphorous atoms in the PJP anion have a single MAS  $^{31}P$  NMR resonance at -13.9 ppm versus  $Na_2HPO_4$  (Figure 6-9). When the PJP ion was exchanged into a  $Zn_2Al-NO_3^-$  LDH, the  $^{31}P$  MAS-NMR was unchanged, verifying that authentic  $NaP_5W_{30}O_{110}^{14-}$  has been intercalated in the LDH layers (Figure 6-9a,b). The absence of any other peak in the NMR spectrum of  $Zn_2Al-NaP_5W_{30}O_{110}^{14-}$  indicated that any impurity salts present in the LDH-POM catalyst must also contain the PJP anion.

However, the observed microporous surface area 65  $m^2/g$  is lower than one may expect from the gallery height and charge density of the PJP ion, even when the high molecular weight of the PJP intercalate is taken into consideration. Limited access to the microporous gallery may be caused by the deposition of the POM salt impurity phase at the LDH edges or by structural defects that result in a higher concentration of POM pillars near the gallery edges.

#### **Catalytic Oxidation by $Zn_2Al-NaP_5W_{30}O_{110}^{14-}$**

The catalytic transfer of oxygen from  $H_2O_2$  to cyclohexene was used as a probe of the relative reactivities of the non-supported  $NaP_5W_{30}O_{110}^{14-}$  catalyst versus the  $Zn_2Al$ -LDH supported catalyst. Cyclohexene, 10%  $H_2O_2$  in  $(BuO)_3PO$ , and catalyst in a molar ratio of 20:30:0.002 were added to a 100 ml

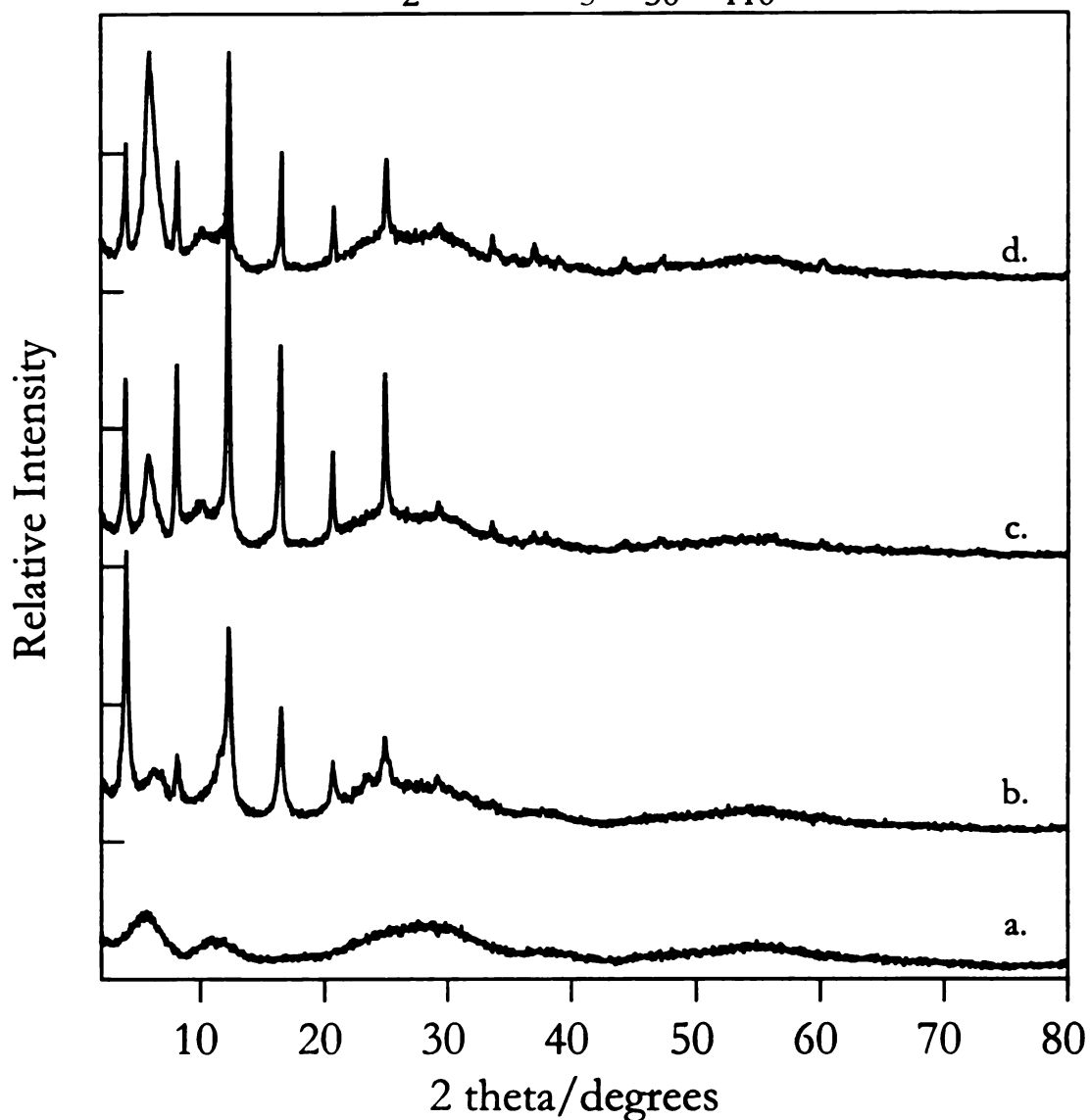
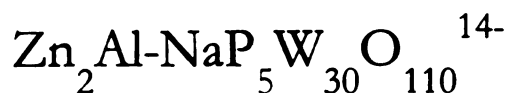


Figure 6-8. a. Powder XRD pattern of an Aluminum- $\text{NaP}_5\text{W}_{30}\text{O}_{110}^{14-}$  salt analogous to the impurity phase in the synthesis of  $\text{Zn}_2\text{Al-PJP}$ . The d spacing of the first peak is 15.5 Å. b. XRD of a thin film sample of  $\text{Zn}_2\text{Al-PJP}$ . The d spacing of the LDH is 21.6 Å and the broad reflection due to the impurity phase is 15.1 Å. c. XRD of a thin film sample of  $\text{Zn}_2\text{Al-PJP}$  with a slightly greater volume of impurity phase. The d spacing of the LDH is 22.0 Å and that of the impurity phase is 15.1 Å. d. XRD of a thin film sample of  $\text{Zn}_2\text{Al-PJP}$  with a the greatest volume of impurity phase. The d spacing of the LDH is 21.7 Å and 14.8 Å for the impurity phase.

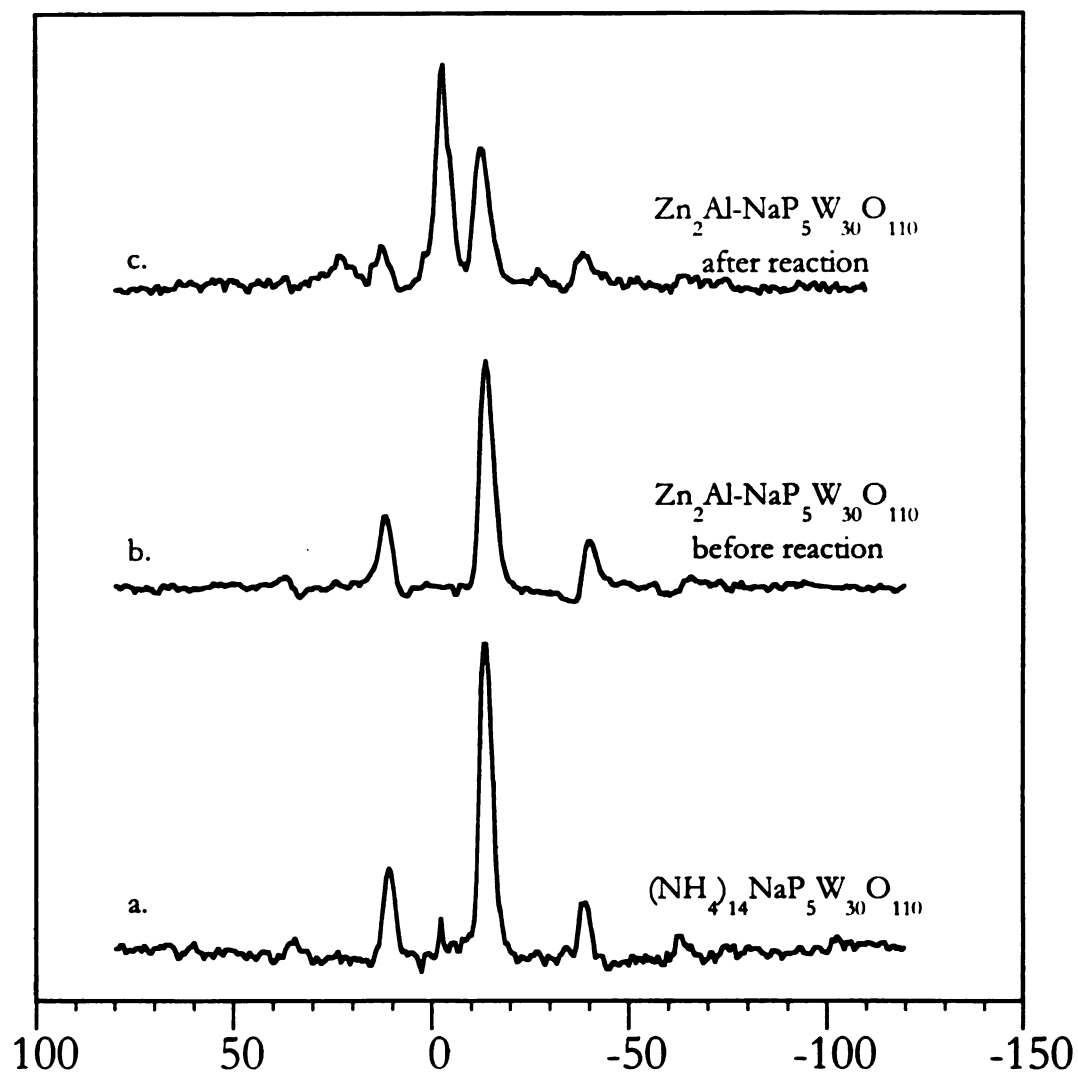


Figure 6-9. a. MAS-NMR of  $(\text{NH}_4)_{14}\text{NaP}_5\text{W}_{30}\text{O}_{110}$ , with a single peak at -13.9 ppm. The two small peaks are side bands. b.  $\text{Zn}_2\text{Al-NaP}_5\text{W}_{30}\text{O}_{110}^{14-}$ , the MAS-NMR of the intercalated anion is the same as a., verifying that only PJP anion is present. c. MAS-NMR of the supported catalyst after use in the oxidation of cyclohexene. The peak at -2.89 ppm is  $(\text{BuO})_3\text{PO}$  and the small peaks are side bands.

flask and stirred at 70 °C for 4 hours. Although  $\text{Zn}_2\text{Al-NO}_3^-$  is unreactive as a catalyst, the corresponding PJP anion intercalates are active epoxidation catalysts (See Table 6-3). In general, the  $\text{Zn}_2\text{Al-PJP}$  LDH intercalates are selective for cyclohexene oxide while the non-supported  $(\text{NH}_4)_{14}\text{NaP}_5\text{W}_{30}\text{O}_{110}^{14-}$  catalyst produces exclusively cyclohexanediol. The basis for this product selectivity is probably due to the less acidic nature of the LDH. The thermal stability of the PJP intercalate has already been demonstrated by the XRD and FTIR.<sup>2</sup> The <sup>31</sup>P MAS-NMR (Figure 6-9c) and the powder X-ray diffraction pattern of  $\text{Zn}_2\text{Al-PJP}$  after use as a catalyst verifies its stability under the reaction conditions.

The turnover numbers reported in Table 6-3 are calculated based on the moles of POM present, as determined by ICP analysis, and include any contribution from the salt-like impurity. This impurity cannot be discounted as a catalyst component. Three samples of the  $\text{Zn}_2\text{Al-PJP}$  intercalate made by the same method, but differing in the amount of impurity present as judged by XRD, were compared for catalytic activity. On comparing the XRD patterns in Figure 6-8 to the turnover numbers in Table 6-3, one finds that the catalytic activity directly correlates to the amount of impurity present. Sample  $\text{Zn}_2\text{Al-LDH-B}$  with the least amount of impurity phase shows only a trace of cyclohexene oxide, while  $\text{Zn}_2\text{Al-LDH-C}$  exhibits 107 turnovers and  $\text{Zn}_2\text{Al-LDH-D}$  with the greatest amount of impurity gave 182 turnovers in 4 hours. But attributing the catalytic activity to the PJP-salt impurity may not be the complete answer. Figure 6-8a shows the diffraction pattern of an  $\text{Al}^{3+}$ -PJP salt made from  $\text{Al}(\text{NO}_3)_3$  and  $(\text{NH}_4)_{14}\text{NaP}_5\text{W}_{30}\text{O}_{110}$  under conditions similar to those used to carry out the  $\text{Zn}_2\text{Al-NO}_3^-$  exchange reaction. The XRD powder pattern is similar to that of the impurity phase in  $\text{Zn}_2\text{Al-PJP}$  intercalate. As can be seen in Table 3, the  $\text{Al}^{3+}$  salt of PJP is basically inactive under the conditions of the

**Table 6-3. Peroxide Oxidation of Cyclohexene in the Presence of Different Forms of  $\text{NaP}_5\text{W}_{30}\text{O}_{110}^{14-}$**

Catalyst	Major Product	Turnovers
$(\text{NH}_4)^+$ Salt	Diol	150
$\text{Zn}_2\text{Al-LDH-b}$	Oxide	<10
$\text{Zn}_2\text{Al-LDH-c}$	Oxide	107
$\text{Zn}_2\text{Al-LDH-d}$	Oxide	182
$\text{Al}^{3+}$ Salt	Oxide	<10

a. Cyclohexene (2 ml) and 10% by wt.  $\text{H}_2\text{O}_2$  (10 ml) were allowed to react with 0.200 gram catalyst at 70 °C in  $(\text{BuO})_3\text{PO}$  for 4 h.

b. The  $\text{Zn}_2\text{Al-LDH}$  supported catalysts correspond to the samples with XRD patterns shown in Figure 6-8.

oxygen transfer reaction. A trace of cyclohexene oxide is observed as a reaction product, indicating the same selectivity as  $\text{Zn}_2\text{Al-PJP}$  catalyst. As discussed previously, the impurity salt is believed to be dispersed on the surface of the LDH particles and this may result in a better access to the catalytically active anion centers of the salt, while at the time limiting access to the intergallery anions of the intercalate. Even though the  $\text{NaP}_5\text{W}_{30}\text{O}_{110}^{14-}$  intercalate has the greatest surface area among the macro polyoxocryptates, access to the gallery region by substrates larger than  $\text{N}_2$  is still restricted.

## Conclusions

The results of the present study clarify the nature of the catalyst precursors used in the earlier work of Tatsumi et al. in terms of mixed phases of salt-like POM impurities and  $\text{Mg}_2\text{Al-LDH}$  intercalates interlayered by  $\text{Mo}_7\text{O}_{24}^{6-}$  and  $\text{W}_7\text{O}_{24}^{6-}$ . Moreover, the  $\text{Mg}_2\text{Al-POM}$  LDH components of the as-synthesized catalysts decompose at the temperatures used to dry the intercalates prior to catalytic reaction. Despite the thermal instability of  $\text{Mg}_2\text{Al-POM}$  intercalates, the substrate selectivity effects observed by Tatsumi for the decomposition products are nonetheless impressive. For instance, the preference of the  $\text{Mg}_2\text{Al-POM}$  catalyst precursor systems for the epoxidation of 2-hexene was enhanced 4 to 6 fold relative to the unsupported catalysts. The origin of the enhanced substrate selectivity cannot be attributed to molecular sieving based on substrate size or shape as originally suggested because the intercalated structure of the LDH is lost after drying and use as a catalyst. Moreover, even if the LDH-POM structure was retained, shape selectivity effects based on sieving would not be expected because of limited access to the solvated gallery anions under reaction conditions. Factors other than pillaring and substrate size selectivity, such as

selective adsorption, may be responsible for the previously observed preference of LDH - POM catalysts toward smaller olefins.

The largest gallery height ( $\sim 16.6 \text{ \AA}$ ) is observed for the  $\text{NaP}_5\text{W}_{30}\text{O}_{110}^{14-}$  intercalate. Because the gallery height is more than three times as large as the layer thickness ( $4.8 \text{ \AA}$ ), this derivative may be regarded as being a supergallery intercalate and is the most likely to have accessible intergallery anions. Catalytic oxidation of cyclohexene with hydrogen peroxide as the oxygen source and the PJP anion as the catalyst resulted in a difference in cyclohexanediol and cyclohexene oxide product selectivity between the non-supported catalyst and the  $\text{Zn}_2\text{Al-NaP}_5\text{W}_{30}\text{O}_{110}^{14-}$  LDH. When the LDH supported PJP catalysts containing varying amounts of impurity phase were compared for catalytic activity, the turnover numbers increased with the presence of the impurity phase. One explanation for this effect, supported by TEM results, is that the impurity is a  $\text{M}^{n+}$  salt of the polyoxometalate dispersed on the surface and edges of the LDH particles. Dispersion of the salt phase on the LDH external surfaces may increase access to the catalytically active impurity salt, while decreasing access to the intercalated  $\text{NaP}_5\text{W}_{30}\text{O}_{110}^{14-}$  anions.

## Experimental Methods

### *Physical Measurements*

Raman spectra in the region  $1200\text{-}200 \text{ cm}^{-1}$  were recorded on a BIO-RAD FT Raman spectrometer equipped with a Spectra-Physics Topaz T10-106c  $1.064 \text{ \mu m}$  YAG laser and a Ge detector. The samples were ground into a fine powder and loaded into glass sampling tubes.

X-ray diffraction patterns were obtained with a Rigaku x-ray diffractometer equipped with DMAXB software, a curved graphite

monochromator and Cu K $\alpha$  radiation. Samples were either thin films on glass slides formed by evaporation of an LDH slurry or dried samples ground into a fine powder.

Proton NMR spectra of the cyclohexene oxidation products were recorded on a VXR 300 or VXR 500s spectrometer. The delay time between pulses was long relative to the proton relaxation time, so that the integral intensities of the cyclohexene, epoxide and diol resonance's were quantitative. <sup>31</sup>P MAS-NMR was used to verify retention of the PJP anion structure following catalysis.

Elemental analyses were performed by ICP emission at the Toxicology Laboratory at MSU. Solutions for analysis were prepared by dissolving 15 mg of solid in 100 mL of 15% HNO<sub>3</sub>.

*Mg<sub>2</sub>Al-Mo<sub>7</sub>O<sub>24</sub><sup>6-</sup> and Mg<sub>2</sub>Al-W<sub>7</sub>O<sub>24</sub><sup>6-</sup> LDHs*

A Mg<sub>2</sub>Al-terephthalate LDH was prepared according to literature methods<sup>7,76</sup> and stored as an suspension in degassed deionized water. The terephthalate-intercalated LDH was converted to the desired POM intercalate according to the procedure used by Tatsumi et al.<sup>7</sup> Na<sub>2</sub>MoO<sub>4</sub> (25.4 g, 0.105 mole) or Na<sub>2</sub>WO<sub>4</sub> (27.7 g, 0.84 mole) was added to 200 mL of the Mg<sub>2</sub>Al-TA slurry and then the pH was lowered to 4.4 with 2 M NaOH. After 10-15 minutes of additional stirring, the product was washed 4 times by centrifuging and resuspending the pellet in deionized water. A thin film sample was made, and the remainder was dried at 120 °C. Mg<sub>2</sub>Al-Mo<sub>7</sub>O<sub>24</sub><sup>6-</sup> - XRD (Å): 10.2, impurity; 6.08,(002); 4.03, (003); 3.03, (004); 2.44, (005); and 1.99 Å, (006). ICP (wt. %): Mg = 11.0, Al = 7.20 and Mo = 25.3. Mg<sub>2</sub>Al-W<sub>7</sub>O<sub>24</sub><sup>6-</sup> - XRD (Å): 12.2, (001); 10.1, impurity; 6.06, (002); 4.04, (003); 3.03, (004); 2.44 (005) and 1.99 (006). ICP (wt. %): Mg = 10.8, Al = 6.73, and W = 32.9.

### *Synthesis of $Zn_2Al-NO_3^-$ LDH*

Taylor's induced hydrolysis method,<sup>102</sup> as modified by Kwon et al.,<sup>188</sup> was used to prepare a stable, highly ordered nitrate - intercalated  $Zn_2Al$  layered double hydroxide. Even though the reaction is not very sensitive to carbonate contamination through exposure to  $CO_2$  in the air,  $N_2$  was bubbled into the reaction mixture, but no other steps were taken to prevent contact with air.

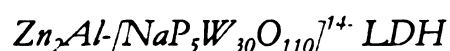
The pH of a 200 mL solution of 0.1 M  $Al(NO_3)_3 \cdot 9H_2O$  in a 1-liter three neck round bottom flask was adjusted to 7.0 with 2 M NaOH. The white slurry was stirred for 1 hour, and then 200 mL of 0.3 M  $Zn(NO_3)_2 \cdot 6H_2O$  was added dropwise. As the  $Zn^{2+}$  solution is added, the pH was allowed to fall to 6.4 and then maintained at that level with the simultaneous addition of 2 M NaOH. Upon complete addition of the zinc nitrate solution, the temperature was raised to 95 °C and digested with gentle stirring for one week. The product was rinsed four times by centrifuging. After the final rinse, the pellet was resuspended in 500 mL water.

In order to maintain a supply of  $Zn_2Al-NO_3^-$  for subsequent anion exchange experiments, the above slurry was purged with  $N_2$  and stored in a stoppered 2-liter single neck round bottom flask. There was no degradation of the LDH over a several month period. XRD (Å): 8.93, (001); 4.46, (002); 2.97, (003); 2.82; 2.61,; and 2.48.

### *$Zn_2Al-Mo_7O_{24}^{6-}$ and $Zn_2Al-H_2W_{12}O_{40}^{6-}$ LDHs*

One hundred mL of  $Zn_2Al-NO_3^-$  LDH slurry was heated to 95 °C and dripped into 100 mL of a  $1.2 \times 10^{-2}$  M solution of  $(NH_4)_6Mo_7O_{24} \cdot 4H_2O$  or  $(NH_4)_6H_2W_{12}O_{40} \cdot 4H_2O$  at room temperature and pH = 5.1 and 4.3, respectively. The pH of the solution was too low for carbonate contamination to be a

significant problem, so there was no attempt to prevent exposure to air. The solution was allowed to stir for 90 min. and rinsed three times by centrifugation and resuspended in 100 mL deionized water. After the final rinse, the pellet was resuspended in 100 mL deionized water and digested for 18 h at 80 °C. A thin film sample was made for X-ray diffraction analysis, and the remainder was dried at room temperature. Powder samples were made from the dried product.  $Zn_2Al-H_2W_{12}O_{40}^{6-}$  - XRD (Å): 14.7, (001); 10.8, impurity; 7.31, (002); 4.86, (003); 3.65, (004); 2.91, (005); 2.43, (006); 2.03 (007) and 1.85 (008). ICP (wt. %): Zn = 16.5, Al = 3.08 and W = 43.4.  $Zn_2Al-Mo_7O_{24}^{6-}$  - XRD (Å): 12.1, (001); 6.02, (002); 4.01, (003); 2.60; 2.44; 2.41, (005); and 2.00, (006). ICP (wt. %): Zn = 26.7, Al = 5.43 and Mo = 21.8.



A hot (95 °C) 100-mL portion of the LDH nitrate suspension (2.6 meq) at pH 6.0 was added dropwise into 200 mL of 0.02 M POM salt solution (4.08 meq, 22 times the LDH AEC). After a reaction time of 2 h, the product was washed several times by suspending in water and centrifuging, and then dried in air at room temperature.  $Zn_2Al-NaP_5W_{30}O_{110}^{14-}$  - XRD (Å) 21.7 (001); 14.8, impurity salt; 10.7, (002); 7.1, (003); 5.34 (004); 4.47, (005); 3.55, (006). ICP (wt %) Zn = 15%, Al = 2.7%, and W = 47.9%.

#### *Oxidation of cyclohexene by supported and non-supported molybdates and tungstates*

Oxidation reactions of cyclohexene were carried out according to previously described methods<sup>7</sup>. The catalyst (1 mmol of W or Mo) and 100 mmol of cyclohexene were stirred at  $73 \pm 2^\circ$  in an oil bath. One hundred mmol of 10%  $H_2O_2$  in  $(BuO)_3PO$  was slowly dripped into the mixture of substrate and catalyst and the reaction was stirred at 73 °C for a total of three hours. The

products were identified by Total Correlation Spectroscopy (TOCSY) NMR, also known as homonuclear Harman-Hahn (HOHAHA) NMR, using purchased standards as reference samples. Yields were calculated from NMR.

*Catalytic Oxidation of Cyclohexene by the supported and non-supported PJP anion.*

Hydrogen peroxide in (BuO)<sub>3</sub>PO (10% by wt., 10 ml) was added to 0.200 g of Zn<sub>2</sub>Al-NaP<sub>5</sub>W<sub>30</sub>O<sub>110</sub><sup>14-</sup> (1.87x10<sup>-5</sup> mol of PJP anion) or an equivalent amount of the control (a potassium or ammonium salt of NaP<sub>5</sub>W<sub>30</sub>O<sub>110</sub><sup>14-</sup>) in a 100 ml three neck flask. Cyclohexene (0.02 mole) was added, and the reaction placed in an oil bath at 70 °C for 4 hr. A sample was taken, and the yield of cyclohexene oxide and diol products determined by <sup>1</sup>H NMR. The non-supported catalyst was recovered in D<sub>2</sub>O and <sup>31</sup>P NMR used to determine that the catalyst was still intact. The supported catalyst was filtered and rinsed with acetone. <sup>31</sup>P MAS-NMR was used to verify that the catalysts were still intact.

1. Sels B. F., de Vos D. E., Jacobs P. A., *Tet. Lett.*, **1996**, 37(47), 8557.
2. Gardner E. A. and Pinnavaia T. J., *Appl. Catal. A: General*, **1998**, 167, 65.
3. Gardner E. A., Yun S. , and Pinnavaia T. J., *Appl. Clay Sci.*, in press
4. Woltermann, US Pat. 4454244 **1984**.
5. Yamada, T., *Petrotech.*, **1990**, 13 627.
6. Aoshima,, A., Tonomurs, S., and Yamamatsu, S., *Polymers Adv. Tech.*, **1991**, 2, 127.
7. (a.) Tatsumi, T., K. Yamamoto, H. Tajima, and H. Tominga, *Chem. Lett.*, **1992**, 815; b. Tatsumi, T., H Tajima, K. Yamamoto and H. Tominga, *New Frontiers in Catalysis*, Guzi et al. (ed), Elsevier Science Publ. B. V. **1993**.
8. Moore D. M. and Reynolds R. C. Jr., *X-Ray Diffraction and Analysis of Clay Minerals 2cnd ed.*, Oxford University Press, N.Y., **1998**, 311.
9. Cavani, F., Trifirò, F., and Vaccari, A., *Catalysis Today*, **1991**, 11, 173.
10. De Roy A., Forano C., El Malki K., and Besse J.-P., in Occelli M. L. And Robson H. E. (eds.) *Expanded Clays and Other Microporous Solids*, **1992**, 108.
11. Newman S. and Jones W., *New J. Chem.*, **1998**, 22(2), 105.
12. Manasse, E., *Atti Soc. Toscana Sc. Nat. Proc. Verb.*, **1915**, 24, 92.
13. Aminoff, G. and B. Bromé, *Kungl. Sven. Vetensk. Handl.* 9, **1930**, 3(no. 5), 23.
14. Frondel, C., *Amer. Min.*, **1941**, 26, 295.
15. Feitknecht C., *Helv. Chim. Acta*, **1942**, 25, 131.
16. Allmann, *Acta Cryst.*, **1968**, B24, 972.
17. Taylor, H. F. W., *Miner. Mag.*, **1969**, 37, 338.
18. Zelinski, N. and Kommarewsky, W., *Chem. Ber.*, **1924**, 57, 667.

19. Bröcker, F. J. and L. Kainer, German Patent 2,024, 282 **1970**, BASF AG, and UK Patent 1,342,020 **1971**, BASF AG.
20. Miyata, S., *Kagaku Gijutsushi MOL*, **1977**, *15(10)*, 32.
21. Ueno, M. and Kubota, US Patent 4,666,919 **1987**.
22. Kyowa Chem. Ind. Co., *Jpn. Kokai Tokkyo Koho JP 60 06,619* 1985; CA **1985**, 102, 226,039f.
23. French Patent 2,091,785 **1971**, to BASF AG.
24. Gardner E. A. and Pinnavaia T. J., *Appl. Catal. A: General*, **1998**, 167, 65.
25. Kang M. J., Rhee S. W., Moon H., Neck V., and Fanghanel T., *Radiochim. Acta*, **1996**, 75, 169.
26. Ikeda T., Amoh H., and Yasunaga T., *J. Am. Chem. Soc.*, **1984**, 106, 5772.
27. Reichle, W. T., *Chemtech.*, **1986**, 58.
28. Miyata, S., and Kuroda, M., US Patent 4,299,759 **1981**, to Toyo Soda Man. Ltd.
29. Miyata, S. And M. Kuroda M., US Patent 4,299,759 **1981** to Kyowa Chem. Ind. Ltd.
30. Miyata, S., Eur. Patent 142,773 **1985** to Kyowa Chem. Ind. Co.
31. Miyata S., *Kagaku Gijutsushi MOL*, **1977**, *15(10)*, 10.
32. Marcon Electronics Co., *Jpn. Kokai Tokkyo Koho JP 60 106,122* 1985; C.A. **1986**, 104, 13785.
33. Suzuki S., Araga T., Tsuji R., Fukushima Y., Banno K., and Hiruta O., Eur. Patent 150,741 **1984**, to Toyota Central R&D Lab.
34. Toyota Central R&D Lab., *Jpn. Kokai Tokkyo Koho JP 59 166,568* 1984; C.A. **1985**, 102, 80,421.

35. Ulmgren, P., *Nordic Pulp and Paper Research J.*, **1987**, 1, 4.
36. Dutta, P. K., and Puri, M. *J. Phys. Chem.*, **1989**, 93, 376.
37. Itaya, K., Chang, H. C., and Uchida, I., *Inorg. Chem.*, **1987**, 26, 624.
38. Zhu K., Liu c., Ye X., and Wu Y., *Applied Catal. A: General*, **1998**, 168, 365.
39. Putyera K., Bandosz T. J., Jagiello J., Schwarz A., *Applied Clay Science*, **1995**, 10, 177.
40. Mousty C. Therias S. Forano C. and Besse J. P., *J Electroanal. Chem.*, **1994**, 347, 435.
41. Tagaya H., Sato S., Kuwahara J., Masa K., and Chiba K., *J. Mater. Chem.*, **1994**, 4, 1907.
42. Dutta P. K., and Robins D. S., *Langmuir*, **1994**, 10, 1851.
43. Tseng W. Y., Lin J. T., Mou C. Y., Cheng S. F., Liu S. B., Chu P. P., and Liu H. W., *J. Am. Chem. Soc.*, **1996**, 118, 4411.
44. Robbins D. S. and Dutta P. K., *Langmuir*, **1996**, 12, 402.
45. Allmann, R. and Lohse, H. H., *N. Jhb. Miner. Mb.*, **1966**, 6, 161.
46. Ingram, L. and Taylor, H. F. W., *Miner. Mag.*, **1967**, 12, 544.
47. Lal, M., and Howe, A. T., *J. Chem. Soc. Chem. Commun.*, **1980**, 15, 737.
48. Bookin A. S. and Drits V. A., *Clays Clay Miner.*, **1993**, 41, 551, 558.
49. Drits, V. A., Sokolova, T. N., Sokolova, G. V., and Cherkashim, V. I., *Clays and Clay Miner.*, **1987**, 35, 401.
50. Miyata, S., *Clays Clay Mineral.*, **1983**, 31, 305.
51. Miyata, *Clays and Clay Minerals*, **1977**, 25, 14.

52. Kooli F., Crespo I., Barriga C., Ulibarri M. A., and Rives V., *J. Mater. Chem.*, **1996**, *6(7)*, 1199.
53. Allmann R., *N. Jhb. Miner. Mb.*, **1977**, *3*, 136.
54. Miyata S. and Kumura T., *Chem. Lett.*, **1979**, *23*, 843.
55. Miyata, S., *Clay Clays Miner.*, **1980**, *28*, 50.
56. Pausch, L., Lohse, H. H., Schürmann, K., and Allmann, K., *Clays Clay Miner.*, **1986**, *34*, 507.
57. Hansen H. C. B. and Koch C. B., *Appl. Clay Sci.*, **1995**, *10*, 5.
58. Boehm H. P., Steinle, J., and Vieweger, C. *Angew. Chem. Int. Ed. Engl.*, **1977**, *16*, 265.
59. Yun S. K. and Pinnavaia Y. J., *Inorg. Chem.*, **1996**, *35*, 6853.
60. Bish D. L., *Bull. Mater.*, **1980**, *103*, 170.
61. Karrado, K. A., Kostapapas, A., and Suib, S. L., *Solid State Ionics*, **1988**, *26*, 77.
62. Giannelis, E. P., Nocera, D. G., and Pinnavaia, T. J., *Inorg. Chem.*, **1987**, *26*, 203.
63. Tagaya H., Kkuwahara T., Sato S., Kadokawa J., Karasu M., and Chiba K., *J. Mater. Chem.*, **1993**, *3*, 317.
64. Miyata S., *Clays and Clay Minerals*, **1975**, *23*, 377.
65. Clearfield A., Kieke M., Kwan J., Colon J. L., and Wnag R. C., *J. Inclusion Phenom. Mol. Recognit. Chem.*, **1991**, *11*, 361.
66. Miyata S., and Kumara T., *Chem. Let.*, **1973**, 843.
67. Boehm H.-P., Steinle J., and Vieweger C., *Angew. Chem. Int. Ed. Engl.*, **1977**, *16*, 265.

68. Wang J. D., Serrette G., Tian Y., Clearfield A., *Appl. Clay Sci.*, **1995**, *10*, 103.
69. Zhao H., and Vance G. F., *J. Chem. Soc., Dalton Trans.*, **1997**, 1961.
70. Chibwe K., and Jones W., *J. Chem. Soc., Chem. Commun.*, **1989**, 926.
71. Dimotakis E. D., and Pinnavaia T. J., *Inorg. Chem.*, **1990**, *29*, 2393.
72. Tagaya H., Sato S., Morioka H., Kadokawa J., Karasu M., and Chiba K., *Chem Mater.*, **1993**, *5*, 1431.
73. Ukrainczyk L., Chibwe M., Pinnavaia T. J., and Boyd S. A., *J. Phys. Chem.*, **1994**, *98*, 926.
74. Carlino S., and Hudson M. J., *J. Mater. Chem.*, **1994**, *4*, 99.
75. Carlino S., Hudson M. J., Husain S. W., and Knowles J. A., *Solid State Ionics*, **1996**, *84*, 117.
76. Drezdzon M. A., *Inorg. Chem.*, **1988**, *27*, 4628.
77. Boehm H.-P., Steinle J., and Vieweger C., *Angew. Chem. Int. Ed. Engl.*, **1977**, *16*, 265.
78. Kanezaki E., Kinugawa K., and Ishikawa T., *Chem. Phys. Lett.*, **1994**, 226, 325.
79. Kanezaki E., Sugiyama S., and Ishikawa Y., *J. Mater. Chem.*, **1995**, *5*, 1969.
80. Franklin K. R., Lee E., and Numm C. C., *J. Mater. Chem.*, **1995**, *5*, 565.
81. Wang J. D., Serrette G., Tian Y., and Clearfield A., *Appl. Clay Sci.*, **1995** *10*, 103.
82. Vichi M. F., and Alver O. L., *J. Mater. Chem.*, **1997**, *7*, 1631.
83. Van der Pol A., Mojet B. L., van de Ven E., and de Boer E., *J. Phys. Chem.*, **1994**, *98*, 4050.
84. Hudson, D. R. and Bussell, M., *Miner. Mag.*, **1981**, *44*, 345.

85. Courtney, P.H., and Marcilly, C. H., in Poncelet, G., Grange, P., and Jacobs, P. A. (Eds.) *Preparation of Catalysts III*, Elsevier, Amsterdam, **1983**, 485.
86. Burba, John L. III; Steve A. Sims, and Thomas M. Knobel, United States Patent 5,084,209, Jan. 28, **1992**.
87. Malherbe, F.; Forano C.; and Besse, J. P.; *Micropor. Mater.*, **1997**, 10(1-3), 67-84.
88. Roy, D. M., Roy, R., and Soburn, E. F., *Amer. J. of Science*, **1988**, 27, 77.
89. Yun, S., *thesis*, Michigan State University, U. S., **1994**, 151.
90. Bish, D. L., and Brindley, G. W., *Amer. Miner.*, **1977**, 62, 458.
91. Clearfield A., *Chem. Rev.*, **1988**, 88, 125.
92. Miyata, S., *Clays Clay Miner.*, **1983**, 31(4), 304.
93. Yamoaka, T., Abe, M., and Tsuji, M., *Mat. Res. Bull.*, **1989**, 24, 1183.
94. Meyn, M., Beneke, K., and Lagaly, G. *Inorg. Chem*, **1990**, 29, 5201.
95. Carlino S. and Hudson M. J., *J. Mater. Chem.*, **1995**, 5, 1433.
96. Reichle, W. T., yang, s. Y., and Everhardt, d. s., *J. Catal.*, **1986**, 101, 352.
97. Chibwe K. and Jones W., *Chem. Of Mater.*, **1989**, 1, 489.
98. Albiston L., Franklin K. R., Lee E., and Smeulders J. B. A. F., *J. Mater. Chem.*, **1996**, 871.
99. Nakamoto Kazuo, *Infrared and Raman Spectra of Inorganic and Coordination Compounds*, third ed., John and Wiley and Sons, NY, **1978**.
100. Ross, G. J. and Kodama, H., *Amer. Min.*, **1967**, 52, 1037.
101. Busetto, C., Del Piero, G., Manara, G., Trifiró, F., and Vaccari, A., *J. Catal.*, **1984**, 85, 260.

102. Taylor R. M., *Clay Minerals*, **1984**, *19*, 591.
103. Kwon T., thesis, Michigan State University, USA, **1988**.
104. Miyata S., *Clays and Clay Miner.*, **1975**, *23*, 369.
105. Reichle W. T. *Solid States Ionics*, **1986**, *22*, 135.
106. Ghosh, P. K. and Bard, A. J. *J. Am. Chem. Soc.*, **1983**, *105*, 5691.
107. Guth, U.; Brosda, S.; and Schomburg, J. *Appl. Clay Science*, **1996**, *11*, 229-236.
108. Lopez, T.; Bosch, P.; Ramos, E.; Gomez, R.; Novaro, O.; Acosta, D.; and Figueras, F. *Langmuir*, **1996**, *12*, 189-192.
109. Pinnavaia, T. J., Chibwe, M., Constantino, V. R. L., and Yun, S., *Applied Clay Science*, **1995**, *10*, 117-129.
110. Sheldon, R. A., J. K. Kochi, *Metal Catalyzed Oxidations of Organic Compounds*, Academic Press New York, N. Y., **1981**.
111. Haber J., *The Role of Molybdenum in Catalysis*. **1981**, Climax Molybdenum Co., Ann Arbor MO.
112. Chibwe, M., and Pinnavaia T. J., *J. Chem Soc. Chem. Commun.*, **1993**, 278.
113. 1. Corma, A., V. Fornis, F. Rey, A. Cervilla, and E. Llopis, *J. of Catal.*, **1995**, *152*, 237. b. Cervilla, A., A. Corma, V. Fornes, E. Llopis, R. Palanca, F. Rey, and A. Ribera, *J. Am. Chem. Soc.*, **1994**, *116*, no.4, 1595.
114. Pope M. T. and Muller, A. *Angew. Chem. Int. Ed. Engl.*, **1991**, *30*, 34.
115. Hill C. L. and Prosser-McCarthy C. M., *Coord. Chem. Rev.*, **1995**, *143*, 407.
116. Katsoulis D. E., *Chem. Rev.*, **1998**, *98*, 359.
117. Kozhevnikov I. V., *Chem. Rev.*, **1998**, *98*, 171.

118. Recent reviews of polyoxometalate chemistry include: a. Hill, C.L., (ed) *Journal of Molec. Catal. A*, **1996** 114; b. I. V. Kozhevnikov, *Catal. Rev.-Sci. Eng.*, **1995**, 37(2) 311; c. Hill, C. L. and Prosser-McCarthy C. M., *Cord. Chem. Rev.*, **1995** 143, 407.
119. Neumann R. and Assael I., *J. Chem. Soc., Chem Commun.*, **1988**, 1286.
120. Sharpless K. B., Townsend J. M., and Williams D. R., *J. Am. Chem. Soc.*, **1972**, 94, 295.
121. Jorgensen K A., Wheeler R. A., and Hoffman R., *J Am. Chem. Soc.*, **1987**, 109, 3240.
122. Venturello C., D'Aloisio R., Bart J. C.J., and Ricci M., *J. Mol. Catal.*, **1985**, 32, 823.
123. Ishii Y. and Ogawa M., in *Reviews on Heteroatom Chemistry*, Ohno A. and Furukawa N., Eds., MY: Tokyo, **1990**, Vol. 3, 121.
124. Aubry C., Chottard G., Plantzer N., Bregault J. M., Thouvenot, R., Chauveau f., Huet C., and Ledon H., *Inorg. Chem.* **1991**, 30, 4409.
125. Neumann R. and Juwiler D., *Tetrahedron*, **1996**, 52, 8781.
126. Neumann R., Khenkin A. M., Juwiler D., Miller H., and Gara M., *J. Mol. Catal. A*, **1997**, 117, 169.
127. Nomiya K., Yanagibayashi H., Nozaki C., Kondoh K., Hiramatsu E., and Shimizu Y., *J. Mol. Catal. A*, **1996**, 114, 181.
128. Kuznetsova L. I., Detusheva L. G., Fedotov M. A., and Likholobov V. A., *J. Mol. Catal. A*, **1996**, 111, 81.
129. Yamase T., Ichikawa E., Asai Y., and Kanai S., *J. Mol. Catal. A*, **1996**, 114, 237.
130. Nuemann R. and Miller H., *J. Chem. Soc., Chem Commun.*, **1995**, 2277.

131. Weinstock I. A., Atalla R. H., Reiner R. S., Moen M. A., Hammil K. E., Houtman C. J., Hill C. L., Harrup M. K., *J. Molec. Catal. A*, **1997**, *116*, 59.
132. Mylonas, A., Hisdia A, and Papaconstantinou E., *J. Molec. Catal. A*, **1996**, *114*, 191. b. Haggin, J., *Chem. and Eng. News*, **1996**, 2530.
133. Harrup M. K. and Hill C. L., *J. of Molec. Catal. A: Chemical*, **1996**, *106*, 57.
134. Gall R. D., Faraj M., and Hill C. L., *Inorg. Chem.* **1994**, *33*, 5015.
135. Serwicka, E. M., Black J. B., Goodenough J. B., *J. Catal.*, **1987**, *106*, 27.
136. Misono M. and Nojiri N., *Appl. Catal.*, **1990**, *64*, 1.
137. Ahmed S. and Moffat J. B., *Appl. Catal.*, **1988**, *40*, 101.
138. Berzelius J., *Pogg. Ann.*, **1826**, *6*, 369.
139. Marignac C., *C. R. Acad. Sci.*, **1862**, *55*, 888; b. *Ann. Chem.*, **1862**, *25*, 362.
140. Rosenheim A., Jaenicke H., *Z. Anorg. Chem.*, **1917**, *100*, 304.
141. *Gmelin Handbuch der Anorganischen Chemie, Verlag Chemie, Berlin: System-No. 53 (Molybdän) 1935; System-No. 54 (Wolfram) 1933.*
142. Keggin J. F., *Nature*, **1933**, *131*, 908.
143. Lipscomb W. N., *Inorg. Chem.*, **1965**, *4*, 132.
144. Izumi Y., Matsuo K., Urabe K., *J. Molec. Catal.*, **1983**, *18*, 299.
145. Preyssler, C., *Bull. Soc. Chim. Fr.*, **1970**, *1*, 30.
146. Pope M. T., Alizadeh M. H., Harmalker S. P., Jeanin Y., and Martin-Frère J., *J. Am. Chem. Soc.*, **1985**, *107*, 2662.
147. Tytko K.-H. and Glemser O., *Inorg. Chem.*, **1990**, *27*, 71.
148. Baker, L. C. W. and Glick. *Chem. Rev.*, **1998**, *98*, 3.

149. Woltermann, G. M., U.S. Pat. 4454244, **1984**.
150. Kwon T., Tsigdnios G. A. and Pinnavaia T. J., *J. Amer. Chem. Soc.*, **1988**, *110*, 3653.
151. a. Chibwe K. and Jones W., *Chem. Mater.*, **1998**, *1*, 489. b. Chibwe K. and Jones W., *J. Chem. Soc. Chem. Commun.*, **1989**, 926.
152. Narita E., Kaviratna P. and Pinnavaia T. J., *Chem. Lett.*, **1991**, 805.
153. Dimotakis E. D. and Pinnavaia T. J., *Inorg. Chem.*, **29**, **1990**, 2393.
154. Sang K. Y. and Pinnavaia T. J. *Inorg. Chem.*, **1996**, *35*, 6853.
155. Han K. S., Guerlou-Demourgues L., and Delmas C., *Solid State Ionics*, **1996**, *84*, 227.
156. Serwicka E., Nowak P., Bahranowski K., Jones W., and Kooli F., *J. Mater. Chem.*, **1997**, *7*, 1937.
157. a. Ulibarri M. A., Labajos F. M., Rives V., Kagunya W., Jones J., and Turjillano R., *Mol. Cryst. Liq. Cryst.*, **1994**, *244*, 167; b. *Inorg. Chem.*, **1994**, *33*, 2592.
158. Kooli F., Jones W., Rives V., and Ulibarri M. A., *J Mater. Sci. Lett.*, **1997**, *16*, 27.
159. Kooli F. and Jones W., *Inorg. Chem.*, **1995**, *34*, 6237.
160. Twu J. and Dutta P. K., *Chem. Mater.*, **1992**, *4*, 398.
161. Hibino T. and Tsumashima A., *Chem. Mater.*, **1997**, *9*, 2082.
162. Kooli F. and Jones W., *Inorg. Chem.*, **1995**, *34*, 5122.
163. Kwon T. and Pinnavaia T. J., *Chem Mater.*, **1989**, *4*, 381 and thesis.
164. Kooli F. and Jones W., *Inorg. Chem.*, **1995**, *34*, 5114.

165. Kooli F., Rives V., and Jones W., *Mater. Sci. Forum.*, **1994**, 152-153, 375.
166. Chibwe K. and Jones W., *Chem. Mater.*, **1989**, 1, 489.
167. Yun, s. K., Constantino V. R. L., and Pinnavaia T. J., *Microporous Mater.*, **1995**, 4, 21.
168. Battacharyya A., Hall D. B., and Barnes T. J., *Appl. Clay Sci.*, **1995**, 10, 57.
169. Depège C., Bigey L., Forano C., de Roy A., and Besse J. P., *J. Solid State Chemistry*, **1996**, 126, 314.
170. Weir M. R., Moore J., and Kydd R. A., *Chem. Mater.*, **1997**, 9, 1686.
171. Evans J., Pillinger M., and Zhang J., *J. Chem. Soc., Dalton Trans.*, **1996**, 27.
172. Hu C.-W., He Q.-L., Zhang Y.-H., Liu Y.-Y., Zhang Y.-F., Tang T.-D., Zhang J.-Y., and Wang E.-B., *J. Chem. Soc., Chem. Comm.*, **1996**, 121.
173. Wang J., Tian Y., Wang R.-C., and Clearfield, A., *Chem. Mater.*, **1992**, 4, 1276.
174. Guo J., Sun T., Shen J. P., Jiang d. Z., and Min E. Z., *Chem. J. Chinese Univ.*, **1995**, 16, 512, in Chinese.
175. Liu Y. Y., Hu C. W., Wang Z. P., Zhang J. Y., and Wang E. B., *Sci. China Series B-Chemistry*, **1996**, 39, 86, in Chinese.
176. Hu C. W., Zhang X., He Q. L., Wang E. B., Wang S. W., and Guo Q. L., *Transition Metal Chem.*, **1997**, 22, 197.
177. Salinas, L. S., Castillo S. P., Ono Y., *Mater. Res. Soc. Symp. Proc.*, **1995**, 371, 163.
178. Yun S. K. and Pinnavaia T. J., *Inorg. Chem.*, **1996**, 35, 6853.
179. Pinnavaia T. J., Kwon T., Dimotakis E. D., and Amarasedera J., US Patent 5,079,203 **1992**.

180. Hu C-W., He Q-L, Zhang Y.-H., Liu Y.-Y., Zhang Y.-F., Tang T.-D., Zhang J.-Y., and Wang E.-B., *Chem. Commun.*, **1996**, 121.
181. Guo J., Jiao Q. Z., Shen J. P., Jiang D. Z., Yang G. H., and Min E. Z., *Catal.Lett.*, **1996**, *40*, 43.
182. Zheng X., Yue W., Heming H., and Dazhen J., in Hattori, Misono, and Ono (eds.), Acid-Base Catalysis II, Elsevier, Amsterdam, *Stud. Surface Sci. Catal.*, **1994**, *90*, 279.
183. Kayunga W., Hassan Z., and Jones W., *Inorg. Chem.*, **1996**, *35*, 5970.
184. Kwon T. and Pinnavaia, *J. Molec. Catal.*, **1992**, *74*, 23.
185. Sels, b. F., De Vos D. E., and Jacobs, P A., *3rd World Conference on Oxidative Catalysis*, Grasselli, jR. K., Oyama S. T., and Lyons J. E., (Eds.) **1997**, 1051.
186. Guo, J., Jiao, Q. Z., Shen, J. P., Jiang, D. Z., Yang, G. H. and Min, E. Z., *Catal. Let.*, **1996**, *40*; 43.
187. Payen E., Grimbolt J., and Kastelan S., *J. Phys. Chem.*, **1987**, *91*, 6642.
188. a. Kwon T. and Pinnaviai T. J., *Chem. Mater.*, **1989**, *1*, 381. b. Kwon T., Thesis, MSU, **1988**.
189. Wang J., Tian Y., Wang R., and Clearfield A., *Chem. Mater.*, **1992**, *4*, 1276.
190. Iannibello A., Marengo S., Tittarelli P., Morelli G., and Zecchina A., *J. Chem. Soc. Farraday Trans. I*, **1984**, *80*, 2209.
191. Fox M. A., Cardona R., and Gaillard P. J., *Inorg. Chem.*, **1987**, *26*, 6347.
192. Harrup M. K. and Hill C. L., *J. Mol. Catal.*, **1994**, 5448.
193. Alizadah M. H., Harmalker S. Pl, Jeanin Y., Martin-Frere J. and Pope M. T., *J. Amer. Chem. Soc.*, *107*, 2662.

MICHIGAN STATE LIBRARIES



3 1293 02206 9953